CHEMICAL REVIEWS

Review

pubs.acs.org/CR

Light Absorption and Energy Transfer in the Antenna Complexes of Photosynthetic Organisms

Tihana Mirkovic,[†] Evgeny E. Ostroumov,[‡] Jessica M. Anna,[§] Rienk van Grondelle,[∥] Govindjee,[⊥] and Gregory D. Scholes*[,†,‡]

[†]Department of Chemistry, University of Toronto, 80 St. George Street, Toronto, Ontario M5S 3H6, Canada

[‡]Department of Chemistry, Princeton University, Washington Road, Princeton, New Jersey 08544, United States

[§]Department of Chemistry, University of Pennsylvania, 231 S. 34th Street, Philadelphia, Pennsylvania 19104, United States

[∥]Department of Physics and Astronomy, Faculty of Sciences, VU University Amsterdam, De Boelelaan 1081, 1081 HV, Amsterdam, The Netherlands

[⊥]Department of Biochemistry, Center of Biophysics & Quantitative Biology, and Department of Plant Biology, University of Illinois at Urbana−Champaign, 265 Morrill Hall, 505 South Goodwin Avenue, Urbana, Illinois 61801, United States

ABSTRACT: The process of photosynthesis is initiated by the capture of sunlight by a network of light-absorbing molecules (chromophores), which are also responsible for the subsequent funneling of the excitation energy to the reaction centers. Through evolution, genetic drift, and speciation, photosynthetic organisms have discovered many solutions for light harvesting. In this review, we describe the underlying photophysical principles by which this energy is absorbed, as well as the mechanisms of electronic excitation energy transfer (EET). First, optical properties of the individual pigment chromophores present in light-harvesting antenna complexes are introduced, and then we examine the collective behavior of pigment−pigment and pigment−protein interactions. The description of energy transfer, in particular multichromophoric antenna structures, is shown to vary depending on the spatial and energetic landscape, which dictates the relative coupling strength between constituent pigment molecules. In the latter half of the article, we focus on the light-harvesting complexes of purple bacteria as a model to illustrate the present understanding of the synergetic effects leading to EET optimization of light-harvesting antenna systems while exploring the structure and function of the integral chromophores. We end this review with a brief overview of the energy-transfer dynamics and pathways in the light-harvesting antennas of various photosynthetic organisms.

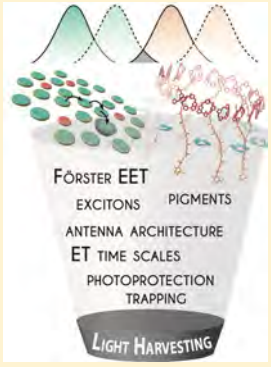

CONTENTS

1. Introduction B
2. Spectral Composition of Light and the Pigments D
3. Light-Harvesting Systems and Their Efficiency F
4. Physical Principles of Antenna Architecture G
5. Mechanism of Förster Excitation Energy Transfer J
6. Beyond Förster Theory of Excitation Energy Transfer M
   6.1. Electronic Coupling and Orbital Overlap M
   6.2. Breakdown of the Dipole Approximation N
   6.3. Solvent Screening N
7. Molecular Excitons Q
8. Structural and Spectral Considerations S
9. Excitonics and Generalized Förster Theory (GFT) S
   9.1. Excitons and Electronic Couplings U
   9.2. Formulating GFT V
10. Structure and Photophysics of Light-Harvesting Complexes of Purple Bacteria V
11. Structure and Absorption of Light-Harvesting Complexes X
   11.1. LH2 Model: Electronic Coupling and Exciton Formation Y
   11.2. LH2 Model: Disorder and Exciton Delocalization AA
12. Energy-Transfer Time Scales AB
   12.1. LH2 of Purple Bacteria AB
   12.2. LHCII of Higher Plants AC
   12.3. FCP and PCP of Brown and Dinoflagellate Algae AD
   12.4. Chlorosomes of Green Sulfur Bacteria AE
   12.5. Phycobilisomes of Cyanobacteria AE
   12.6. Phycobiliproteins of Cryptophyte Algae AE
13. Carotenoids and Photoprotection AF
14. Trapping of Energy AG
15. Concluding Remarks AH
Author Information AH
   Corresponding Author AH
   Notes AH
   Biographies AH
Acknowledgments AI
References AI

Special Issue: Light Harvesting

Received: January 8, 2016

DOI: 10.1021/acs.chemrev.6b00002
Chem. Rev. XXXX, XXX, XXX−XXX

Scheme 1. (Top) Fine Tuning of the Function of a Light-Harvesting Apparatus Occurs through Photophysical Properties of Its Constituent Chromophores and Synergetic Effects Resulting from Their Collective Interactions and (Bottom) the Light-Harvesting Complexes of Purple Bacteria Illustrate Phenomena Affecting Excitation Energy Transfer

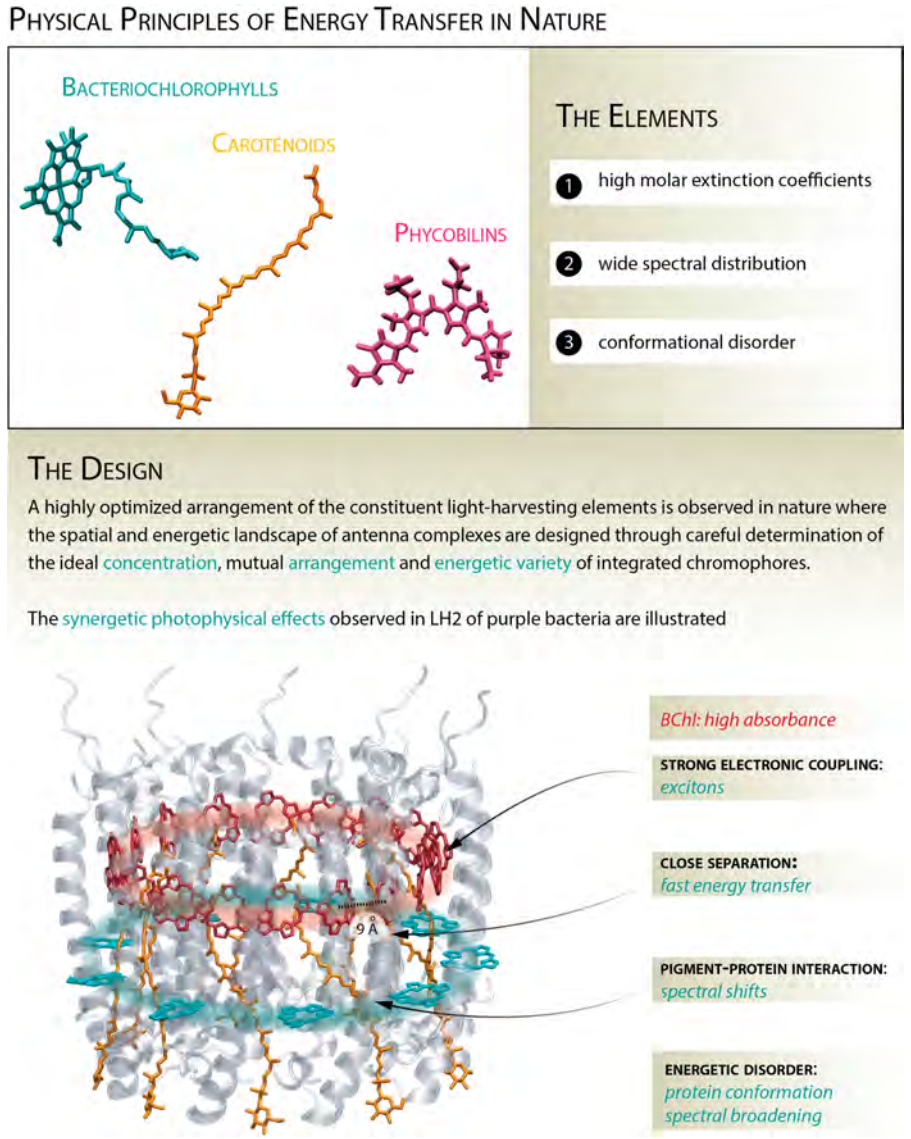

1. INTRODUCTION

The development, nourishment, and regulation of all forms of life on our planet are directed by sunlight. Photosynthesis, the most important light-induced process, allows plants, algae, cyanobacteria, and anoxygenic photosynthetic bacteria to convert energy harvested from light into a chemical form.[1,2] It is initiated by a sequence of remarkable and finely tuned photophysical and photochemical reactions (see Scheme 1, top). The process of photosynthesis, which takes place over a hierarchy of time scales and distances, ultimately powers, directly or indirectly, all living cells on the planet.[3] Planet Earth reflects 30% of the incident 166 PW (1 PW = 10^{15} W) of solar power back into space; 19% is absorbed by the clouds, leaving 85 PW available for terrestrial energy harvesting. Of this 85 PW of solar radiation, only a small fraction, 75 TW (1 TW = 10^{12} W), is utilized for products of terrestrial photosynthesis or the net global primary production through photosynthesis.[4] To put these numbers in perspective, the average total power consumption of the human world in 2010 was 16 TW.

In the past century, curiosity-driven research led to the discovery of the intricate structural and functional organization of the photosynthetic apparatus, which has more recently also been fueled by the opportunity to mimic these natural processes in man-made energy-harvesting systems. A number of reviews have discussed the development of artificial systems based on molecular and supramolecular architectures, and prospective redesigns of photosynthetic plant systems on various scales have been presented as plausible solutions to global food and bioenergy demands.[5−11] We have exciting days ahead.

There are two types of photosynthesis: oxygenic photosynthesis and anoxygenic photosynthesis. Plants, algae, and cyanobacteria carry out oxygenic photosynthesis, whereby carbon dioxide is reduced to carbohydrate and the oxidation of water delivers the necessary electrons and eventually leads to oxygen production.[12] However, in bacteria, other than cyanobacteria, water is not used as the primary electron donor, and no oxygen is produced during anoxygenic

DOI: 10.1021/acs.chemrev.6b00002
Chem. Rev. XXXX, XXX, XXX−XXX

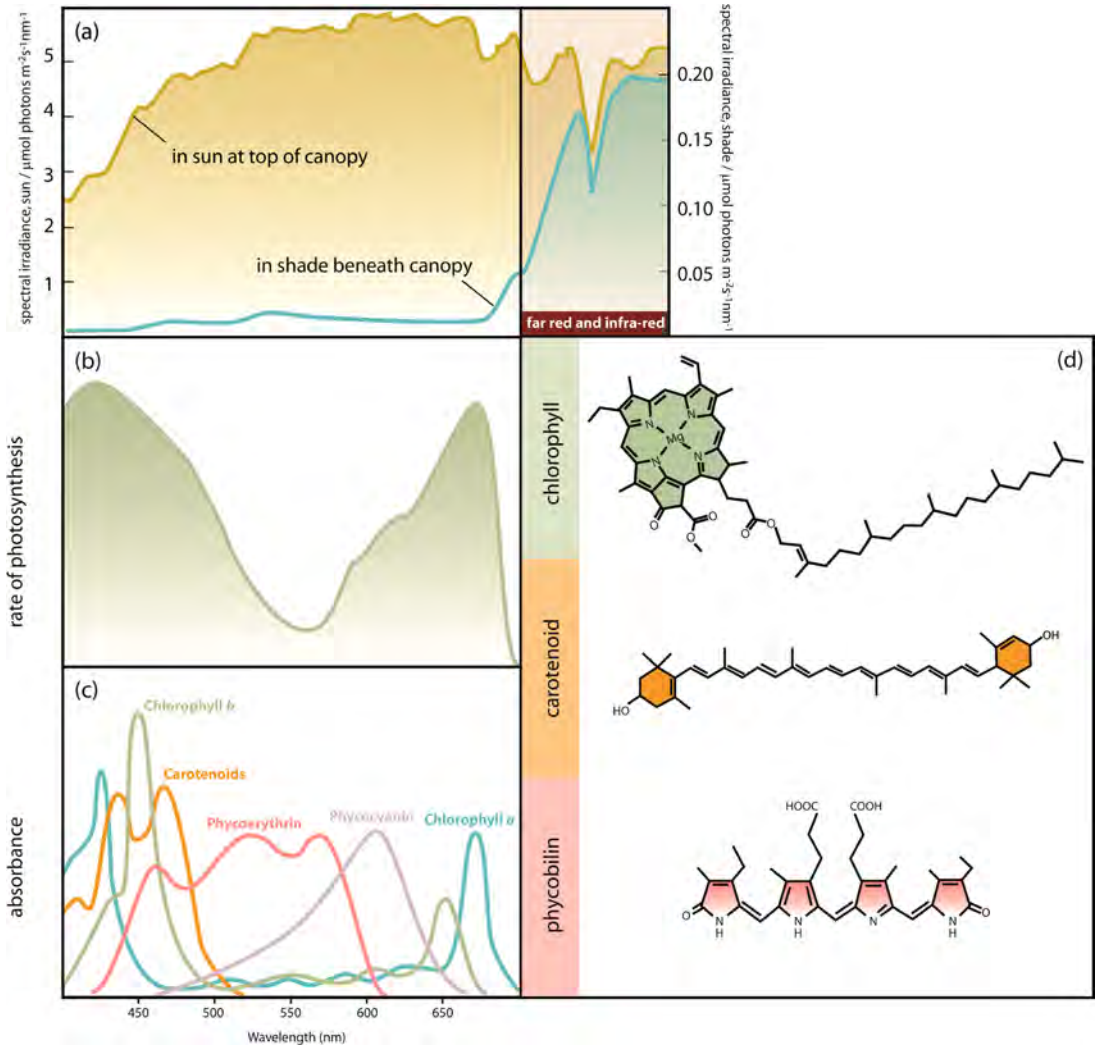

Figure 1. (a) Spectral distributions of sunlight that reaches the top and base of a dense canopy. (b) Photosynthetic action spectrum for a higher plant. Adapted with permission from ref 64, p 183. Copyright 2005 Pearson Education, Inc. (c) Absorption spectra of photosynthetic pigments utilized in light harvesting.[65,66] (d) Chemical structures of the chlorophyll, carotenoid, and phycobilin pigments. Adapted with permission from ref 37. Copyright 2015 Springer.

photosynthesis.[13,14] For example, purple sulfur bacteria utilize hydrogen sulfide or thiosulfate as the electron donor, whereas purple nonsulfur bacteria consume organic compounds, such as fatty and amino acids.[15] In fact, many studies have concluded that oxygenic photosynthesis appeared later, having evolved from anoxygenic photosynthesis, because geochemical evidence points strongly to a largely anoxic atmosphere up until the "Great Oxidation Event", which occurred about 2.4 billion years ago.[16]

The three stages of photosynthesis take place in the presence of light: (1) light harvesting from sunlight; (2) use of that energy for the production of ATP and reducing power, reduced ferredoxin, and NADPH; and (3) capture and conversion of CO_2 into carbohydrates and other cell constituents. However, the only true light reactions are over when charge separation has ended at the reaction centers (see, e.g., Govindjee and Govindjee, 1974).[17] During the third stage, namely, the carbon reactions, long incorrectly designated as the "dark reactions" or "light-independent reactions", the energy-rich products of the light reactions are used to reduce CO_2. Certain enzymes of the carbon reactions require light for regulation (see, e.g., Wolosiuk and Buchanan, 2015).[18] Thus, the division of even "light-dependent" and "light-independent" reactions is hazy, to say the least.

Robert Emerson and William Arnold performed pioneering experiments, in 1932, exposing a suspension of the green alga *Chlorella pyrenoidosa* to a series of light flashes and measuring the maximum oxygen evolution.[19] Their surprising findings suggested that about 2500 chlorophyll (Chl) molecules are involved in the production of a single molecule of oxygen. In 1934, Arnold and Henry Kohn, after examining several other photosynthetic systems, confirmed the existence of a "unit" of ~2400 Chl molecules per oxygen molecule, calling it a "chlorophyll unit".[20] In 1936, Kohn concluded that the physical number of chlorophylls in a chlorophyll unit was closer to 500, a number consistent with the idea developed by Warburg and Negelein (1922) that four photons were required for the production of oxygen.[21,22] The controversy over the minimum quantum requirement for oxygen evolution and the opposing views of Warburg and Emerson were reviewed in a nice historical perspective by Nickelsen and Govindjee (2011)[23] and summarized by Kärin Hill and Govindjee (2014).[24] Also in 1936, Hans Gaffron and Kurt Wohl expanded on Emerson and Arnold's 1932 experiment, where exposure of a *Chlorella*

DOI: 10.1021/acs.chemrev.6b00002
Chem. Rev. XXXX, XXX, XXX−XXX

suspension to weak light immediately initiated the evolution of oxygen.[25] They determined that it would take one single chlorophyll molecule an average of 1 h to capture 4−12 photons, the number required for the evolution of one oxygen molecule.[26]

These observations forced Gaffron and Wohl to be the first to come up with the concept of quantum energy being transferred from one molecule to another. They envisioned a model where energy absorbed by pigment molecules anywhere in the unit (today termed the "photosynthetic unit") would be transferred and utilized efficiently at the center (today termed the "reaction center") where photochemistry would commence. Roderick Clayton (1965) later formulated this model in terms used today: "The pigment aggregate acts as an antenna, harvesting the energy of light quanta and delivering this energy to the reaction center".[27]

So, in terms of size, is there something special about 2400 Chl/oxygen evolution? Other studies confirmed even higher numbers, such as 3200−5000 in *Lemna* sp., in the moss *Selaginella* sp., and in the alga *Stichococcus bacillaris*, whereas Georg Schmid and Gaffron (1968) observed photosynthetic units of various approximate sizes (300, 600, 1200, 1800, 2400, and 5000) while conducting experiments on photosynthetic organisms under different physiological conditions.[20,28] These observations have provided clues, and in conjunction with further detailed biochemical and biophysical information, they form the physical basis for the photosynthetic unit (PSU) model of today.

The typical physical size of the PSU encompasses the two reaction centers of photosystems I and II (PSI and PSII, respectively), each associated with approximately 200−400 light-harvesting molecules (in higher plants and green algae). In their review "The Absolute Size of a Photosynthetic Unit", David Mauzerall and Elias Greenbaum (1989) highlighted the importance of this concept in the relationship between the size of the oxygen forming unit, the total chlorophyll per O_2 (the classical Emerson−Arnold unit), and the quantum requirement for O_2 formation.[29] They pointed out that a theoretical limit exists for the PSU size—the same limit as in a homogeneous antenna—that the mean time before trapping increases with the size of the antenna, owing to the random walk of the energy-transfer steps. However, modulation of the light-harvesting architecture through incorporation of pigments that absorb at higher energies, that is, shorter wavelengths of light (e.g., Chl *b*, phycobilins, carotenoids), adjacent to Chl *a* leads to directed downhill energy transfer and a considerably shorter time before trapping. The existence of pigment heterogeneity allows for the existence of larger PSUs that are still efficient.[30] Furthermore, determining the PSU size, in terms of the numbers and classes of the constituent pigments, is of great value for the elucidation of adaptive mechanisms of photosynthetic organisms in varied environments.[31]

The photosynthetic unit comprises numerous light-harvesting complexes that have diversified and optimized through evolution.[32] The mechanism of highly efficient energy capture—first light absorption, followed by rapid excitation energy transfer within light-harvesting antennas, culminating in trapping at the reaction-center chlorophylls—has fascinated biophysicists for a long time.[33,34] Elucidation of this challenging puzzle still continues today. Here, we examine the compositional and architectural arrangement of the main building blocks of the light-harvesting machineries that photosynthetic organisms utilize. The well-established foundations of electronic excitation energy transfer (EET) are described in this review, and the effects of the structural organization of light-harvesting pigments are also examined with respect to the efficient energy-transfer mechanisms that have evolved.

2. SPECTRAL COMPOSITION OF LIGHT AND THE PIGMENTS

Even though the intensity and spectral quality of light can be vastly different on temporal and spatial scales, the light-harvesting machinery of photosynthetic organisms has evolved adaptation mechanisms that allow these organisms to thrive in diverse environments.[35−37] For example, plant canopies provide a vertical gradient of sunlight, attenuating the intensity of visible light by a factor of up to 100 as it passes from the top of the canopy to the shade beneath (Figure 1a). For algae growing in oceans or lakes, water plays an important role in filtering specific wavelengths of light.[38,39] Short wavelengths of the visible light spectrum, such as blue and green, penetrate the water much farther than red light does. The turbidity of the water from particulate matter plays another important role in defining the depth profile of irradiance.[40] For example, downwelling irradiance can vary by orders of magnitude when comparing depth profiles in lakes, depending on the local conditions of dissolved organic matter and scattering particulates (e.g., humus from vegetation distinctly stains the water).[41]

Microbial mats present another interesting example of light penetration, but in this case, the light profile is controlled by the stratification of photosynthetic organisms.[42] In 2012, Zoee Perrine and co-workers[43] noted that, in general, light-harvesting antennas have developed to maximize light capture under both low- and high-intensity light conditions. However, that leads to the antenna size not being optimized for the achievement of the maximal apparent quantum efficiency, as poor kinetic coupling between fast photon capture and the slower downstream process of photosynthetic electron transfer leads to energy losses of up to 50%. A large antenna size might offer a competitive advantage in mixed cultures when competition for energy harvesting arises at low flux densities, but it might be redundant in monocultures where competition between different species is absent.[43]

Additionally, one needs to consider the variation in the efficiency with which different wavelengths of light are able to drive photosynthesis. The photosynthetic action spectrum (Figure 1b), a plot of a physiological activity such as oxygen evolution as a function of the wavelength of light, reveals the spectral region of light harvesting that is effective in photosynthesis.[44,45] Diversification and optimization of the light-harvesting machinery is essential to achieve short- and long-term adaptation under varying light conditions.

In all photosynthetic organisms, initial light absorption is performed by special pigments, which are chemically and structurally subdivided into three major groups: chlorophylls, carotenoids, and phycobilins (Figure 1c,d). In green plants, for example, the action spectrum of photosynthesis is only approximately in agreement with the absorption spectrum of chlorophylls and carotenoids and has prominent bands in the violet-blue and red regions of the spectrum. Two major differences are (1) lowered efficiency in the carotenoid region because of diminished efficiency of energy transfer from carotenoids to chlorophylls and (2) a red drop in efficiency even in the far-red end of the chlorophyll absorption.[46,47] The

DOI: 10.1021/acs.chemrev.6b00002
Chem. Rev. XXXX, XXX, XXX−XXX

reflection and/or transmission of the central part of the spectrum causes leaves to appear green.

One might wonder why plants evolved to reflect green light.[48] One suggestion is that chlorophyll absorption is complementary to that of bacteriorhodopsin, a purple chromophore that was employed as a light-driven proton pump in the earliest aquatic organisms (e.g., halobacteria), which relied on light-driven energy generation while inhabiting oceanic surface waters. Further, organisms that evolved later optimized their light-harvesting apparatus based on chlorophyll systems to maximize absorption of available sunlight after it was attenuated by bacteriorhodopsin. Electron transport mediated by metal porphyrins already existed before that in photosynthetic transport.[49] Mauzerall (1973)[50] and Björn et al. (2009)[51] have speculated that biosynthetic pathways for metal porphyrins and implementation of the existing precursor for the production of chlorins through porphyrins was a clear evolutionary advantage.

The optimal absorption wavelength range for the light-harvesting pigment has been suggested to be in the red region (680−690 nm), as chlorophylls utilize that part of the spectrum for the energy required to split water and to reduce ferredoxin.[52] The evolution of chlorophyll *a* as the most widely utilized photosynthetic pigment can be attributed perhaps to its efficient absorption of red light and also, perhaps, its chemistry (such as redox potential).[53,51] Particularly in land plants, for which light was abundant, there was an absence of evolutionary pressure to generate innovative light-harvesting architectures that would utilize other parts of the solar spectrum. See Björn and Govindjee (2015)[47] for a discussion of the evolution of photosynthesis.

The photosynthetic action spectra of cyanobacteria and red algae show strong activity in the blue-green region, attributed to the specific class of accessory pigments called phycobilins (Figure 1c).[54−56] Green light penetrates through great water depths, and utilization of green-light-absorbing pigments allows red algae and cyanobacteria to live at greater depths than organisms that primarily use chlorophyll, such as green algae and sea grasses, which tend to grow in shallow waters where the visible spectrum is similar to the spectrum of incident sunlight. However, all photosynthesis in these organisms occurs through chlorophyll *a*, because energy absorbed by phycobilins is transferred very efficiently to chlorophyll *a*.[57−59] Phycobiliproteins exhibit a high nitrogen content, and under conditions of limited nitrogen supply, their synthesis tends to be unfavorable. In cyanobacteria, rhodophytes, and cryptophytes, phycobiliproteins are selectively lost during nutrient stress conditions, because photosynthesis can function in the absence of phycobiliproteins but chlorophyll is essential not only for the light-harvesting apparatus but also for the reaction centers.[60−63] Consequently, for higher plants that grow on land under an abundance of sunlight, it is energetically inefficient to utilize phycobiliproteins for harvesting of green light. Thus, in the interest of energy conservation, higher plants, which are exposed to an abundance of light when growing on land, do not utilize phycobiliproteins for the capture of green light.[51] One reason why "red" carotenoids are not utilized is possibly that red carotenoids have their S_1 transition degenerate or even below the Chl lowest excitonic transitions, which would therefore quench the excited state of chlorophyll fluorescence and thus make light harvesting inefficient.

The variety of chromophores employed in light harvesting is considerably smaller than the enormous diversity of photosynthetic organisms that exists. Certainly, the types of LHC "designs" outnumber chromophore types by a lot. So what optimizations in their structure and function have led to the dominance of these pigments in light-harvesting systems? Chlorophyll molecules are based on a cyclic tetrapyrrole ring, chlorin, coordinated to a central atom, a structure very similar to that found in the heme group of hemoglobin, with the difference being that, in chlorophyll, magnesium is the central atom, whereas heme contains iron (Figure 1d). Attachment of different side chains to the chlorin ring allows for structural diversification of the chlorophyll family and production of chlorophylls (*a*, *b*, *c*, *d*, *e*, and *f*). The different side chains on the chlorophylls are responsible for tuning the absorption spectra of the pigment molecules.[67] Carotenoids, yellow-orange chromophores, exhibit a characteristic triple peak absorbance in the range of 400−500 nm, more or less coinciding with the B_X and B_Y Soret bands of chlorophyll.

Carotenes occur naturally in a number of isomeric forms; α-carotene and β-carotene are the primary isomers, differing only in the position of the double bonds in the cyclic group at the end of the molecule (Figure 1d). Phycobilins are linear open-chain tetrapyrroles that bear a resemblance to a porphyrin that has been split open (Figure 1d). Photosynthetic pigments are cyclic or linear examples of conjugated π-electron systems with exceptional molar extinction coefficients, $\sim 10^5$ M^{-1} cm^{-1}. The scaling laws for linear chromophores, such as carotenoids and π-conjugated polymers, predict that the dipole strength of their lowest allowed electronic transition will depend on the length squared.[68] However, the scaling plateaus at lengths of about 10−15 double bonds are due to effects such as conformational disorder that twists bonds and breaks conjugation.[69]

Up to this point, we have treated pigment chromophores only as individual entities characterized by a large absorption strength, but in the following sections, we reveal that their synergetic interactions as constituent elements of light-harvesting machineries play a crucial role. They have clearly different biochemical and biophysical properties when they are associated with different amino acids within specific proteins.[70]

The path toward realization of artificial light-harvesting model systems has, thus far, faced two major challenges: synthesis of well-suited chromophores and construction of the scaffolding that would avoid the difficulties of assembling large numbers of integral pigment molecules. Recently, a synergetic combination of bioinspired and synthetic building blocks led to the development of a series of multichromophore biohybrid complexes that can be utilized in the realization of multifunctional light-harvesting assemblies.[71,72] The rationale for the design of these biohybrid architectures is to overcome limitations faced by synthetic chemists, as it is an extremely challenging task to fabricate a framework structure that would allow for an organized assembly of a large number of pigment molecules. The model is based on creating a framework from native photosynthetic peptide analogues. The native chromophores, bacteriochlorophylls and their derivatives, on the other hand, have often limited synthetic malleability. However, recently developed bacteriochlorins exhibit good stability, and their structural tailoring enables wavelength tuning, giving these structures an advantage over naturally occurring systems that face limitations in terms of the extent of spectral coverage.[72]

Through static and time-resolved optical studies on these oligomeric biohybrid antenna, Reddy et al. (2013)[71] observed efficient (90%) excitation energy transfer from the attached bacteriochlorin to the BChl *a* target.

DOI: 10.1021/acs.chemrev.6b00002
Chem. Rev. XXXX, XXX, XXX−XXX

Realization of artificial photosynthetic model systems is contingent on the awareness that the role of constituent pigment molecules in these large light-harvesting assemblies is manifold, as they can act as initial light absorbers, efficient energy conduits, or facilitators of charge separation. Furthermore, the photophysical properties and spectral features of pigment molecules within these light-harvesting assemblies is highly affected by the synergetic interactions of all of the constituent elements. Some aspects of the photophysics governing these constraints are discussed in the following sections.

In summary, the main pigment groups are chlorophylls, carotenoids, and phycobilins. Pigments are examples of conjugated π-electron systems and have exceptionally high molar extinction coefficients ($\sim 1 \times 10^5$ M^{-1} cm^{-1}).

3. LIGHT-HARVESTING SYSTEMS AND THEIR EFFICIENCY

Pigments in pigment−protein (antenna) complexes, usually called light-harvesting complexes (LHCs), are responsible for most of the absorption of sunlight. Excitation energy is subsequently funnelled, first among the other surrounding molecules of the same complex, then from one light-harvesting complex to another before being trapped at a photochemical reaction center (RC), where it is converted into a charge separated state with >90% quantum efficiency.[73]

Although many measurements of photosynthetic quantum yield, or the efficiency of energy conversion, are available, we stress the importance of the measurement techniques and conditions when comparing the values reported in different ecophysiological studies.[74] In early days, evaluation of absolute quantum efficiency was most often performed on intact algae or bacteria, but the respiratory activity complicated those investigations of the primary photochemical act.[75] Usually, the internal (intrinsic) quantum efficiency of the primary reactions of photosynthesis is close to unity when one compares the percentage of absorbed photons converted to charge carriers.[76] The absolute quantum yield of primary photochemistry, measured in the reaction centers of *Rhodopseudomonas sphaeroides*[73,77] and *Rhodospirillum rubrum*,[78] has been found to be near unity. Further, measurements on singlet−singlet energy transfer from carotenoid to BChl in LH2 showed typical efficiencies ranging from 50% to 100%, with a strong dependence on both the type of carotenoid(s) and the type of LH complex. In *Rhodopseudomonas* (*Rps.*) *acidophila* [now *Rhodobastus* (*Rbl.*) *acidophilus*] LH2, carotenoid to BChl energy transfer is about 55% efficient,[79] whereas in *Rhodobacter* (*Rb.*) *sphaeroides* 2.4.1 LH2, it is about 95% efficient.[80]

Wientjes et al. (2012)[81] determined the PSII efficiency in *Arabidopsis thaliana* by studying the thylakoid membrane of the plant under varying light conditions. In high light, the plant had a smaller PSII antenna size and an efficiency of 91%, whereas an increase of the antenna size in low light led to an increase in the absorption cross section but at the cost of a lowered PSII efficiency (84%). Time-resolved Chl *a* fluorescence experiments yielded higher values of quantum efficiency than those obtained from the ratio of the variable to maximum Chl fluorescence, F_v/F_m (~80%), a parameter that is widely used to indicate the PSII quantum efficiency.[81] (Note: $F_v = F_m - F_o$, where F_o is the minimal fluorescence.)

In the case of green sulfur bacteria, the energy from absorbed photons is transferred down an energy gradient from BChl *c* (absorbing at 742 nm) in the chlorosome antenna, to BChl *a* (absorbing at 792 nm) in the chlorosome baseplate, through the membrane-bound Fenna−Matthews−Olson (FMO) complex (BChl *a*, ~805 nm), before finally reaching the reaction center (BChl *a*, ~865 nm).[82] The energy transfer from BChl *c* to the BChl *a* component of the chlorosomes occurs with an efficiency of about 55%, whereas the energy transfer within the pigment−protein complex proceeds with an efficiency close to 100%.[83,84] For the determination of the overall efficiency in the baseplate and the reaction-center environment of the Fenna−Matthews−Olson (FMO) protein, which connects the outer antenna system (chlorosome/baseplate) with the reaction-center complex in green sulfur bacteria, much more detailed structural information is needed.[85] On the other hand, in red algae, such as *Porphyridium cruentum*, the efficiency of energy transfer from the phycobiliproteins to chlorophyll *a* is higher than 80−90% .[56,57,86]

The reason for the development of an elaborate energy-collecting system is that the reaction-center chlorophylls (present in 1 of ~300 antenna molecules) cannot absorb sunlight at a rate anywhere near high enough for efficient photosynthesis to occur. [See its first discussion by Gaffron and Wohl (1936), where the concepts of "antenna" and "reaction center" were born.[25]] The inefficiency of the system is due to the fact that chlorophyll molecules absorb only a few photons each second, which would be completely insufficient to drive the multielectron process of photosynthesis if only reaction centers were found in the membrane.[25] The solution to the shortcoming of independently functioning reaction centers is the association of intricate antenna pigment−protein assemblies, light-harvesting complexes, with reaction centers. These proteins associate approximately 100−800 additional chlorophylls (or other pigments) with each reaction center.[29] Electronic excitation resulting from the absorption of sunlight by pigments in light-harvesting complexes is transferred very efficiently to reactions centers, thus increasing their effective absorption cross section. Light-harvesting complexes are vital for photosynthetic organisms in that they ensure, through a combination an increase in effective absorption and regulation, a steady supply of excitation to each reaction center.[2,69,87]

The diversity in antenna systems is remarkable, differing in the number of pigments they associate and their composition and structural organization at the nanoscale, in addition to the location relative to the reaction center, emphasizing the importance and necessity of the light-gathering mechanism in photosynthesis. The existence of such a variety is also suggestive of independent evolutionary origins that have led to the development of optimized multichromophoric energy collector systems. Specific examples will be examined in later sections, with a more focused look at the antenna complexes of purple bacteria such as *Rhodobastus* (*Rbl.*) *acidophilus*, which is a model case for studying the physical principles that govern light absorption and energy transfer.[88]

The sites in which key photosynthetic processes, including light harvesting, subsequent charge separation, and electron transport, occur are multifunctional membrane systems, which vary greatly both in their architecture and composition. In green sulfur bacteria, the antenna complexes, chlorosomes, are associated with the plasma membrane, whereas purple phototrophic bacteria have intracytoplasmic membranes.[14,89] Cyanobacteria are quite different from these anoxygenic bacteria in that their membrane system comprises stacks of parallel sheets of thylakoids, which are closely positioned to the cytoplasmic membrane.[13,14,90,91] Other photosynthetic organ-

DOI: 10.1021/acs.chemrev.6b00002
Chem. Rev. XXXX, XXX, XXX−XXX

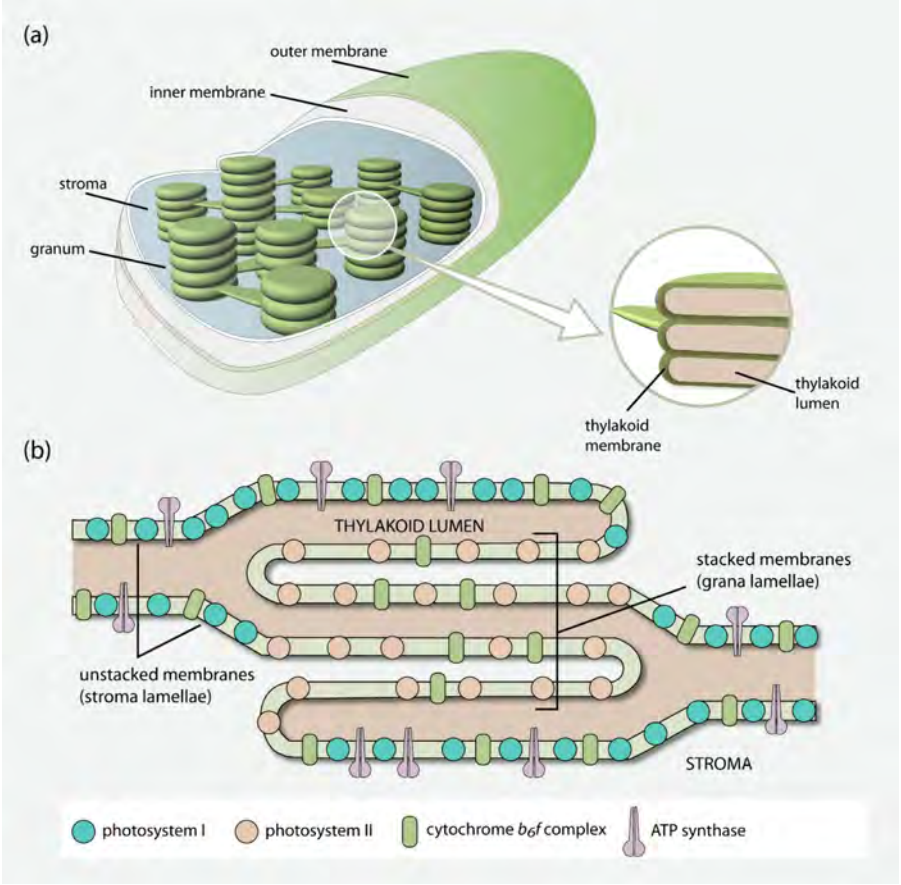

Figure 2. (a) Schematic representation of a chloroplast, where the flattened thylakoids are stacked into grana. (b) Spatial distribution of complexes embedded in the thylakoid membrane.

isms, such as algae and plants, house their light-harvesting machinery and carry out photosynthesis in organelles called chloroplasts. The schematic in Figure 2a illustrates the double-membrane encapsulating stroma, which contains numerous enzymes involved in carbon fixation. The internal membranes, thylakoids, fold into disklike stacks called grana.

The spatial distribution of pigment clusters is shown in Figure 2b, where we note that these molecular components are not arranged randomly. The significance of their relative position lies in the optimization of the energy- and electron-transfer efficiency. Enhancement of photosynthetic plasticity is achieved by enabling the protein components to redistribute dynamically, thereby allowing the vital self-protective and repair processes to be performed.[92] These dynamics play a fundamental role in the adaptability of photosynthetic organisms to different environments, where long-term acclimation is based on the compositional alteration of the photosynthetic membrane, whereas short-term adaptation requires reorganization of existing protein components.[93]

4. PHYSICAL PRINCIPLES OF ANTENNA ARCHITECTURE

Remarkable variations exist in architectures of light-harvesting antenna structures, but there are also parallels in the physical principles leading to the construction of chromophore assemblies (Scheme 2).[94,95]

Most antenna systems have architectures based on pigment–protein complexes, where the precise position, mutual separation, and relative orientation of light-harvesting pigment molecules is determined by their association with the protein backbone.

James Franck and Edward Teller, in their original 1938 PSU model, assumed that exciton migration occurred by Förster energy transfer (dipole–dipole interaction; section 5) along a one-dimensional chlorophyll crystal before reaching the photochemical site at the end.[96] However, the energy-transfer times extracted from the one-dimensional model were not compatible with the observed fluorescence yields, leading to Franck and Teller's (erroneous) conclusion that "the existence of the photosynthetic unit is improbable".[96]

As details about the thylakoid structure in chloroplasts emerged, researchers were encouraged to investigate two- and three-dimensional model structures, which would allow for a larger number of pathways and would thus greatly speed up the process.[97−99] Figure 3 illustrates the clear advantage that three-dimensional models have over one-dimensional arrangements. Random-walk properties suggest that, for an equal ratio of traps and donors, energy-transfer efficiency between two distant chromophores will be much smaller in one-dimensional models than in two- or three-dimensional systems.

In the 1960s, a statistical approach to describe exciton trapping in photosynthetic units was developed based on a model of an infinite periodic lattice of unit cells, each composed of N points of which one is a trap and the other $(N - 1)$ are represented by chlorophyll molecules.[100−104] In this model, excitation-transfer steps are allowed only between nearest-neighbor lattice points, while the probability of carrying the excitation was equal for all nontrapping chlorophylls.

DOI: 10.1021/acs.chemrev.6b00002
Chem. Rev. XXXX, XXX, XXX−XXX

Scheme 2. Schematic Illustration of Light-Harvesting Architectures of Various Classes of Photosynthetic Organisms[a]

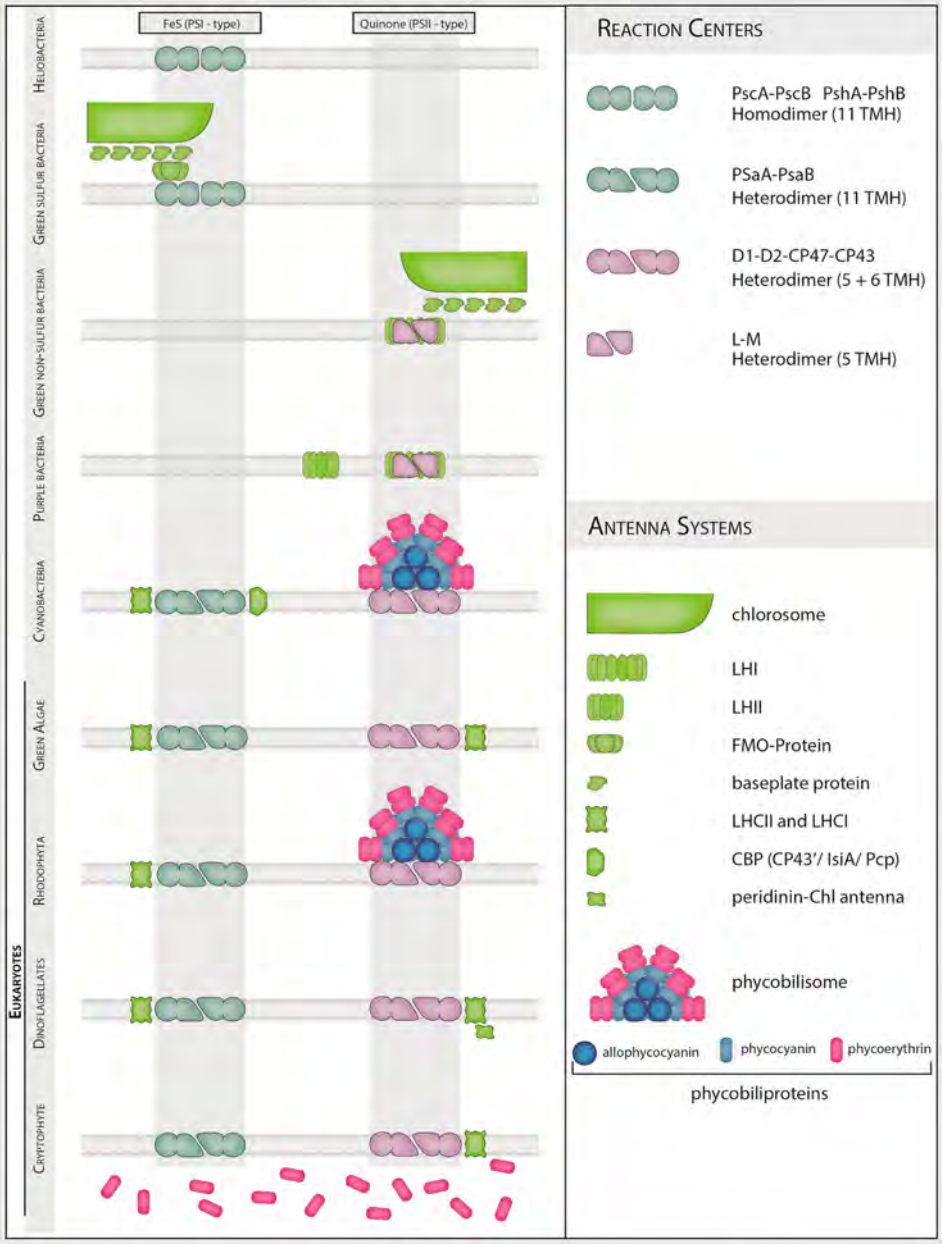

[a]Adapted with permission from ref 37. Copyright 2015 Springer.

Expressions were derived for an infinite lattice (i.e., as $N \rightarrow \infty$) for the required number of steps, n, to arrive at the trap

$$\langle n \rangle = \begin{cases} N^2/6 & \text{linear chain} \\ \pi^{-1} N \log N & \text{square lattice} \\ 1.5164N & \text{single cubic lattice} \end{cases} \quad (1)$$

For example, applications of eq 1 in conjunction with fluorescence decay data enabled the estimation of the single-step transfer time between communicating Chl molecules in PSI of the green alga *Chlamydornonas reinhardii*.[105] Physiological data indicated the presence of 220 chlorophyll molecules, but fluorescence decay data suggested that only 50.3% of the 220 Chl molecules actually transfer their absorbed excitation to PSI, so that the average number of steps required to reach the trapping center, $\langle n \rangle$, for a value of N = 111 (i.e., 0.503 × 220) is 167 steps (assuming a cubic lattice model). Consequently, the lifetime for trapping (53 ps) divided by the number of steps (167) yields a single-step transfer time of 317 fs.[105]

The classical random-walk model can be biased if one introduces a downhill energetic landscape into the chromophore ordering and effectively constructs an energy funnel in

DOI: 10.1021/acs.chemrev.6b00002
Chem. Rev. XXXX, XXX, XXX−XXX

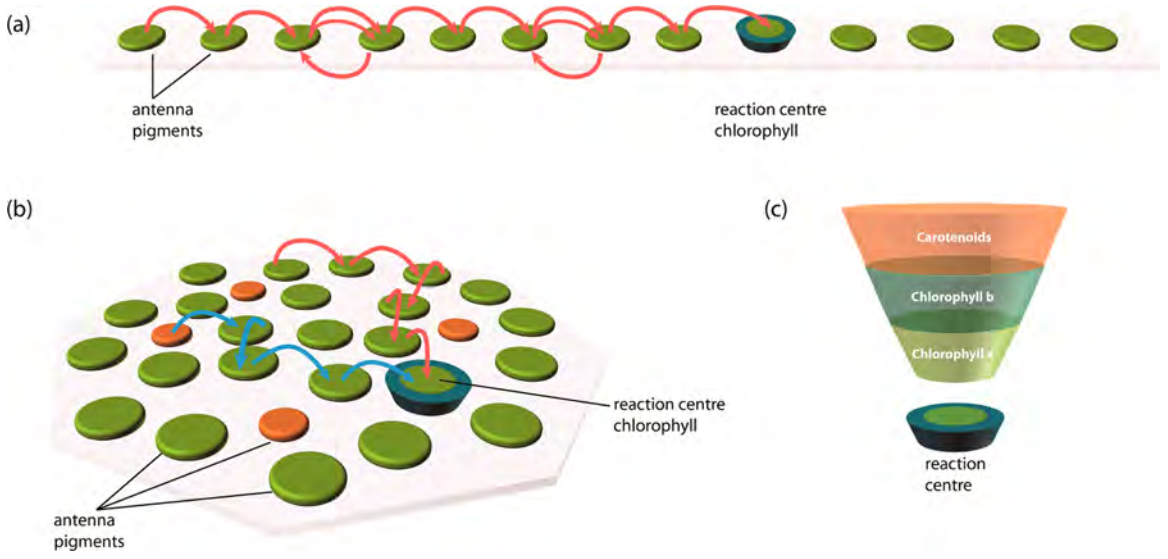

Figure 3. Schematic depicting excitation-transfer pathways in models where chromophores are arranged in (a) a linear (one-dimensional) format and (b) a two-dimensional planar distribution. The inefficiency of the one-dimensional model compared to the two-dimensional arrangement is manifested in the larger number of steps needed for energy transfer to the reaction center. (c) Energy collection in an antenna system depicted as an energy funnel. Shorter wavelengths of light are absorbed by peripheral antenna complexes, followed by energy-transfer processes to the lower-energy pigments located closer to the reaction center.[66] Adapted with permission from ref 37. Copyright 2015 Springer.

which high-energy chromophores (i.e., those absorbing on the blue side of the spectrum) transfer excitation energy to more red-shifted (lower-energy) chromophores (Figure 3c). The overlap of the spatial and energetic landscapes in energy-funnel models ensures that energy is transferred "downhill" from the periphery to the reaction center, with a small energy loss in the form of heat associated with each step. Although energetically costly, the justification for the integrated irreversibility is that one ensures that the excitation energy is concentrated at the reaction center. Control over the different steps in the funnel can also be achieved by modulating the energy differences between the constituent pigments and, thereby, changing the slope of the "funnel". An example of this phenomenon is discussed in more detail in section 11, highlighting the ability of some purple bacteria to implement accessory pigments that absorb at 820 nm instead of the usual 850 nm, thereby increasing the slope of the funnel and preventing back transfer. This alteration in the energy-transfer apparatus allows these species to grow under lower-light conditions than their competitors who cannot realize this modification.

The basic elementary unit of the light-harvesting apparatus of photosynthetic cells is a photosynthetic unit (PSU), a complex composed of a large number of antenna chromophores coupled to a reaction center. PSUs are characterized by the ratio of antenna pigments to reaction-center complexes. Theoretically, energy migration has been modeled either through a random-walk process, where all pigments are considered individual entities, or by focusing only on interactions between defined elementary units.[106,107] Microscopic models with a high degree of sophistication and a large number of parameters, including structural details, relative distances, and orientations between pigment molecules, would be required to precisely model the interactions of N interacting pigments. The introduction of simplifying assumptions, such as infinitely fast energy transfer within elementary units or isoenergetic antenna chromophores, can aid in the reduction of the complexity of these microscopic models. This type of global approach was discussed in 1999 by Kay Bernhardt and Hawi Trissl when they contrasted so-called "lake" and "puddle" assemblies (Figure 4).[108] In the puddle model, the separate units do not interact mutually, and the

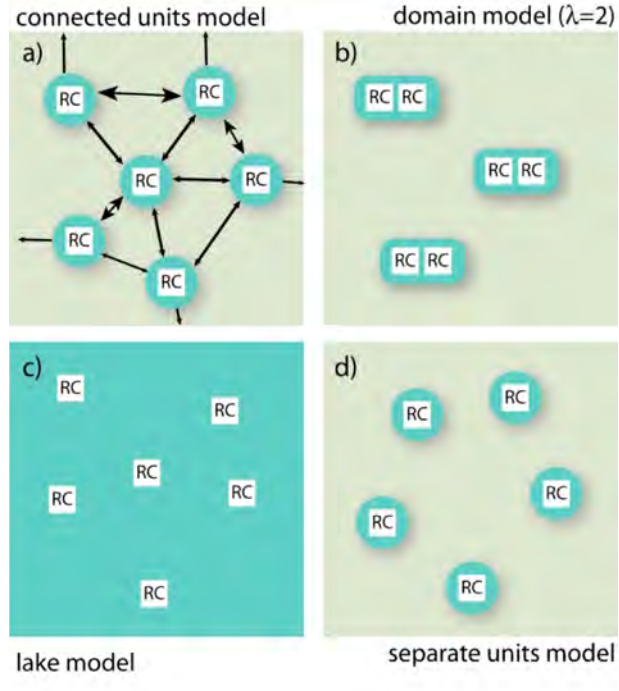

Figure 4. Models of antenna organization: (a) "connected units model", where all reaction centers are connected to each other; (b) "domain model", where two reaction centers are close to each other but the groups of two are not connected to each other; (c) "lake model", characterized by perfect connectivity where energy moves freely between constituent units; and (d) "puddle model" (or separate units model), an extreme case in which excitation energy absorbed by antenna chromophores is always transferred to the same reaction centers. Adapted with permission from ref 108. Copyright 1999 Elsevier.

DOI: 10.1021/acs.chemrev.6b00002
Chem. Rev. XXXX, XXX, XXX−XXX

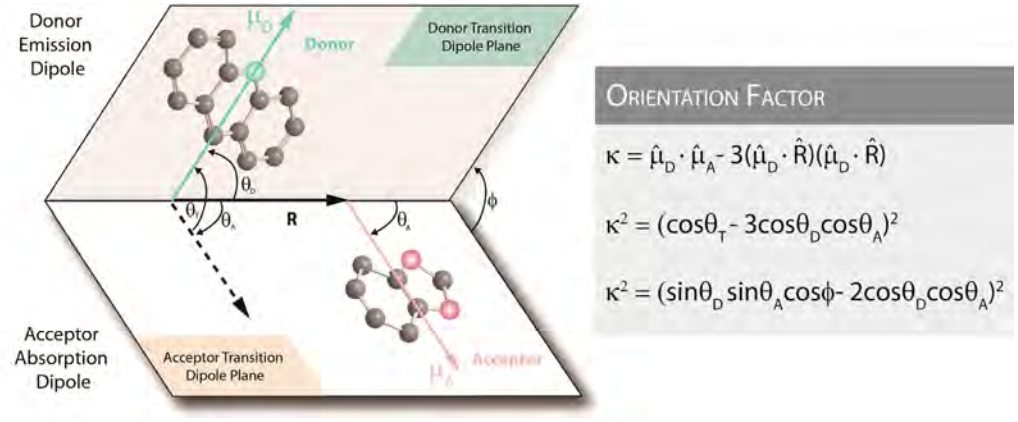

Figure 5. Depiction of angles and vectors relevant to the calculation of the orientation factor, κ. $\hat{\mu}_D$ and $\hat{\mu}_A$ are the transition-dipole-moment unit vectors of the donor and acceptor, respectively, and $\hat{R}$ is the center-to-center separation vector.

excitation energy absorbed by antenna chromophores is always transferred to the same reaction center within the specific photosynthetic unit. The lake model allows for unrestricted exciton transfer as antenna chromophores form a matrix with embedded reaction centers (Figure 4c).[103] In the latter model, which is often used for PSII and purple bacteria, excitation energy can visit multiple reaction centers before eventually being trapped at a reaction-center complex that is open for photochemistry.[2,109−111]

Most photosynthetic organisms fall somewhere between the two extremes in terms of their antenna organizations and the degree of connectivity between different PSUs. The basic properties of such an intermediate case were first suggested within the framework of the "connected units model" developed by Pierre Joliot and Anne Joliot (1964). In this model, a partial connectivity between puddles exists, but energy transfer among pigments within a specific puddle is more probable than energy transfer between chromophores located in distinct puddles.[112] Alternatively, limited excitation transfer can be taken into account by dividing the photosynthetic membrane into domains (mini-lakes) comprising clusters of photosynthetic units. The domain model allows for unrestricted excitation migration within a domain but restricts exciton exchange between the separate units.[113,114] This model is well-suited for scenarios in which dimeric aggregation of reaction centers exist, as in the case of the chlorosome antenna complex of green photosynthetic bacteria.[2,108]

Today, our understanding of the structure and function of PSUs has become much more sophisticated through information obtained from studies employing statistical models of PSUs in conjunction with a number of fluorescence techniques. Elucidation of structural details of a number of light-harvesting complexes through high-resolution crystallography has fueled the generation of more sophisticated energy-transfer models.[115−118] Even models that contain chromophore−protein interactions treated with atomistic detail have recently been reported.[119−122] See the basic discussion by Amarnath et al. (2016)[123] and the review by Stirbet (2013).[124]

In summary, light-harvesting antennas exhibit a large variation in the architectural assembly of their constituent chromophores. Pigment−protein associations allow for control over the separation and mutual orientation of light-harvesting molecules. Spatially, a three-dimensional arrangement of chromophores is statistically preferred for efficient energy transfer. The principle of an energy funnel biases the random walk but contributes to the irreversibility of the concentration of energy at the reaction center. Variations in the models of antenna organization are based on photosynthetic units (PSUs) on the macroscopic level. High-resolution crystal structures and models with atomistic details allow for sophisticated models of energy transfer on a microscopic level.

5. MECHANISM OF FÖRSTER EXCITATION ENERGY TRANSFER

During 1927−1929, Jean Perrin and Francis Perrin observed energy transfer as they researched fluorescence quenching of fluorophores in solution.[125−127] They noted that molecules in solution could interact without collisions and at distances exceeding their molecular diameters. It was then postulated that this observed phenomenon, which leads to electronic energy transfer, derives from an inductive resonance interaction between transition dipole moments of the molecules. In other words, the semiclassical oscillation of the electrons on the donor, during de-excitation, induces oscillations of the acceptor electrons, causing electronic excitation. This interaction is a Coulombic dipole−dipole interaction, which varies as the inverse of the cube of the center-to-center intermolecular distance between donor and acceptor. It can thus be effective at distances on the order of several nanometers.

The semiclassical idea of a classical inductive resonance that transfers energy from donor to acceptor in the same way as mechanical energy can be transferred among oscillators is conceptually appealing. Classical analogues are well-known in classical mechanics, such as the transfer of oscillations from one tuning fork to another by mechanical coupling of the tuning forks to sound waves through the intervening medium (air). Technically, however, the coupling V is a quantum mechanical interaction between the reactant wave function $|\psi_{D,excited}\psi_{A,ground}\rangle$ and the product wave function $|\psi_{D,ground}\psi_{A,excited}\rangle$, where D and A stand for donor and acceptor, respectively. In shorthand, we can write these wave functions equivalently as $|D'A\rangle$ and $|DA'\rangle$. These wave functions are written as product states of one excited-state molecule (initially D) and a ground-state molecule (initially A). Physically, what one need to ascertain is the interaction that causes de-excitation of the donor, $D' \rightarrow D$, synchronously with excitation of the acceptor, $A \rightarrow A'$. This picture is worth keeping in mind because it indicates that, to understand energy transfer, one must explicitly include four electronic states in the

DOI: 10.1021/acs.chemrev.6b00002
Chem. Rev. XXXX, XXX, XXX−XXX

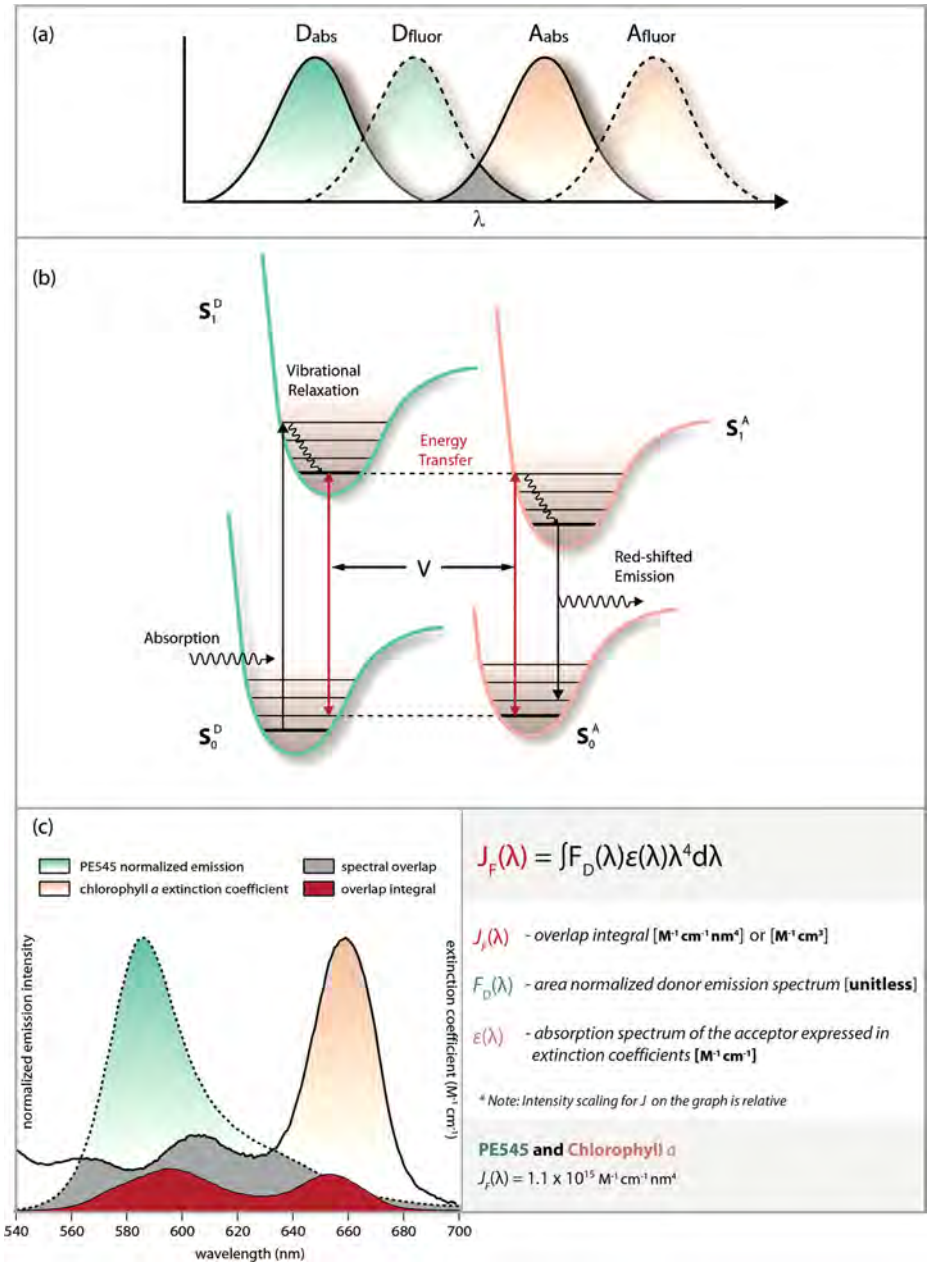

Figure 6. (a) Spectral overlap of the emission spectrum of the donor and the absorption spectrum of the acceptor, a requirement for FRET. (b) S_0^D is the ground state of the donor, S_1^D is the excited singlet state of the donor, S_0^A is the ground state of the acceptor, and S_1^A is the excited singlet state of the acceptor. Light is initially absorbed by the donor, which then undergoes radiationless decay to the lowest excited state. De-excitation is achieved through spontaneous emission or nonradiative energy transfer to a suitable acceptor, resulting in a further red shift of the emission. (c) Illustration of the spectral overlap and the calculated overlap integral for an acceptor (chlorophyll *a*)/donor [phycoerythrin 545 (PE545)] pair. Adapted with permission from ref 37. Copyright 2015 Springer.

model: the ground and excited states of each of the chromophores.[128]

The coupling that promotes excitation to jump from donor to acceptor is primarily a Coulombic interaction between "transition densities" (vide infra).[129] In the dipole approximation, the interaction potential between these transition densities is expanded as an infinite sum of transition multipole−multipole interactions.[130] As long as the donor and acceptor molecules are widely separated compared to their physical size, one can simply take the first (leading) term of this expansion, which is the transition dipole−dipole interaction

$$V = \frac{1}{4\pi\varepsilon_0}\left[\frac{\vec{\mu}_D\cdot\vec{\mu}_A}{R^3} - \frac{3(\vec{\mu}_D\cdot\vec{R})(\vec{\mu}_A\cdot\vec{R})}{R^5}\right] \equiv \frac{1}{4\pi\varepsilon_0}\frac{\kappa|\vec{\mu}_D||\vec{\mu}_A|}{R^3} \quad (2)$$

Here, $\vec{\mu}_D$ and $\vec{\mu}_A$ are the transition dipole moments (SI units of the coulomb-meter) of the donor and acceptor, respectively, and R is the center-to-center separation between the donor and acceptor molecules. The orientation factor, κ, is given by

$$\kappa = \hat{\mu}_D\cdot\hat{\mu}_A - 3(\hat{\mu}_D\cdot\hat{R})(\hat{\mu}_A\cdot\hat{R}) \quad (3)$$

where $\hat{\mu}_D$ and $\hat{\mu}_A$ represent unit vectors of the donor and acceptor, respectively, in the direction of the appropriate

DOI: 10.1021/acs.chemrev.6b00002
Chem. Rev. XXXX, XXX, XXX−XXX

transition dipole moment and $\hat{R}$ is their mutual displacement unit vector pointing from D to A. The schematic in Figure 5 illustrates the vectors and angles relevant to the orientation factor, and the following expression describes the dependence of the orientation factor on the relative orientation between the donor and acceptor transition-dipole-moment vectors

$$\kappa^2 = (\cos\theta_T - 3\cos\theta_D \cos\theta_A)^2 = (\sin\theta_D \sin\theta_A \cos\phi - 2\cos\theta_D \cos\theta_A)^2 \quad (4)$$

When the orientations of D and A are independent and random, either dynamically or in the ensemble average, the isotropic average of the dipole orientation factor equals $^2/_3$. In photosynthetic light harvesting, transition dipoles have fixed relative positions, in which case κ^2 can range from 0 to 4. For a detailed discussion of κ^2, see van der Meer.[131]

In 1946, Theodor Förster provided a notable advance by relating the predicted energy-transfer rate to the spectra of the donor and acceptor molecules. He first became interested in the subject following the realization that, in photosynthesis, the efficiency of energy collection is much greater than if one assumes that reaction centers are responsible for direct photon capture. Förster's "hopping" energy-transfer mechanism described this process of exciton migration as a kind of random walk in which a series of energy-transfer steps shuttle the excitation from chromophore to chromophore. Each hop is induced by the weak point-dipole−point-dipole interaction between chromophore transition dipole moments.

Förster first showed that the rate of energy transfer ($k^{\text{Förster}}$) between a donor and acceptor chromophore is determined by several parameters: the donor lifetime (τ_D), the quantum yield of the donor fluorescence (ϕ_D), the interchromophore distance R (cm), the relative orientation of the donor−acceptor pair (κ) (Figure 5), and the overlap integral (J_F) (Figure 6c). The rate is expressed as

$$k^{\text{Förster}} = \frac{1}{\tau_D} \frac{9(\ln 10)\kappa^2 \phi_D J_F}{128\pi^5 N_A n^4} \frac{1}{R^6} \quad (5)$$

where n is the medium index of refraction and N_A is Avogadro's number.[132] The Förster spectral overlap (J_F) (M^{-1} cm^3 or M^{-1} cm^{-1} nm^4) measures the overlap of the donor emission spectrum and the acceptor absorption spectrum and ensures energy conservation. The expression for J_F is a function of the area-normalized spectrum of the donor emission, $F_D(\lambda)$, and $\varepsilon_A(\lambda)$, the extinction coefficient spectrum of the acceptor in units of M^{-1} cm^{-1}

$$J_F = \int_0^\infty F_D(\lambda)\, \varepsilon_A(\lambda)\lambda^4\, d\lambda \quad (6)$$

An example of Förster overlap $J_F(\lambda)$ is illustrated in Figure 6c for an acceptor (chlorophyll a)/donor [phycoerythrin 545 (PE545)] pair. The two y axes on the plot represent the spectral intensities of the donor and acceptor, and thus, the scaling for J_F in the graph is arbitrary.

In Förster theory, energy conservation is determined by the overlap of the fluorescence spectrum of the donor and the absorption spectrum of the acceptor. Part of the electronic coupling (the quantum mechanical inductive resonance interaction) comes from the magnitude of the donor transition dipole moment and is provided by the radiative rate of fluorescence, $k_{rad} = \phi_D/\tau_D \propto |\mu_D|^2$, where ϕ_D is the fluorescence quantum yield, τ_D is the fluorescence lifetime. and μ_D is the transition dipole moment of the donor. The magnitude of the acceptor dipole moment is encoded in the molar extinction of the acceptor absorption spectrum. Deconvolving the required information from the experimental spectra and discarding information that is not needed for the energy-transfer theory is what clutters Förster's equation with so many constants. See references by Silvia Braslavsky et al. (2008)[132] and Robert Knox and Herbert van Amerongen (2002)[133] for further details on this matter.

Förster realized that spectral line broadening for molecules in solution leads to phase decoherence before incoherent excitation energy transfer occurs.[134] This means that a model based on the Fermi golden rule rate expression is sufficient. In that framework, the rate of energy transfer scales as the square of the electronic coupling. Hence, the $1/R^3$ distance dependence of the dipole−dipole interaction translates to a $1/R^6$ distance dependence for the rate of energy transfer.

To conserve energy during the excitation transfer from donor to acceptor, the fluorescence emission spectrum of the donor molecule should overlap to some degree with the absorption spectrum of the acceptor molecule, illustrated by the gray area in Figure 6a. This is the basis of Förster's famous spectral overlap integral. The larger the spectral overlap, the higher the energy-transfer rate. Notably, the spectral overlap integral depends not only on the donor fluorescence being coincident with frequencies at which the acceptor can absorb light, but also on the line broadening.[135] Details on how and why spectral lines are broadened can be neglected in Förster theory; however, they can be important for the understanding of the modern, more advanced treatments of coherent energy transfer.[136,137] We do not discuss the topic here, but some background reading on line broadening can be found in articles by Clegg et al. (2010)[33] and Fleming and Cho (1996)[138] and in section 2 of the article by Oh et al. (2011),[139] as well as the references cited therein.

At low temperature, spectral overlap can be much smaller, as molecules in the gas phase have very sharp vibronic transitions and, therefore, need to be close to degenerate to overlap. Nevertheless, by examining a schematic diagram of the donor and acceptor vibronic transitions in the gas phase (Figure 6b), one can see most clearly an important aspect of Förster's theory. That is, vibronic progressions in the donor fluorescence spectrum and acceptor absorption spectrum provide important contributions to the spectral overlap (energy conservation during energy transfer), especially when the two chromophores are different. The Förster spectral overlap sums over possible combinations of these energy-conserving coupled transitions. This vibronic overlap is a powerful attribute of Förster theory that is often neglected in contemporary theories. Indeed, it is because of this aspect that Förster theory remains one of the foremost quantitatively predictive theories.

The sensitivity of the rate of energy transfer and the critical distance range also correspond to a number of biologically significant dimensions, including the thickness of cell membranes and the separations between chromophore sites on different protein subunits. Therefore, EET measurements can be employed as an effective molecular ruler, resolving the spatial relationships between molecules, as it is capable of quantitatively determining distances between chromophores (10−100 Å), thereby providing more insight into the structural and dynamic aspects of macromolecules.[140−142]

DOI: 10.1021/acs.chemrev.6b00002
Chem. Rev. XXXX, XXX, XXX−XXX

6. BEYOND FÖRSTER THEORY OF EXCITATION ENERGY TRANSFER

Despite the general success of conventional Förster theory, especially for predicting energy transfer from phycocyanins to chlorophyll *a* in cyanobacteria and elsewhere, it can provide a complete description of energy transfer for only a few cases of photosynthetic light-harvesting complexes. Typically, light-harvesting antenna structures contain chromophores at very high concentrations, reaching levels of up to 0.6 M in some pigment−protein assemblies. Interchromophoric distance between neighboring chlorophyll molecules in light-harvesting systems can vary between 5 and 20 Å, consequently resulting in variations in the strength of intermolecular coupling, which directly influences the quantum mechanical nature of the energy-transfer mechanism. This has inspired advances that have extended Förster's original theory.[115,117,136,143,144]

Four principle modifications to the energy-transfer theories are needed to predict energy transfer in light-harvesting complexes.

First, electronic coupling must be calculated without invoking the dipole approximation, because of the close intermolecular separation mentioned previously. Second, solvent screening of the electronic coupling needs to be reconsidered hand-in-hand while dealing with a breakdown in the dipole−dipole approximation.[122,145] Third, the presence and role of molecular exciton states as excitation donors and acceptors needs to be considered. Typically, the generalized Förster theory (GFT) or the modified Redfield theory are employed to do this.[115,146−149] We introduce GFT in a section below after describing molecular excitons. Fourth, quantum-mechanical corrections need to be introduced into energy-transfer dynamics to account for coherence effects.[136,144,150−152] In models beyond Förster theory, it is essential to know and account for details about the bath, especially the time scales of fluctuations that produce line broadening—and correlations of these fluctuations. Emphasizing this point was an important contribution of Akito Ishizaki and Graham Fleming (2009), who introduced the hierarchical equations of motion (HEOM) approach for calculating energy-transfer dynamics.[153] The HEOM method provides an accurate prediction of the dynamics of a reduced system coupled to a quantum bath, regardless of the relative strength of electronic coupling and coupling of the system to the bath (i.e., the intermediate coupling regime). It takes advantage of the Gaussian property of the phonon operators in the exciton−phonon interaction Hamiltonian. This approach has been highly useful for many cases.[136]

6.1. Electronic Coupling and Orbital Overlap

In photosynthetic light harvesting, energy-transfer processes can be driven by different interaction mechanisms: the long-range dipole−dipole Coulombic interactions (electrodynamic interactions[154]), V^{ed}, and interactions due to intermolecular orbital overlap, V^{ioo}, which operate at short range and become critical at distances of less than 5 Å..[135,155] The coupling term, V^{total}, is defined as the sum of the long-range and short-range contributions, which is worth emphasizing because it is often misunderstood that the dipole−dipole mechanism (V^{ed} term) and the Dexter mechanism (V^{ioo} term) are mutually exclusive[128]

$$V^{total} = V^{ed} + V^{ioo} \tag{7}$$

The electronic coupling is strongly influenced by interchromophore orbital overlap effects at small intermolecular distances. For example, these effects play an important role when transitions involving simultaneous donor de-excitation and acceptor excitation are spin-forbidden.[156] In photosynthesis, processes that are mediated by V^{ioo} include triplet−triplet energy transfer, as well as the chlorophyll-sensitized generation of singlet oxygen. This topic is described later in this review.

In molecular systems, the part of the electronic coupling that depends on orbital overlap, V^{ioo}, comes from the fact that electrons are not definitively associated with a particular molecule when orbitals overlap. It is most convenient to include this effect by rendering the model for the reactant and product wave functions more flexible by including so-called charge-transfer (or ionic) configurations in addition to the locally excited configurations that mediate V^{ed}.[157] In this model, V^{ioo} appears as an intuitive double-step electron transfer between donor and acceptor that effectively exchanges electronic excitation.

The formal derivation[157] takes a bit more work than the intuition suggests, but the net result is that the primary electronic coupling for EET that is mediated by orbital overlap is not the exchange interaction but the product of two one-electron transfers, each quantified by a matrix element (eq 8), called a bond integral (β) in the old literature. The β_{ET} term accounts for transfer of an electron from D′ to A, and the β_{HT} term moves a hole from D′ to A (equivalently, an electron from the highest occupied molecular orbital of A to D′). The net effect of these two virtual and synchronous electron transfers is that electronic excitation is transferred from D to A. See ref 157 for details and ref 135 for a review. Note that the electron transfers are conceptual, stemming from the classical valence-bond formulation of the problem; they are not a real sequence of one-electron-transfer events because they do not separately and sequentially induce solvent reorganization.

The part of the electronic coupling that promotes EET through explicit orbital overlap effects, therefore, has a steep distance dependence. Each of the β terms in eq 8 depends exponentially on donor−acceptor separation. Therefore, the magnitude of V^{ioo} depends exponentially on R and increases exponentially twice as steeply as the rate of a hypothetical electron transfer between the same molecules with a decrease of R. The sign of V^{ioo} can be positive or negative (it depends on how the donor is oriented with respect to the acceptor), and the sign of V^{ioo} does not have to correlate with the sign of the Coulombic interaction V^{ed}. The specific form of V^{ioo} is

$$V^{ioo} \approx 2\beta_{ET}\beta_{HT}/A \tag{8}$$

where A is the energy difference between charge-transfer configurations and the locally excited donor configuration (corresponding to ΔE^{CT} in Figure 9). The distance dependence of V^{ioo} is directly proportional to $\exp(-2\alpha R)$ given that the electron and hole transfer matrix elements are $\beta_{ET} \propto \exp(-\alpha R)$ and $\beta_{HT} \propto \exp(-\alpha R)$.[158,135] Owing to this very steep scaling of V^{ioo} with R, V^{ioo} dominates at close separations when the molecules are in van der Waals contact. Figure 7 shows a calculation of the electronic coupling between naphthalene chromophores at various separations. The distinction between the electrodynamic (approximately dipole−dipole) coupling regime and the regime where orbital overlap effects matter is quite clear.

DOI: 10.1021/acs.chemrev.6b00002
Chem. Rev. XXXX, XXX, XXX−XXX

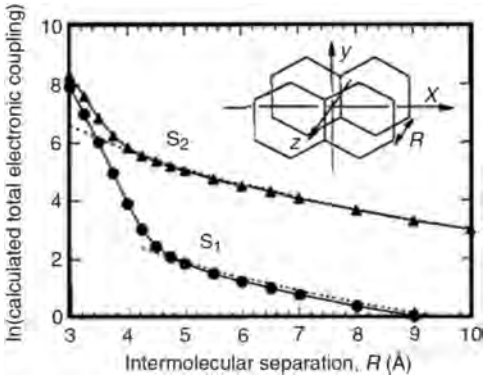

Figure 7. Total electronic coupling between the S_1 states of naphthalene and the S_2 states as a function of interchromophore separation. The steep rise at short separations indicates the onset of interactions depending on interchromophore orbital overlap. Reproduced with permission from ref 128. Copyright 1994 American Chemical Society.

In Förster theory, the weakly coupled chromophores are assumed to be well-separated compared to their size, so that the short-range term, V^{ioo}, is neglected and the Coulombic coupling can be approximated as a point-dipole−dipole interaction. Such a model based on the localized donor−acceptor states is reasonable for the weakly coupled B800 ring of purple bacterial LH2. (For readers unfamiliar with LH2, structural details presented in section 10 would be helpful in a further discussion of this topic.[129]) The main problem with the dipole−dipole approximation is that it works well only when the separation between the chromophores is large compared to the size of those molecules.

6.2. Breakdown of the Dipole Approximation

At small separations, the dipole−dipole approximation fails, and the calculation of the Coulombic coupling between chromophores requires a more realistic account of the shape of the transition densities. A straightforward method is to use the transition density cube (TDC) method developed by Brent Krueger et al.[129] How and why this method is useful is reviewed in detail elsewhere.[116,155] In section 9 of this review, we discuss the TDC method further. The essential picture of the TDC method is illustrated in Figure 8.

The first concept to understand when thinking about V^{ed} and any accurate way to calculate it, including the TDC method, is the transition density. The properties of an electronic transition

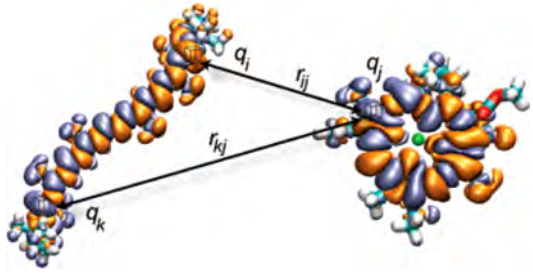

Figure 8. Plot of transition densities calculated for (right) a chlorophyll molecule and (left) a carotenoid molecule. The Coulombic interaction V^{ed} is determined by the integral over all interactions between the molecules in a way that maps over the shapes of the donor and acceptor. Reprinted with permission from ref 156. Copyright 2011 Wiley-VCH.

are determined by the transition density: it is a virtual charge distribution that captures the way a molecule's electronic wave function jumps from one state to another as a result of the action of a resonant electromagnetic field. One can calculate transition densities and plot them as if they were a real (classical) charge distribution, as shown in Figure 8. For example, it is a common procedure in freshman chemistry to plot charge distributions to illustrate the shapes of atomic orbitals; for example, the shape of the $2p_x$ orbital wave function ψ_{2p_x} is indicated by the one-electron spinless density $\rho(x,y,z) = |\psi_{2p_x}(x,y,z)|^2$. This is the real (quantum mechanical) charge distribution for an electron in the $2p_x$ atomic orbital. The transition density is not quite the same because it is constructed from wave functions of two different electronic states. The transition density connecting electronic state Ψ_0 to state Ψ_1 is given by

$$P^k_{0\delta}(r_1) = N \int \Psi_0(x_1, x_2, ..., x_N)\, \Psi_1^*(x_1', x_2', ..., x_N')\, dx_2 ... dx_N dx_2' ... dx_N' ds_1 \quad (9)$$

where N is a normalization constant, x_i includes both the spatial and spin coordinates of each electron i, and s_1 is the spin of electron 1. In other words, the wave-function outer product has been integrated over all space and spin coordinates of all electrons except electron one.

When light interacts with a molecule to instigate the transition from state Ψ_0 to state Ψ_1, it averages over the detail of the transition density, because the wavelength of the light being absorbed or emitted is very large compared to the size of the molecule. This averaging means that absorption and emission observables, such as extinction coefficients and radiative rates, are well-quantified by a simple vector, the transition dipole moment. Just as a dipole moment can be calculated for any real charge distribution, it can be calculated for the transition density simply by applying the dipole operator. The resulting quantity is called the transition dipole moment.

There is a difference between how light interacts with molecules and how molecules, such as those shown in Figure 8, interact with each other through their transition densities. The molecules and the distance separating them are comparable in size. Thus, the Coulombic interaction, proportional to $1/r$, effectively traces out the shapes of the molecules. $1/r$ is quite a steep interaction, so it weights closely separated parts of the transition density more than distantly separated parts. For instance, in Figure 8, the interaction between transition charge elements i and j with separation r_{ij} is stronger than the interaction between transition charge elements k and j with separation r_{kj} by the ratio r_{kj}/r_{ij}, if the charge elements are all of similar magnitude.

The net effect of averaging over the interactions, instead of first averaging over the transition densities and then calculating the interaction, can be significant and is the reason for the failure of the dipole−dipole approximation. Failure of the dipole−dipole approximation is related to the shapes of molecules, and therefore, when the dipole approximation fails, so does the multipole expansion (taken to reasonable, low, order).

6.3. Solvent Screening

It is known that the solvent environment, or the host medium surrounding the donor and acceptor molecules, modifies the electronic coupling. For example, the EET rate in a polarizable

DOI: 10.1021/acs.chemrev.6b00002
Chem. Rev. XXXX, XXX, XXX−XXX

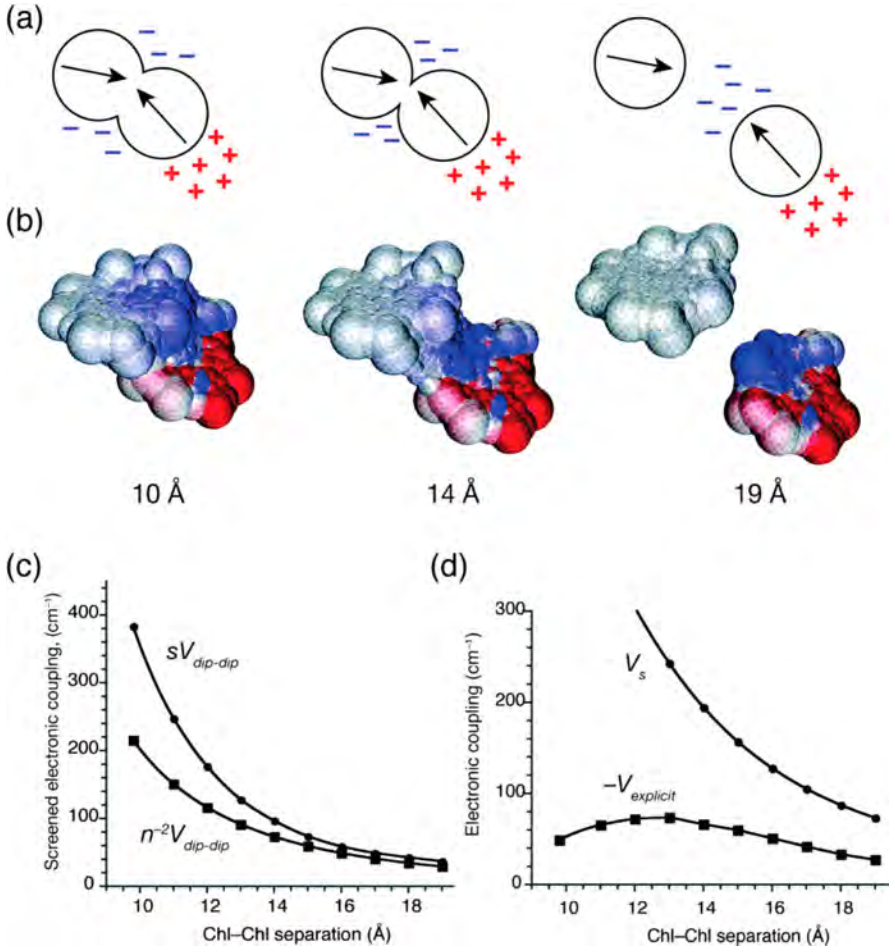

Figure 9. (a) Schematic depiction of the interaction between two transition dipoles (arrows) immersed within cavities in a polarizable medium. The effective charges representing the response of the medium to one transition dipole are drawn. As the cavities converge, the effective charges remain held away from the transition dipoles. (b) On the basis of quantum mechanical calculations, the dependence of s on the separation between the Chl_{602}–Chl_{607} molecules in the dimer structure from LHCII is explained by the formation of a common cavity, physically representing exclusion of solvent from the intermolecular region. The result is represented by a progressive spread of the effective surface charges over the acceptor microenvironment, as shown for three Chl–Chl separations. (c) The spread of the surface charges over the cavities changes the magnitude and functional form of the electronic coupling. The dipole–dipole coupling (screened by n^2), $V_{dip-dip}/n^2$ (squares), is compared here to $sV_{dip-dip}$. The difference corresponds to a factor of at least 2 in the calculated rate of EET. (d) The origin of the distance dependence of s is seen by inspecting the ratio of the direct electronic coupling, V_s, to the explicit solvent contribution, $V_{explicit}$. As the intermolecular separation decreases, V explicit assumes diminishing significance, and thus, $s = V_s/V_{tot} \rightarrow 1$ because the total coupling $V_{tot} \approx V_s$. Figure reproduced with permission from ref 145. Copyright 2007 American Chemical Society.

medium is reduced by the factor $1/n^4$ according to Förster theory, where n is the refractive index of the medium at optical frequency. This factor (often somewhat misleadingly referred to as screening; see below) comes from a modification of the dipole–dipole electronic coupling, $V^{dip-dip(solv)} = V^{dip-dip(vacuum)}/n^2$. A similar equation is easily derived for the interaction energy between charge dipoles in a polarizable medium, but there is an important distinction for transition dipole: The medium effects come only from the high-frequency dielectric response of the medium, not from the low-frequency dielectric response. Hence, the refractive index and not the dielectric constant of the solvent is the parameter that matters. The other confusing point is that Förster theory is formulated in terms of spectra, and the donor emission and acceptor absorption spectra each also contain refractive index factors. Knox and van Amerongen (2002)[133] provided a very clear account disentangling the different refractive index terms that appear in the derivation of Förster theory and showed how only the solvent "screening" term ends up in the final equation.

The Förster treatment of the dielectric medium is adequate only for two chromophores found at large distances compared to their molecular dimensions in a nondispersive, isotropic host medium and for which the dipole approximation holds.[159] These conditions are quite restrictive. Given that the EET is strongly affected by solvent effects, for example, if $n = 1.4$, then compared to unscreened electronic couplings, the rate differs by a factor of almost 4. It therefore makes sense that estimations of electronic couplings using more accurate methods such as TDC should also incorporate more sophisticated treatments of solvent effects. It turns out that quantum chemical theory is needed to provide a realistic solution, as was worked out by Iozzi et al. (2004)[160] and Jurinovich et al. (2015).[161] Johannes Neugebauer described how to calculate solvent screening in the framework of time-dependent density functional theory.[162] Another important contribution was from Julia Adolphs and Thomas Renger, who developed ways to calculate electrochromic shifts of transition energies in protein environments.[163] In that work, an electrostatic method, now known as the

DOI: 10.1021/acs.chemrev.6b00002
Chem. Rev. XXXX, XXX, XXX–XXX

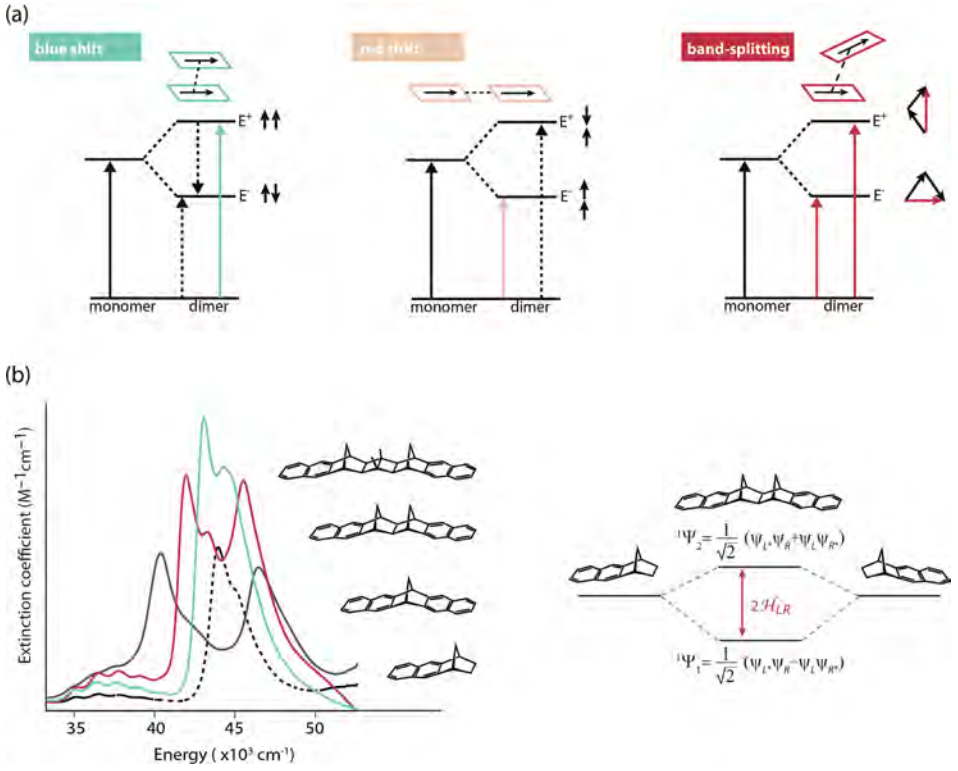

Figure 10. (a) Exciton band energy diagrams for a molecular dimer with three different mutual arrangements: parallel transition dipoles, in-line transition dipoles, and oblique transition dipoles. (b) Absorption spectra of a series of naphthyl dimer molecules compared to the monomeric model chromophore (dashed line). Exciton delocalization over two molecules is manifested in the absorption spectrum of the dimers, as it splits into two bands, where the splitting is related to the electronic coupling between the naphthyl moieties. Spectra redrawn with permission from ref 158. Copyright 1993 American Chemical Society. Figure adapted with permission from ref 173. Copyright 2006 Nature Publishing Group.

Poisson-TrEsp method,[164,165] was introduced for the parameter-free calculation of excitonic couplings including screening effects. It was applied to calculate electronic couplings in the FMO protein and, thereby, provided a microscopic explanation of the small effective oscillator strength inferred from spectroscopic studies, reported by Louwe et al. (1997).[166]

Using the polarizable continuum model (PCM), the molecular system under study (the donor−acceptor pair) is represented as a quantum mechanical charge distribution within a molecular cavity, characterized by a realistic shape, whereas the complex host environment comprising the protein medium, intrinsic water, and surrounding medium is collectively modeled as a structureless polarizable continuum. This model can more precisely elucidate solvent effects for realistic systems because it accounts for the shapes of interacting molecular transition densities. The calculation includes the way solvent responds to the interaction between transition densities and how the transition densities in turn respond, through a reaction field, to the polarization of the solvent (Figure 9).[145] Combined with TDC calculations, one thereby finds the general form of the screened (or, better, solvent-corrected) electronic coupling: $V^{\mathrm{Coul(solv)}} = sV^{\mathrm{Coul(vacuum)}}$. In the limit of the dipole−dipole approximation, $s = 1/n^2$.

As an example, calculations of electronic couplings were performed for more than 100 pairs of molecules taken from different photosynthetic proteins, with variations in the molecular dimensions, shapes, and orientations.[145] By analyzing these results, a functional form of the solvent screening factor s, was evaluated

$$s = A \exp(-\beta R) + s_0 \qquad (10)$$

where the pre-exponential function $A = 2.68$ and the separation-dependent dielectric screening is fitted by the exponential term. Two contributions to the electronic coupling interplay: the direct coupling, implicitly altered by the medium (V_s), and the coupling involving the explicit solvent effect (V_{explicit}), such that $s = V_{\mathrm{tot}}/V_s = (V_s + V_{\mathrm{explicit}})/V_s$. At decreasing intermolecular separations, the difference of the dipole−dipole coupling (screened by n^2), $V_{\mathrm{dip-dip}}/n^2$, compared to $sV_{\mathrm{dip-dip}}$ increases dramatically (Figure 9c). Additionally, at diminishing intermolecular separations, the explicit-solvent contribution, V_{explicit}, becomes increasingly less significant compared to the direct electronic coupling V_s (Figure 9d).

In contrast to these results, Renger and Müh (2012)[164] reported calculations of screening of electronic couplings in photosystem I trimers. In their work, no notable distance dependence of the screening was predicted. Instead, the screening depended on the mutual orientation of pigments and the local protein environment.[163,164,167−169] For example, in photosystem I, the screening factor was found to be dominated by the protein itself, leading to red-shifted site energies, whereas smaller contributions from chlorophyll molecules, lipids, and water molecules gave rise to blue-shifted site energies.[167] In these works by Renger and colleagues, inclusion of large number of amino acids was required to produce screening factors that led to calculated spectra that were in good agreement with experimental results. These results indicate that long-range electrostatic interactions are important for determining site energies for reproducing experimental spectra.[163,167,168]

DOI: 10.1021/acs.chemrev.6b00002
Chem. Rev. XXXX, XXX, XXX−XXX

In summary, according to Förster theory, the major factors affecting energy transfer are the center-to-center separation between chromophores, the relative orientation of their transition dipoles, and the Förster spectral overlap integral (between the fluorescence spectrum of the donor and the absorption spectrum of the acceptor). The distance between interacting chromophores has a direct impact on the quantum mechanical characteristics of the energy-transfer mechanism. Extensions of the original theory include the following considerations: electronic coupling without invoking the dipole approximation, molecular exciton states, solvent screening of the electron coupling, and dynamic effects of coherence. Regarding the electronic coupling between donor and acceptor chromophores, the coupling term, V^{total}, is defined as the sum of long-range and short-range contributions, given by the electrodynamic interaction (V^{ed}) and the interchromophore orbital overlap (V^{ioo}), respectively.

7. MOLECULAR EXCITONS

In the strong coupling limit, in contrast to the weak electronic coupling limit where excitation is transferred as localized states, electronic states are not localized on individual chromophores. Instead, closely spaced pigments coherently share electronic excitation. This is described by the molecular exciton model.[170−172] Studies of molecular excitons provide insight into the collective absorption and redistribution of excitation energy in nanoscale systems.[173] Sometimes, the term "exciton" is used to mean electronic excitation of a molecule. We prefer to reserve the term exciton for excitation that is coherently shared among two or more molecules.

The Frenkel model, which is relevant for photosynthetic antenna and can also describe molecular aggregates such as J-aggregates (Figure 10), is based on the principle that, if one cannot physically distinguish the cases of electronic excitation of, say, molecule A from excitation of molecule B, then the correct quantum states that absorb light are linear combinations of the two possibilities. Thus, the strong electronic coupling between molecules comprising a molecular exciton results in the electronic excited states being linear combinations of excitations of different molecules. The result for two indistinguishable molecules is the symmetric and antisymmetric linear combinations of excitation

$$\Psi_{\text{symm}} = \frac{1}{\sqrt{2}}(\text{A}'\text{B} + \text{AB}') \tag{11a}$$

$$\Psi_{\text{antisymm}} = \frac{1}{\sqrt{2}}(\text{A}'\text{B} - \text{AB}') \tag{11b}$$

where the prime indicates electronic excitation. These linear combinations are reminiscent of how bonding and antibonding orbitals are constructed.

The oscillator strengths of transitions from the ground state to different excitonic energy levels are influenced by the relative arrangement of the monomers (Figure 10a). For example, when two molecules are arranged in a "sandwich" configuration, their transition dipoles are parallel, and the electronic coupling has a positive sign (dictated by the orientation factor κ; see eq 4). The linear combination where the transition dipoles point in the same direction results in the higher-lying excitonic state being bright (allowed), whereas transition dipoles oriented in an antiparallel fashion result in the lower-energy excitonic state being dark (forbidden).

In this sandwich geometry (called an H-aggregate), a blue shift in the absorption spectrum compared to that of the monomer is observed because the oscillator strength is exclusively carried by the upper exciton state. A simple calculation shows why this is the case. Note that the oscillator strength is proportional to the magnitude squared of the dipole transition moment, so one must calculate the dipole transition moment for each exciton state. The lowest-energy state is the antisymmetric linear combination, eq 11b, because of the positively signed electronic coupling. The transition dipole moment for this state is

$$\begin{aligned}\vec{\mu}_{\text{anti}} &= \left\langle \frac{1}{\sqrt{2}}(\text{A}'\text{B} - \text{AB}')|\hat{\mu}|\text{AB} \right\rangle \\ &= \frac{1}{\sqrt{2}}(\langle \text{A}'|\hat{\mu}|\text{A}\rangle\langle \text{B}|\text{B}\rangle - \langle \text{A}|\text{A}\rangle\langle \text{B}'|\hat{\mu}|\text{B}\rangle) \\ &= \frac{1}{\sqrt{2}}(\vec{\mu}_{\text{A}} - \vec{\mu}_{\text{B}})\end{aligned} \tag{12}$$

which equals zero in the case of parallel transition moment vectors with the same magnitude, $\vec{\mu}_{\text{A}}$ and $\vec{\mu}_{\text{B}}$. Note that the overlap is $\langle \text{A}|\text{A}\rangle = \langle \text{B}|\text{B}\rangle = 1$, $\hat{\mu}$ is the dipole operator, and $|\text{AB}\rangle$ is the ground-state wave function. The upper exciton state is the symmetric linear combination, and it can be seen that this will have a dipole transition moment of $\vec{\mu}_{\text{symm}} = (\vec{\mu}_{\text{A}} + \vec{\mu}_{\text{B}})/\sqrt{2} = \sqrt{2}\vec{\mu}$, and therefore, its oscillator strength is proportional to twice that of one monomer.

In J-aggregates (in-line or head-to-tail; Figure 10a), the electronic coupling is negative, so the symmetric exciton state lies lowest in energy. Therefore, the lower-energy state is characterized by a larger transition dipole moment, resulting in a red shift of the absorption band. Intermediate, oblique, orientations are characterized by band splitting, which is dependent on both the separation between the dipoles and the angles with the vector connecting them, resulting in the appearance of two bands in the absorption spectrum.

In the very weak coupling limit, differences between the absorption spectra of the exciton system and isolated molecules are minimal, whereas small spectral perturbations are observed in the weak coupling case. A clear example can be seen for a series of naphthalene-bridge-naphthalene dyads (DN-2, DN-4, and DN-6) with two naphthalene chromophores held in position by a rigid polynorbornyl-type bridge, where the distance and orientations of the interacting chromophores is fixed and well-controlled (Figure 10b).[158] As the electronic coupling is reduced by increasing the separation between the chromophores, the exciton splitting diminishes. The strong coupling limit is defined as the case when the exciton splitting is larger than the line broadening of the absorption bands.

When the molecules are not identical or when there are more than two interacting molecules, the exciton states are obtained by solving a suitable secular determinant. For example, in the general case of a dimer, the exciton transition energies are given by

$$\begin{vmatrix} H_{11} - \text{E} & H_{12} \\ H_{21} & H_{22} - \text{E} \end{vmatrix} = 0 \tag{13}$$

$$E = \frac{(H_{11} + H_{22}) \pm \sqrt{(H_{11} - H_{22})^2 + 4|H_{12}|^2}}{2}$$

where H_{11} and H_{22} are the two diagonal Hamiltonian elements (e.g., the total energies of the charge-localized state), whereas

DOI: 10.1021/acs.chemrev.6b00002
Chem. Rev. XXXX, XXX, XXX−XXX

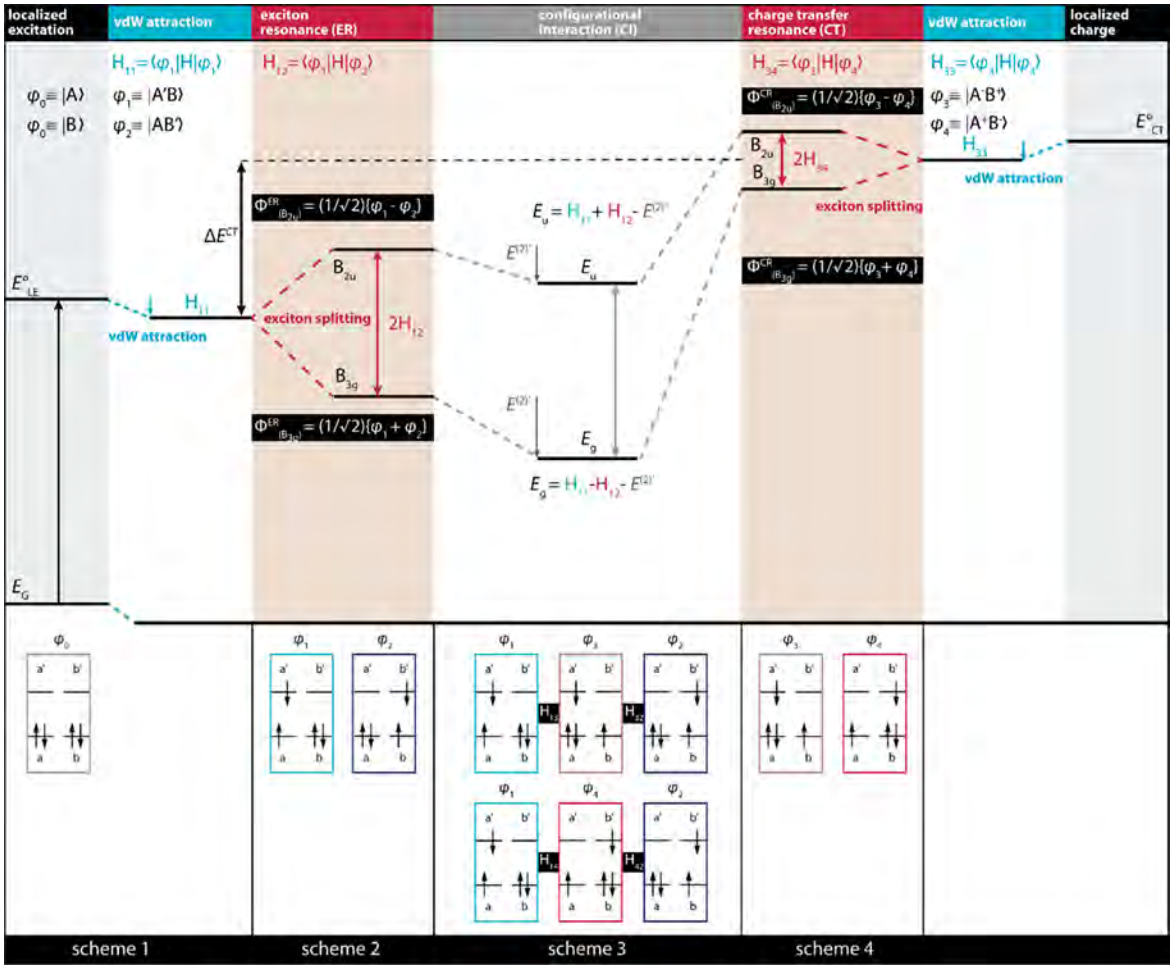

Figure 11. Schematic representation of the electronic transitions in a dimer based on molecular exciton theory. van der Waals attraction lowers the energies of the locally excited (E°_{LE}) and charge-transfer (E°_{CT}) states to H_{11} and H_{33}, respectively. These states are subsequently split by exciton interactions (H_{12} and H_{34}), and the configurational interaction between exciton-resonance (ER) and charge-transfer-resonance (CT) states results in final dimer states with energies of E_u and E_g. Note that the symmetry labels are for illustration only and refer to a D_{2h}-symmetry dimer.

H_{12} and H_{21} are the off-diagonal matrix elements, representing interaction terms. More sophisticated treatment of exciton spectroscopy incorporates coupling of electronic states to vibrations.[171,174] In some cases, one should also consider contributions resulting from interchromophore orbital overlap.[128] Although the exciton splitting is still equal to twice the total electronic coupling in the case of identical molecules in a dimer, the absorption bands are often collectively red-shifted, and oscillator strength can be redistributed because of orbital overlap effects. Figure 11 summarizes the electronic transitions for a dimer system comprising identical chromophores A and B (Figure 11, scheme 1). In the weak coupling limit, the chromophores retain their individuality (Figure 11, left side), and in the limiting case of infinite separation, the excited states are described as localized and degenerate, $|A'B\rangle$ and $|AB'\rangle$, where the prime means electronically excited. The attractive van der Waals interaction lowers the energy of the excited dimer (H_{11}). Then, at smaller separations, the degeneracy of the excited states is removed through exciton resonance (ER), where the exciton splitting between the two states ($2H_{12}$) (Figure 11, scheme 2) is proportional to the electronic coupling between the two chromophores.

For close-range interactions, orbital overlap must be taken into account, and in that case, the energies are modified by configuration interaction (CI) between exciton states and charge-transfer (CT) states (Figure 11, scheme 4).[175,176] This mixing is a methodology that allows inclusion of the primary intermolecular orbital overlap effects and is not necessarily a physical process such as an electron-transfer reaction. Moreover, it is specific to a classical valence-bond formalism—historically, a way to improve the Heitler–London wave function. It is easily shown that a valence-bond model including locally excited and intermolecular charge-transfer configurations is equivalent to a supermolecule molecular orbital calculation of excited states using the CI-singles level of theory. The relationship between the local orbital basis and molecular orbitals for a dimer is shown in ref 177.

In Figure 11, the localized charge-transfer states are on the right (scheme 4). The attractive forces lower the localized charge-transfer state (H_{33}), before the exciton interaction lifts the degeneracy, which leads to the formation of B_{2u} and B_{3g} states with a splitting equivalent to $2H_{34}$.[158] The final dimer states with energies of E_u and E_g are obtained following the configuration interaction (Figure 11, center, scheme 3). That is, one must solve a 4×4 secular determinant analogous to eq 13.

In summary, in the very weak coupling limit, electronic states are localized on individual chromophores, and there are minimal differences between the absorption spectra of the

DOI: 10.1021/acs.chemrev.6b00002
Chem. Rev. XXXX, XXX, XXX−XXX

exciton system and the isolated molecules. In the weak coupling limit, small spectral perturbations are observed. In the strong coupling limit, closely spaced pigments coherently share electronic excitation, as described by the molecular exciton model. The oscillator strengths of excitonic energy levels depend on the geometry and mutual arrangement of monomers. Interchromophore orbital-overlap-dependent interactions become significant at small separations.

8. STRUCTURAL AND SPECTRAL CONSIDERATIONS

With variations in the interchromophoric interactions (as discussed above), it is important to discuss the principles behind the organizational structure in multichromophoric systems. By modulating the structure and arrangement of chromophores, organisms are able to maximize the collection of light and the subsequent funneling of that energy to the reaction centers. The optimization of the spatial and energetic landscapes of the antenna complex involves balancing the concentrations of the constituent chromophores, their mutual arrangement, and the integration of pigments of various absorption energy gaps.

The phenomenon of concentration quenching, originally observed in solutions of organic dyes, describes the rapid decrease in fluorescence quantum yield when the fluorophore is present in a high concentration. Fluorescence emission of dissolved Chl *a* was found to be completely quenched at a concentration of 0.3 M.[178,179] Light-harvesting antennas have succeeded in circumventing this phenomenon, and a very high packing density of pigments can therefore be attained before quenching is observed. For example, chlorophyll in LHCII has an effective concentration of 0.25 M, yet its lifetime is hardly quenched.[180] One of the classic examples is the aggregated bacteriochlorophylls (BChls) in chlorosomes, the light-harvesting organelles of green sulfur bacteria. BChl *a* protein in the Fenna−Matthews−Olson (FMO) complex in green sulfur bacteria is found at a concentration of 0.1 M.[181]

These examples serve as evidence that, although high local concentrations of chromophores in these supramolecular pigment structures are achieved, concentration quenching is generally avoided. This suggests a highly optimized arrangement of the constituent light-harvesting elements. It also emphasizes that the chromophores in light-harvesting complexes can be closely packed and, therefore, electronic coupling can be strong in many instances. This has profound implications for energy-transfer mechanisms, as we discuss in the following section. Note that there is quenching of excitation in chlorosomes by quinones, but this redox-activated quenching is not concentration quenching.[182]

We argue that pigment separations have been optimized to minimize electron transfer, a process enhanced proportional to the overlap of the molecular wave functions. A recent study[183] of light harvesting by a purple bacterium, *Rhodopseudomonas palustris*, mutant showed the quenching role of charge-transfer states. This mutant has a blue-shifted B850 Bchl band in the LH2 ring such that the LH2 absorption spectrum peaks solely at about 800 nm (unlike the wild-type LH2, which shows the typical B800−B850 absorption spectrum). Upon excitation of LH2, a red-shifted charge-transfer (CT) state, hidden in the wild-type bacterium by spectral overlap, was observed to be populated in <100 fs, quenching the emissive excited state. This indicates that CT states are close in energy to the excitonic states. The light-harvesting system "protects" itself by red shifting the excitonic manifold, which results in a uniform mixing of the CT state with many of the exciton states. This will still quench the states, but the effect is far less dramatic than having a CT state below the exciton manifold. This mixing of the red states with CT states will, of course, strongly enhance charge separation in RCs— this is a major point of many articles on PSII charge separation.[184−187] CT states are employed by the RC-antenna supercomplex to (i) escape quenching by unavoidable CT states, (ii) red shift the spectrum, and (iii) provide a fast and effective pathway in the RC for charge separation.

9. EXCITONICS AND GENERALIZED FÖRSTER THEORY (GFT)

Strong electronic coupling produces new chromophores because light is absorbed and emitted collectively (and nonadditively) by two or more coupled molecules. This has implications for light harvesting because now the donor and/or acceptor of excitation energy are/is not a single molecule, as in the case treated by normal Förster theory, but instead the exciton states shared between strongly interacting chromophores. In other words, new effective chromophores can be formed based on pigments already present in the organism. A modified version of Förster theory, called generalized Förster theory (GFT), can be used to account for excitonic donors and acceptors.[188]

Klaus Schulten and co-workers modeled exciton energy transfer in LH2 between exciton states,[189] which was a precursor to the GFT formalism. Mukai et al. (1999),[147] Sumi (1999),[190] and Scholes and Fleming (2000)[146] independently developed the GFT method for treating energy transfer in excitonic systems using a model with most of the Förster theory attributes. The key insight was the way electronic coupling must be taken into account, which we describe below. Scholes and Fleming delayed publication of their work because they were working (unsuccessfully) on how to include dynamic localization in the donor state and they were trying to formulate the theory in terms of a spectral overlap analogous to that of Förster. This "coupling-weighted spectral overlap" turned out to be interesting because it explains how averaging over the measured optical line shapes hides information about how donor and acceptor excitons couple. A few years later, Seogjoo Jang and co-workers (2004) reported a theory very similar to GFT that they called MC-FRET (multichromophoric Förster resonance energy transfer).[148]

There are three essential elements in the rate theory for excitation energy transfer that need to be addressed.[188] First, the electronic coupling is broken down into a linear combination of molecule-to-molecule electronic couplings, where the coefficients in the linear combination are simply those defining the exciton wave functions of donor and acceptor. Second, instead of one electronic state associated only with the donor and one associated only with the acceptor, there are two or more excitonic states, and one must sum over all permutations of donor and acceptor interactions. The key is to associate with each pair of excitonic donor and acceptor state couplings a corresponding spectral overlap. This leads to the rate expression containing a sum over coupling-weighted spectral overlaps in place of the simple Förster spectral overlap.[146] Third, when there is significant inhomogeneous broadening (disorder), one must perform the averaging "outside" this sum of coupling-weighted spectral overlaps because disorder makes each realization of exciton states (their

DOI: 10.1021/acs.chemrev.6b00002
Chem. Rev. XXXX, XXX, XXX−XXX

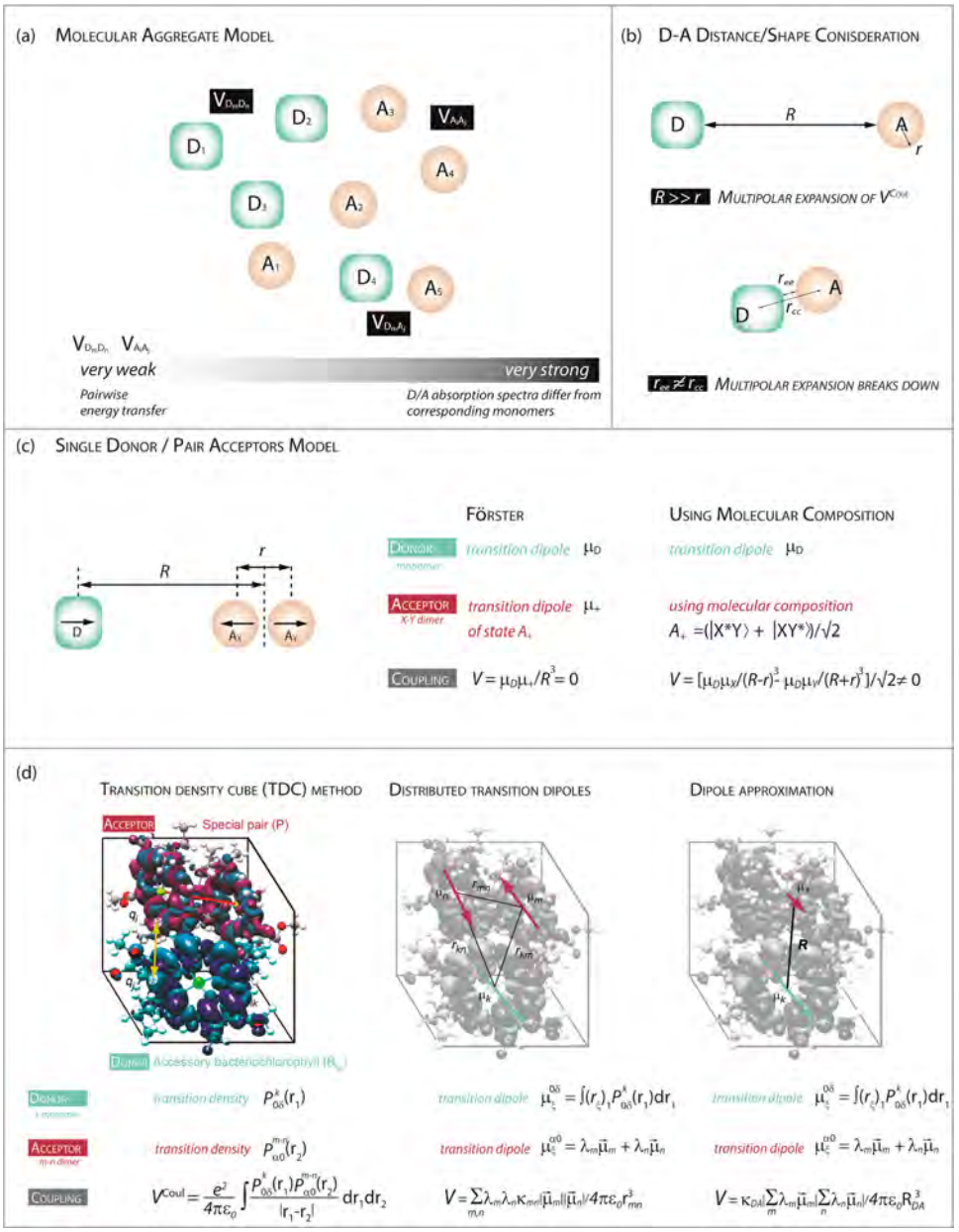

Figure 12. Elements of generalized Förster theory (GFT): (a) Schematic illustration depicting the composition of an aggregate comprising several donor (D) and several acceptor (A) molecules. The model takes three classes of coupling into consideration: coupling between donors V_{DmDn}, coupling between acceptors V_{AiAj}, and coupling between donors and acceptors V_{DmAj}. (b) Distance and shape considerations are major factors for GFT. (c) Illustration of the arrangement of a model aggregate comprising a donor (D) and a dimer (X and Y molecules arranged in a tail-to-tail orientation). The donor is separated by a distance of R from the center of the X−Y dimer. (d) Summary graphic depicting three different schemes for calculating the electronic coupling between the accessory bacteriochlorophyll (B_M) and the special pair (P) in the photosynthetic reaction center of a purple bacterium. Panel d adapted from ref 188. Copyright 2001 American Chemical Society.

coefficients and spectra) unique. Below, we discuss the essential elements of GFT in detail.

When GFT is applied to predict B800−B850 energy transfer in LH2, spectral overlap is determined in terms of B800 emission and the B850 absorption band density of states weighted by the associated electronic coupling factor (i.e., not the measured spectra, which are weighted by transition moments).[146] As a consequence of the delocalization of excitation in the B850 ring, the ring itself acts as a special chromophore when accepting energy from B800. Excitation can jump from B800 to any of the exciton states of B850; the electronic coupling must therefore be calculated on the basis of excitons through GFT.[146,147] The calculation shows that the primary acceptor states in B850 are actually the spectroscopically dark exciton states—quite a remarkable result compared to Förster theory, which counts only bright states. The GFT calculation predicts the B800-to-B850 energy-transfer time constant to be similar to that measured by experiment, whereas Förster theory predicts a rate that is a factor of 10 too low. This is an example of how the collective effects of an excitonic acceptor promote accelerated energy transfer, which has been called "supertransfer" in some recent work.[191,192]

DOI: 10.1021/acs.chemrev.6b00002
Chem. Rev. XXXX, XXX, XXX−XXX

9.1. Excitons and Electronic Couplings

Förster theory, despite being successful at predicting EET rates through donor emission and acceptor absorption spectra in some systems, has failed to provide a quantitative prediction of energy-transfer dynamics in multichromophoric assemblies, architectural models typically encountered in photosynthetic systems. These molecular aggregates are often characterized by groups of strongly interacting chromophores that can collectively donate or accept excitation energy. The dynamics of the energy transfer are therefore governed by three classes of electronic couplings: coupling between donors $V_{D_mD_n}$, coupling between acceptors $V_{A_iA_j}$, and coupling between donors and acceptors $V_{D_mA_j}$.[188] The Förster-type pairwise energy hopping model works well in the limit when all three of these couplings are very small, but if there are strong electronic interactions between constituent molecules of the donor (D) or acceptor (A), significant modifications of the D/A absorption spectra and electronic couplings will be found compared to those of corresponding monomers (Figure 12a).

Recall that, for the dipole approximation to be adequate and for convergence of the multipole expansion of Coulomb interactions, the separation between the donor and the acceptor molecules must be much larger than their size (Figure 12b). When interacting molecules are at close separations relative to their size or when the center-to-center (r_{cc}) and edge−edge (r_{ee}) separations differ considerably, the dipole approximation becomes inadequate for electronic couplings as it averages away the shapes of the D and A molecules (Figure 12b). Instead, one must consider V^{Coul} in terms of local interactions between the donor and acceptor transition densities. Similarly, when molecular exciton states associated with aggregated donors and acceptors are larger in spatial extent than the separation of these exciton wave functions, the dipole approximation breaks down, and one must include much more detail in the analysis of donor−acceptor interactions. We now discuss the levels of treatment that can be used.

A hypothetical aggregate model, comprising a monomer donor (D) and a dimer acceptor (X−Y pair) coupled in a confined geometry, as shown in Figure 12c, is used to illustrate the contribution of each molecular center. Consider the interaction between the donor and the symmetric acceptor molecular exciton state A_+, with a transition dipole moment of μ_+. For this geometry, μ_+ is evaluated to be zero. Application of Förster theory, where constants and the orientation factors are set to unity, results in eq 14a. If the acceptor is treated in terms of a molecular composite, $A_+ = (|X^*Y\rangle + |XY^*\rangle)/\sqrt{2}$ and the dipole approximation is again employed, but now only for site−site couplings, eq 14b is obtained. Similar values of r (the center-to-center separation between acceptors X and Y) and R (the center-to-center separation between the donor and the acceptor dimer) result in a pronounced difference in electronic coupling (see eqs 14a and 14b).

$$V = \mu_D\mu_+/R^3 = 0 \tag{14a}$$

$$V = [\mu_D\mu_X/(R - r)^3 - \mu_D\mu_Y/(R + r)^3]/\sqrt{2} \neq 0 \tag{14b}$$

Close proximity of donor and acceptor chromophores compared to molecular dimensions leads to the breakdown of the analogy between synergistic absorption and emission processes (coupled dipoles). Additionally, there is a distinct and crucial variation between averaging over wave functions and then coupling them (eq 14a and 15a) and averaging over the coupling between wave functions (eq 14b using eq 15b)

$$V = \kappa_{DA}|\sum_m \lambda_m\vec{\mu}_m||\sum_n \lambda_n\vec{\mu}_n|/4\pi\varepsilon_0 {R_{DA}}^3 \tag{15a}$$

$$V = \sum_{m,n} \lambda_m\lambda_n\kappa_{mn}|\vec{\mu}_m||\vec{\mu}_n|/4\pi\varepsilon_0 {r_{mn}}^3 \tag{15b}$$

Here, R_{DA} is the center-to-center separation between D and A, and κ_{DA} is the orientation factor between transition moments $\vec{\mu}_D = \sum_m \lambda_m\vec{\mu}_m$ and $\vec{\mu}_A = \sum_n \lambda_n\vec{\mu}_n$. In the latter case, transition dipoles μ_m and μ_n are separated by r_{mn} with a characteristic orientation factor κ_{mn}. The coefficients λ_m and λ_n define the composition of wave functions D and A in terms of configurations m and n according to the molecular exciton model.

Three different schemes with increasing levels of simplification for evaluating electronic coupling are illustrated in Figure 12d, where a monomeric donor (B_M), an accessory bacteriochlorophyll, and a dimeric acceptor, the special pair (P), of the photosynthetic reaction center of a purple bacterium are used as the model system. Figure 12d (left) depicts the transition density cube (TDC) method, where accurate interaction energies between transition density cubes of each chromophore, represented in a three-dimensional grid, were evaluated. First, through quantum chemical calculations of the ground and relevant excited states, transition densities, $P^k_{0\delta}(r_1)$ and $P^{m-n}_{\alpha 0}(r_2)$, of the monomeric donor chromophore k and the upper exciton state of the dimeric acceptor comprising molecules m and n, respectively, are evaluated. Then, the coupling is described primarily by a Coulombic interaction between the transition densities of the chromophores[193]

$$V^{Coul} = \frac{e^2}{4\pi\varepsilon_0}\int \frac{P^k_{0\delta}(r_1)\, P^{m-n}_{\alpha 0}(r_2)}{|r_1 - r_2|}\, dr_1 dr_2 \tag{16}$$

Unlike the multipole expansion (and the dipole−dipole limit), which is only valid at separations beyond the van der Waals radii of the donor and acceptor, the TDC method is applicable at all interchromophore separations.

A simplification of the TDC method is illustrated in the case of distributed transition dipoles (Figure 12d, middle), where reduction of the transition densities to transition dipoles on each chromophoric center was performed.[190,194] Constituent chromophores of molecular aggregates retain nonvanishing transition dipoles even if their collective dipole strength vanishes for optically forbidden exciton states. Therefore, EET can be observed from or to an exciton state that might even be optically dark as a result of interactions attributed to individual transition dipoles in the molecular aggregate when D and A are found at close separations. The transition dipole moment for the donor monomer k is obtained by applying the dipole operator to the transition density $\mu^{0\delta}_\zeta = \int (r_\zeta)_1 P^k_{0\delta}(r_1)\, dr_1$ (where components of the vector are described by ζ). The wave function of the acceptor dimer is a superposition of monomer wave functions, where coefficients λ_m and λ_n define the admixture, $\mu^{\alpha 0}_\zeta = \lambda_m\mu^{m0}_\zeta + \lambda_n\mu^{n0}_\zeta$. The couplings can then be evaluated through eq 15b.

A yet further simplification is achieved by averaging within the donor or acceptor aggregates, as illustrated in Figure 12d, where the acceptor exciton state in the model system has been reduced to corresponding point dipoles. Coupling is then evaluated using $\mu^{0\delta}_\zeta$ and $\mu^{\alpha 0}_\zeta$ and eq 15a. The dipole

DOI: 10.1021/acs.chemrev.6b00002
Chem. Rev. XXXX, XXX, XXX−XXX

approximation, corresponding to the Förster method, treats donors and acceptors as point dipoles associated with each spectroscopic band. This approach, however, has serious flaws because absorption and emission spectra do not provide adequate information on length scales on the order of molecular dimensions and are thus not well-suited for assessing energy-transfer dynamics in multichromophoric assemblies.

In summary, EET in molecular aggregates is best described to occur through exciton states. Extraction of EET dynamics for a generalized picture of a multichromophoric assembly (Figure 12a) comprising m donor chromophores and n acceptor chromophores requires the evaluation of $m \times n$ distinct electronic couplings. In the next section, we show how to construct these electronic couplings and incorporate them into a modification of Förster theory for molecular aggregates, GFT.

9.2. Formulating GFT

The generalized Förster theory (GFT) described here enables structural information to be preserved in the model for EET. For the treatment of multichromophoric aggregates, the coupling between D and A, $V_{D_mA_j}$, is classified as "weak", allowing the Förster-type approach to be retained and the modified theory to still be based on the Fermi golden rule rate expression. Donors and/or acceptors are collected into groups where electronic couplings ($V_{D_mD_n}$ and $V_{A_iA_j}$) are strong. GFT also allows for the incorporation of energetic disorder, which affects both site energies and couplings and is commonly significant in photosynthetic systems. By retaining the Förster-type approach, which allows for donor and acceptor characteristics to be extracted from spectroscopic measurements, we must assume that electronic states are linearly coupled to the phonon bath and that coherence or memory effects are insignificant.[195−198]

Formulation of the effective states of the donor δ and acceptor α in molecular assemblies proceeds by first grouping donor and acceptor units into separate blocks in the Hamiltonian matrix

$$\mathbf{H} = \begin{pmatrix} \mathbf{H}_{dd} & \mathbf{H}_{da} \\ \mathbf{H}_{ad} & \mathbf{H}_{aa} \end{pmatrix} \tag{17}$$

where all quantities at this stage are in the site basis, so that $\mathbf{H}_{dd}$ is a matrix that contains on its diagonal the transition energies for the chromophores grouped in the donor aggregate (we label these molecules by the index m) and its off-diagonal part contains electronic couplings between the donor chromophores. $\mathbf{H}_{aa}$ is the analogous matrix for the acceptor aggregate (we label these molecules by the index n). The electronic couplings between each donor chromophore and each acceptor chromophore are in the off-diagonal blocks $\mathbf{H}_{da} = \mathbf{H}_{ad}$ (these are denoted by V_{mn}).

The next step is to block-diagonalize the donor and acceptor blocks of eq 17. This yields a partitioned matrix containing the effective donor δ and acceptor α states, whereas the diagonal blocks $H_{\delta\delta}$ and $H_{\alpha\alpha}$ define the effective donor and acceptor states as the eigenvectors in terms of the donor- and acceptor-molecule wave functions ψ_m and ψ_n

$$\Psi_\delta = \sum_m \lambda_{\delta,m}\psi_m \tag{18a}$$

$$\Psi_\alpha = \sum_n \lambda_{\alpha,n}\psi_n \tag{18b}$$

Thus, we obtain the electronic couplings between these effective donor and acceptor states $V_{\delta\alpha}$

$$V_{\delta\alpha} = \langle\Psi_\alpha|V|\Psi_\delta\rangle = \sum_{m\neq(a)}\sum_{n\neq(d)} \lambda_{\delta,m}\lambda_{\alpha,n}V_{mn} \tag{19}$$

This is the key step underpinning GFT. We now associate a spectral overlap $J_{\delta\alpha}$ with each effective donor and acceptor and thus sum over each pairwise energy-transfer term, taking care with the ensemble average over disorder, to obtain the rate of EET as

$$k_{GFT} = \frac{2\pi}{\hbar}\langle\int_0^\infty d\varepsilon \sum_{\delta,\alpha} P_\delta |V_{\delta\alpha}(\varepsilon_d, \varepsilon_a)|^2 J_{\delta\alpha}(\varepsilon, \varepsilon_d, \varepsilon_a)\rangle \tag{20}$$

where we average over the disordered site energies ε_d and ε_a and P_δ indicates the Boltzmann distribution of population of the donor exciton states.

Averaging over disorder needs to be carried out in a special way: For each realization of disorder (physically, each LH2 ring), the sum of coupling-weighted spectral overlaps must be calculated, and the average must be taken over many realizations of disorder (LH2 rings).[146] The importance of disorder in these calculations, through generalized Förster theory, for B800 to B850 EET is shown in Figure 13.[146,188]

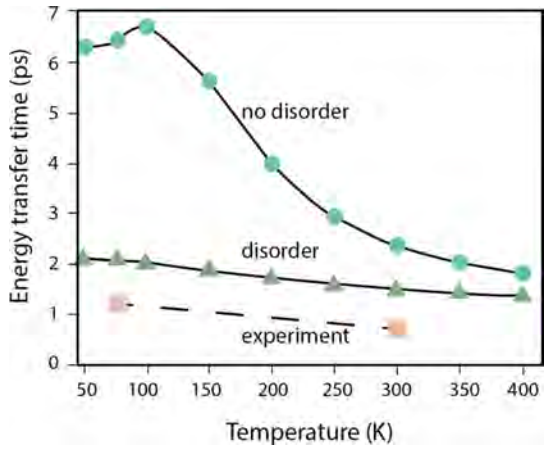

Figure 13. Comparison of the temperature dependence of the B800−B850 energy-transfer time for (i) calculations with no disorder, (ii) calculations with disorder but without accounting for the carotenoids, and (iii) experimental results for *Rb. sphaeroides*. Data adapted with permission from ref 146. Copyright 2000 American Chemical Society.

Without disorder, the EET time is predicted to be strongly temperature-dependent, but with disorder included, the results are relatively insensitive to temperature, in agreement with experimental results.

10. STRUCTURE AND PHOTOPHYSICS OF LIGHT-HARVESTING COMPLEXES OF PURPLE BACTERIA

Here, we discuss in detail light-harvesting LH2 antenna complexes from purple bacteria (see Scheme 1, bottom). Because of its very special molecular structure, this protein complex reveals a wide diversity of processes associated with energy transfer and lends itself as a perfect model system.

Anoxygenic phototrophic purple bacteria are widespread photosynthetic prokaryotes that inhabit stratified lakes (particularly the anoxic zone), ponds, estuaries, waste lagoons,

DOI: 10.1021/acs.chemrev.6b00002
Chem. Rev. XXXX, XXX, XXX−XXX

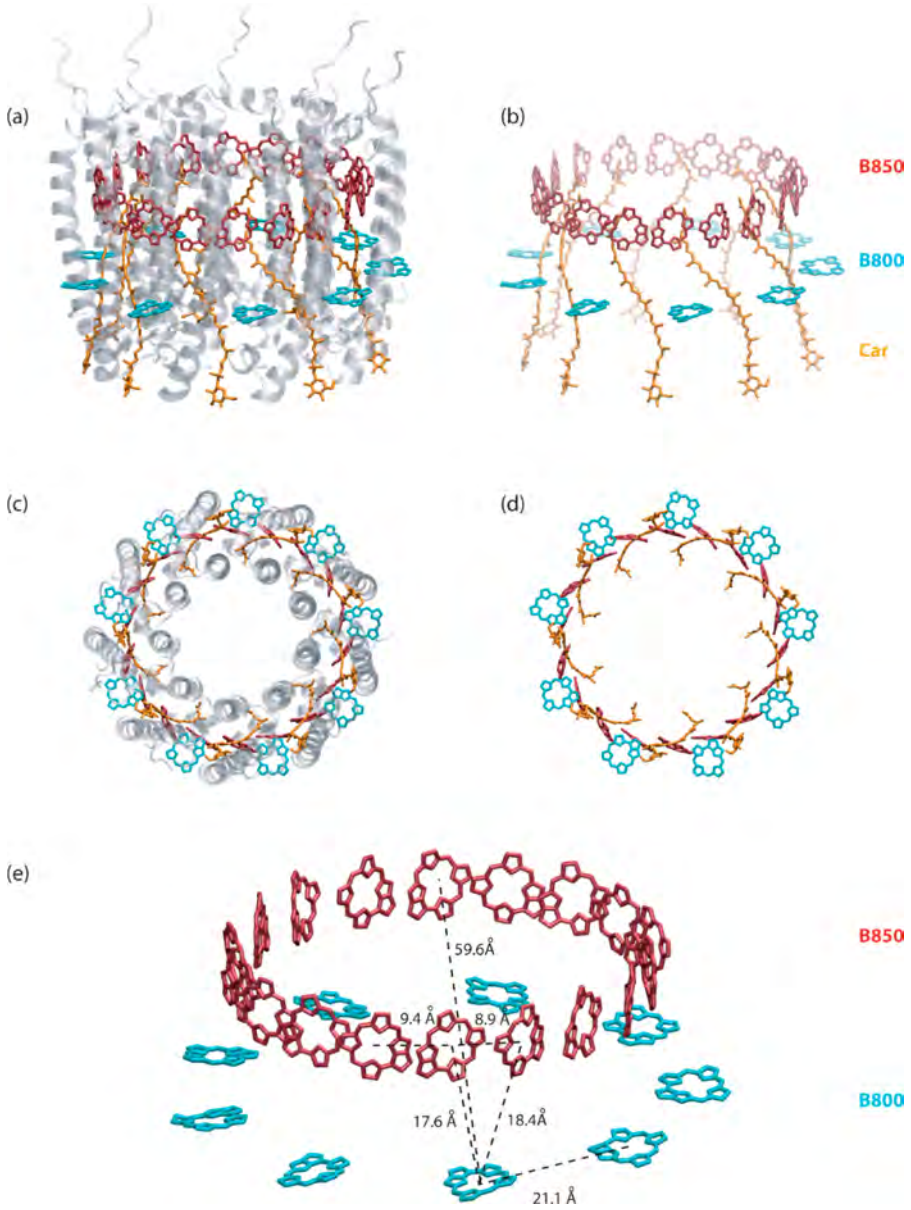

Figure 14. Structural model of the LH2 complex of *Rhodopseudomonas acidophila* [now *Rhodobastus* (*Rbl.*) *acidophilus*]. Views (a,b) parallel and (c,d) perpendicular to the membrane. On the left-hand side, the whole pigment–protein complex is illustrated (apoprotein is in gray), whereas on the right-hand side, the spatial arrangement of BChl *a* chromophores (B800 cyan, B850 red) and carotenoids (orange) is indicated. The phytyl tails of pigments have been removed for clarity. (e) Spatial arrangement illustrating the range of distances between BChl *a* pigments in B800 and B850 rings.

microbial mats, and soil. They are broadly classified as purple sulfur bacteria and purple nonsulfur bacteria and photosynthesize only under anoxic conditions.[13] They contain a range of various bacteriochlorophylls and carotenoids, depending on the species. Purple bacteria utilize one or both of the two types of pigment–protein complexes known as light-harvesting 1 and 2 complexes (LH1 and LH2). LH2, also termed B800–B850, has the role of a peripheral light-harvesting complex, whereas RC-LH1 is the core complex. Both LH1 and LH2 bind carotenoids (Car) and bacteriochlorophylls to maximize the absorption of available light in the green and far-red light of wavelengths above 750 nm.

In this section, the photophysics of light harvesting in species that contain LH1 and LH2 complexes is briefly presented, providing an overview of the energy-transfer pathway. Particular focus is placed on examining the synergetic contributions of the structural and photophysical characteristics of LH2, including spectral shifts originating from variations in the chromophore environment, electronic coupling and the excitonic nature of the B850 ring in LH2, and contributions of disorder and its effect on exciton delocalization.

In various species of purple bacteria that synthesize LH2, this complex serves as the principle light harvester. LH2 transfers excitation energy to LH1, from where excitation is transferred to the reaction centers. LH2 has a characteristic circular nonamer (or octamer) structure consisting of nine (or eight) $\alpha\beta$-apoprotein subunits, as illustrated in Figure 14. The absorption of the LH2 complex in the near-infrared (NIR) region shows bands at 800 and ~850 nm, whereas LH1 shows a single peak at 875 nm. The LH1 core antenna is similar in

DOI: 10.1021/acs.chemrev.6b00002
Chem. Rev. XXXX, XXX, XXX–XXX

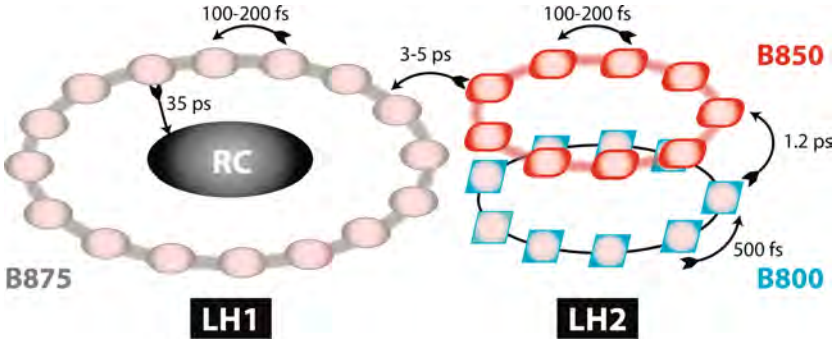

Figure 15. (a) Energy-transfer rates (inverse of the times shown) in the photosynthetic unit of purple bacteria. Figure adapted with permission from ref 199. Copyright 1997 Elsevier. (b) Schematic illustration of the transition dipole moments in neighboring BChl *a* dimers in the B850 ring of LH2 in *Rps. acidophila* [now *Rhodobastus* (*Rbl.*) *acidophilus*].

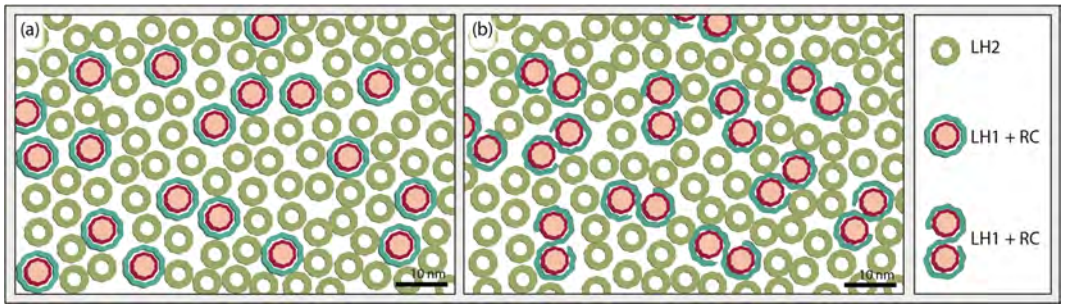

Figure 16. Schematic representation of the diversity of core-complex architectures observed among purple photosynthetic bacteria: (a) monomeric core complex (in, e.g., *Bcl. viridis* and *Rsp. photometricum*) and (b) dimeric core complex comprising two reaction centers surrounded by an S-shaped LH1 assembly (in, e.g., *Rhodobacter*).[206,207]

structure to LH2 but has a larger aggregation number with 16-fold symmetry, where the 32 closely spaced BChl *a* pigments surround the reaction-center complex (Figure 15). The core antenna complex, LH1, is intimately associated with the reaction center (RC). Two primary LH1-RC associations have been identified (Figure 16). In a monomeric "core" complex, the LH1 subunit surrounds the RC, forming a ring, which can be either closed[200] or interrupted.[201] A dimeric core complex $(RC\text{-}LH1)_2$ is observed when two LH1 rings are associated in a "figure eight" structure and is seen in certain *Rhodobacter* species.[202]

High-resolution atomic force microscopy (AFM) experiments have provided incredible pictures of the membranes of purple bacteria.[203−205] Table 1 lists some examples of purple bacteria and their features. Most species of purple bacteria use bacteriochlorophyll *a* (BChl *a*). However, *Blastochloris viridis* uses BChl *b* (absorbing more to the near-infrared range than BChl *a*) and employs only LH1-RC complexes (no LH2).

Table 1. Overview of LH Complexes in Selected Species of Purple Bacteria

species	LH complex
Rhodobacter sphaeroides	LH1, LH2 (BChl *a*)[208]
Rhodopseudomonas (*Rps.*) *acidophila* strain 7050 (and 7750)	LH1, LH2/LH3 (BChl *a*)[209−211]
Rhodopseudomonas (*Rps.*) *acidophila* strain 10050	LH1, LH2 (BChl *a*)[212]
Rhodopseudomonas (*Rps.*) *palustris*	LH1, LH2, LH4 (BChl *a*)[213]
Rhodovulum sulfidophilum	LH1, LH2 (BChl *a*)[214]
Rhodospirillum rubrum	only LH1 (BChl *a*)[215]
Blastochloris viridis	only LH1 (BChl *b*)[215,216]
Rhodobium marinum	only LH1 (BChl *a*)[217]
Halorhodospira abdelmalekii	LH1, LH2 (BChl *b*)[217,218]
Thermochromatium (*Tch.*) *tepidum*	LH1, LH2 (BChl *a*)[219,220]

11. STRUCTURE AND ABSORPTION OF LIGHT-HARVESTING COMPLEXES

The light-harvesting complexes of purple bacteria are notable for their beautiful symmetric ring structures. Determination of the high-resolution structural model of LH2 for *Rhodopseudomonas acidophila* strain 10050, reported in 1995 by Richard Cogdell and co-workers, was a turning point for interpreting spectroscopic data and elucidating detailed molecular-level specifics of the mechanism of light harvesting.[212] This crystal structure together with an abundance of ultrafast and polarized light spectroscopic data have ensured this light-harvesting antenna system to be one of the most studied.[87,221] Here, we do not review the full array of studies of LH2, but instead focus on examples of some of the key concepts that emerged soon after the structure was reported.

One of the best studied structures is that of LH2 from *Rps. acidophila* (Figure 14), a circular nonamer comprising nine $\alpha\beta$-apoprotein subunits, each incorporating three bacteriochlorophyll pigments and one carotenoid molecule.[212,222] The chromophore assembly is best visualized in Figures 14b,d and 17. In the B850 ring, the Mg^{2+} ions in BChls are coordinated alternatively to His30 on the β-apoprotein (β-His30) and to His31 on the α-apoprotein (α-His31). These are key interactions that have both structural and functional importance for the complex. Alia and co-workers (2001) provided a complete assignment of the histidine residues in LH2, indicating that several histidines (α-His37, β-His12, β-His41)

DOI: 10.1021/acs.chemrev.6b00002
Chem. Rev. XXXX, XXX, XXX−XXX

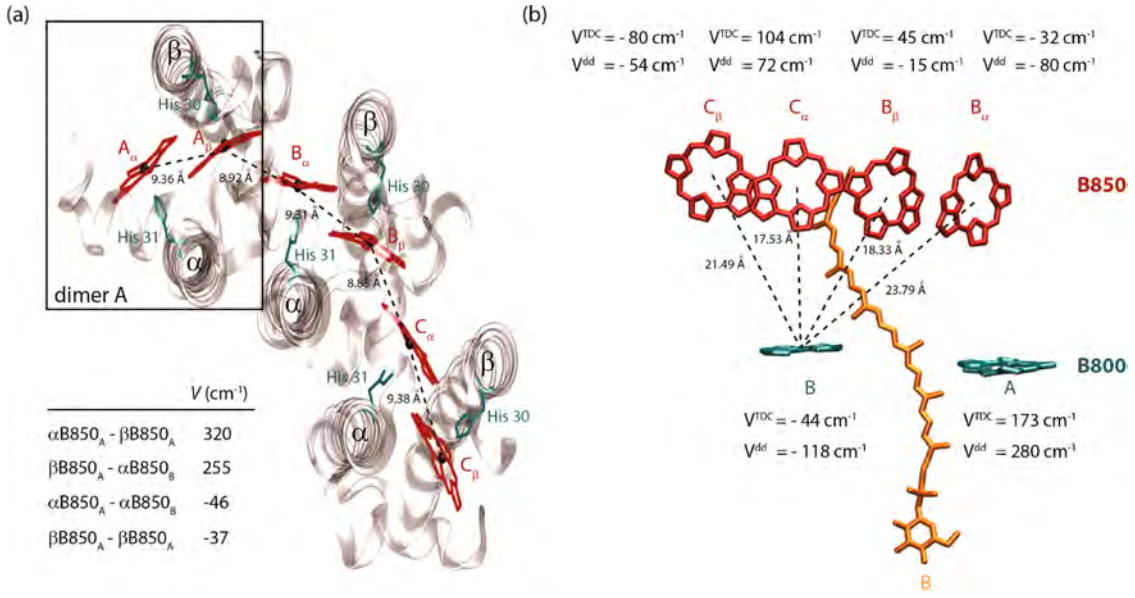

Figure 17. (a) Top view of B850 of *Rhodopseudomonas acidophila* (PDB ID 2FKW) showing the distances (Mg^{2+}–Mg^{2+}) between BChls in one section of the ring. The Mg^{2+} ions are coordinated alternatively to His30 on the β apoprotein (β-His30) and to His31 on the α apoprotein (α-His31). The coupling values can be found in ref 116. (b) Summary of couplings calculated between the BChl Qy transition and the carotenoid S2 transition for LH2. The V^{TDC} values are those calculated by the TDC method for *Rps. acidophila*.[129]

are not coordinated to BChls (Figure 17a).[223] The nine pigments comprising the B800 ring are axially coordinated at their central Mg^{2+} ion by the carboxyl-αM1 at the N-terminus of the α-subunit.[224] Carotenoids make only van der Waals contacts with the three BChl *a* pigments. The LH2 apoprotein structure and its interactions with the pigments are presented in more detail elsewhere.[225]

Room-temperature absorption spectra of the chromophores that constitute LH2 of *Rps. acidophila* are shown in Figure 18a,b. Clear spectral shifts are evident when these pigments are in association with the apoprotein, as in vivo measurements of the membrane indicate (Figure 18c). These red shifts arise from a combination of interactions between chromophores and the protein and electronic interactions between closely spaced chromophores. The kinds of pigment–protein interaction that shift the BChl *a* absorption band include (1) specific coordination of amino acids (e.g., tyrosine) with functional groups on the BChl *a* ring, (2) local polarization of the protein environment, and (3) subtle distortion of the chromophore and its local protein environment.[226−228]

The story of the LH2 structure and spectrum becomes even more fascinating when considering organisms grown under different light conditions. Purple bacteria are known to adapt in two ways when grown under low-light conditions: Some increase the ratio of LH2 to LH1-RC in the membrane, yet others do nothing. A summary is provided in Table 2.

The modified LH2 complex from low-light-adapted purple bacteria shows a distinctly blue-shifted B850 band, typically peaking at ~820 nm. This kind of low-light-adapted LH2 complex is often called LH3 or B800–B820. Incorporation of this blue-shifted antenna into the membrane provides potentially a more directed energy funnel to LH1 (LH3 → LH2 → LH1). This mechanism for low-light adaptation is genetically controlled. The LH2 α/β polypeptides are encoded by a cluster of genes known as the *puc* operon. It turns out that there are multiple genes that encode the LH2 proteins, and members of this family of *puc* operons are selectively expressed depending on light conditions.[229,230] The structural changes responsible for the spectral blue shift were explored by McLuskey et al. (2001) for *Rps. acidophila* strain 10050.[211] Considerable work has also focused on the low-light-adapted LH2 from *Rps. palustris*, LL-LH2 (occasionally referred to as LH4).[230] Brotosudarmo et al. (2011) further confirmed that absorption bands at 800, 820, and 850 nm result not from a mixture of B800–B820 and B800–B850 complexes, but rather from individual low-light LH2 complexes having a heterogeneous $\alpha\beta$-apoprotein composition that varies the site energies of constituent BChl *a* molecules.[230]

One of the insights from these experiments is about the way the membrane is reorganized in response to light conditions during growth. For example, in *Rsp. photometricum* and *Rb. sphaeroides*, the number of LH2 complexes per LH1-RC increases significantly.[204,205] In some cases, a striking development of LH2-rich domains surrounding clusters of LH1-RC complexes has been found (Figure 16a).[235]

11.1. LH2 Model: Electronic Coupling and Excition Formation

Incorporation of structural and functional information on constituent components of the light-harvesting antenna is paramount in elucidating energy-transfer mechanisms and parameters that govern EET processes. As mentioned above, bacteriochlorophyll molecules are present in LH2 antenna complexes at high concentrations forming two rings. Consequently, their spatial arrangement relative to each other has critical implications for chromophore–chromophore interactions and energy transfer.

The monomeric BChl *a* molecules of LH2 associated with the 800-nm absorption band and constituting the B800 ring lie almost flat in *Rsp. acidophila*, positioned at a right angle to the transmembrane α-helix. At a center-to-center distance of approximately 21.1 Å (Figure 14e, Figure 17b), these chromophores are weakly coupled, estimated at ~24 cm^{-1}, resulting in spectral properties associated with localized excitations.[236,237] The anisotropy decay, measured using

DOI: 10.1021/acs.chemrev.6b00002
Chem. Rev. XXXX, XXX, XXX–XXX

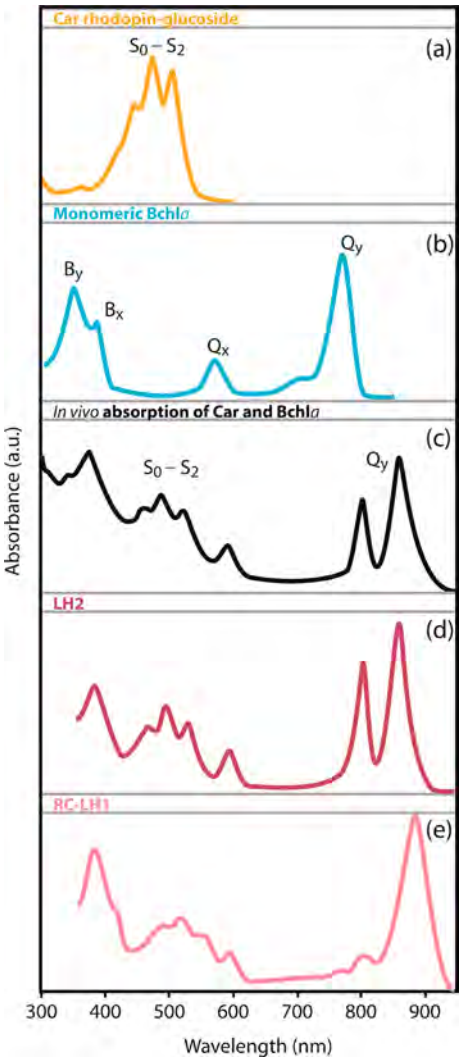

Figure 18. Room-temperature spectra of BChl and Car pigments from *Rps. acidophila*. (a) Solvent-extracted Car rhodopin glucoside in hexane with the characteristic (S_0−S_2) ground-state absorption peak. (b) Monomeric BChl *a* with Soret (B_x and B_y) bands in the UV region and Q_x (590 nm) and Q_y (772 nm) electronic transitions. (c) In vivo absorption of the isolated membrane indicates a red shift of the Car and Q_y absorption bands when the pigments are in association with the apoprotein. The variation in color of isolated and purified (d) LH2 and (e) RC-LH1 complexes is attributed to the difference in Cars that they preferentially bind. Figure adapted with permission from ref 88. Copyright 2006 Cambridge University Press.

polarized excitation pulses, indicates an energy hopping time of ∼1.5 ps between B800 chromophores, but newer pump−probe kinetics experiments in the B800 band showed a biexponential decay of the isotropic transient absorption. A slow component of 1.2−1.9 ps is assigned to the B800−B850 transfer, whereas the B800−B800 hopping is attributed to the fast phase of 0.3−0.8 ps (Figure 15).[238,115]

The second group of bacteriochlorophyll chromophores makes up the 18-member B850 ring (a BChl *a* dimer in each $\alpha\beta$-apoprotein subunit). These pigments are oriented perpendicular to those in the B800 ring. The spacing between the B850 BChl *a* molecules is much smaller than that in B800, at ∼9 Å center-to-center (Figure 14e), resulting in strong intermolecular interactions with electronic coupling between nearest neighbors of ∼300 cm^{-1}.[237,239−242] A simpler picture of the interactions contributing to the B850 excited state is illustrated in Figure 17b, where nearest-neighbor interdimer interactions, V_{ext}, and nearest-neighbor intradimer interactions, V_d, are depicted schematically.[88] As a consequence of the quite strong electronic coupling in the B850 ring, several interesting quantum mechanical effects are observed (vide infra). Examples of such effects are the delocalization of the excitation over the ring, the shift of the absorption of the constituent bacteriochlorophylls to 850 nm, and the development of a band of exciton states distributed over a bandwidth of ∼1200 cm^{-1}.[88] Superradiance, a phenomenon discussed in more detail in section 11.2, is a valuable indicator of exciton delocalization.[243]

The excitonic states of the B850 ring can be described by a well-known model of the circular aggregate.[244,245] In its simplest form, the model consists of *N* identical monomers evenly spaced along a ring. Although this model is a bit too simple to describe the B850 ring of LH2, it serves as a good starting point for understanding the excitonic transitions.[246,247]

Calculation of the ideal circular aggregate model for LH2 (N = 18) results in 18 excitonic states (and therefore absorption bands), labeled k = 0, ±1, ±2, ..., ±8, 9. The wave functions for these purely electronic states are delocalized, extending over the entire ring. Because of the symmetry of the excitonic states for a perfect ring, only the degenerate k = ±1 states are optically allowed. This produces an absorption spectrum that has a single peak that is red-shifted with respect to the monomer transition. The other 16 states are not observed in the absorption spectrum.

Experiments performed on an LH2 mutant lacking the B800 ring enabled the absorption spectrum of the B850 ring to be obtained.[242] Using a combination of linear absorption and

Table 2. Light Adaptation in Purple Bacteria

bacteria	LH2/LH1-RC ratio: normal or high light	LH2/LH1-RC ratio: low light	LH2 blue shift under low-light growth?
Rhodopseudomonas acidophila[231]	5.1[231]	5.9[231]	LH2 (863 nm) → LH3 (823 nm)
Rhodopseudomonas palustris[231]	2.2[231]		LH2 (861 nm) → LH4 (820 nm)
			low-850-nm-absorbing B800−850 complex[232]
Chromatium vinosum[231]	2.2[231]		
Chromatium purpuratum[231]	7.8[231]		
Rhodobacter sphaeroides 2.4.1[231,205]	3.4[231]	increased[205]	no
	1[233]	3[233]	
	2.8[234]	8[234]	
Phaeospirillum molischianum[229]			LH2 (850 nm) → LH3 (820 nm)[229]
Rhodospirillum photometricum[204]	3.5[204]	7[204]	no

DOI: 10.1021/acs.chemrev.6b00002
Chem. Rev. XXXX, XXX, XXX−XXX

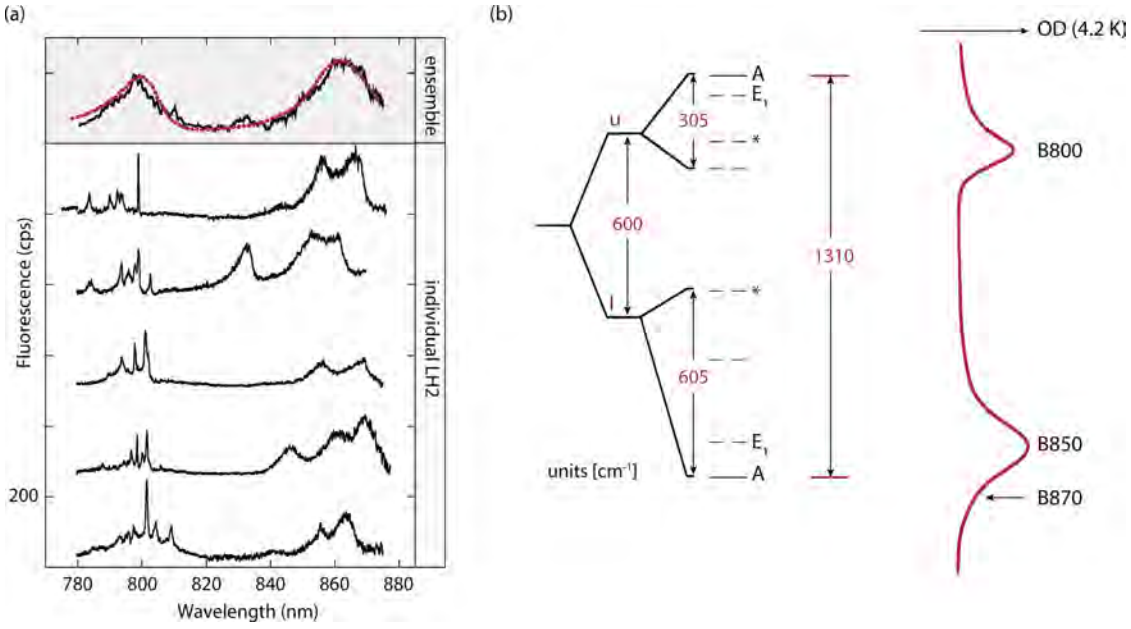

Figure 19. (a) Fluorescence−excitation spectra of individual LH2 complexes of *Rps. acidophila*. The ensemble spectrum (dashed trace, pink) and the sum of the spectra recorded from 19 individual complexes (solid, black) are compared at the top of the panel. Spectra reprinted with permission from ref 248. Copyright 1999 AAAS. (b) The 4.2 K absorption spectrum of LH2 complex from *Rps. acidophila* (strain 10050) (right) and exciton manifold of the B850 ring (left). u and l refer to the upper and lower components, respectively, of the basic B850 dimer, and the energy levels are labeled based on the C_9 symmetry. The $k = 0$ (A) level is nondegenerate and lies lowest for the l manifold and highest for the u manifold. Significant absorption intensity (B850 ring) coincides with the $k = \{1,8\}$ (E_1) level of the l manifold, whereas the u manifold coincides with absorption of the B800 ring. The asterisks indicate two closely spaced doubly degenerate levels. Figure adapted with permission from ref 249. Copyright 1997 American Chemical Society.

circular dichroism spectroscopies, Koolhaas et al. (1998) observed transitions at 780 and 850 nm that were attributed to the B850 ring.[242] The apparent disagreement between this experimental observation and the ideal circular aggregate model is not surprising because the αBChl and βBChl monomeric units comprising the B850 ring lie in different electrostatic environments and have slightly different structures resulting in slightly different energies and couplings.[226] A more realistic model for LH2 would be a circular aggregate consisting of coupled dimeric units. There are two possible ways to apply this model to LH2, either with nine coupled dimers where each dimer unit consists of an $\alpha\beta$BChl pair (Figure 17) or with two coupled monomeric rings of nine βBChls and nine αBChls. The introduction of this heterogeneity into the model changes the selection rules so that the $k = \pm 1$ and $k = \pm 8$ states are allowed transitions. This model explains the experimentally observed transitions at 780 and 850 nm, with the 780-nm transition being assigned to the upper excitonic state and the 850-nm transition to the lower excitonic state (Figure 19b).

11.2. LH2 Model: Disorder and Exciton Delocalization

Although the model based on electronic coupling and two distinct site excitation energies captures some of the main features of the spectroscopic properties, it cannot fully reproduce all of the spectroscopic observables. For example, a low-temperature absorption spectrum of LH2 has a peak at 870 nm that lies lower in energy than the 850-nm transition (Figure 19b).[249] To fully reproduce the experimental observables, theoretical models must also include disorder.[115] Disorder accounts for the fact that, in real systems, the environment of each chromophore of the protein complex is different. As a result, instead of having two values of energies and two values of electronic couplings for αBChl and βBChl monomers, the protein complex exhibits two statistical distributions of energies and two statistical distributions of electronic couplings. When disorder is incorporated into the theoretical model, the excited states are no longer delocalized over the entire ring, but are localized on a few BChl molecules. This leads to a relaxation of the selection rules, with almost all of the excitonic transitions gaining some oscillator strength. The degeneracy of the resulting excitonic states is also lifted.

Disorder in the energies of spectroscopic transitions can be caused by variations in the local environment around the BChl chromophores. Variations in the orientation or relative positions of the chromophores will result in distribution of the electronic coupling, the so-called "off-diagonal" disorder. On the other hand, specific changes in a local molecular environment of pigments, for instance, a change in the protonation state of amino acids near the BChl molecule or structural fluctuations of a hydrogen bond between the pigment and protein, will lead to variations in the exciton energies—"diagonal" disorder. Fluctuations that can cause spectral disorder can be considered "static" on the time scale of the time-resolved spectroscopy experiments.

Although the presence of disorder is accepted, it is a challenge to characterize disorder quantitatively. Typical measurements, such as linear absorption, are ensemble averages that hide detailed information about line broadening.[250,251] Single-molecule spectroscopic techniques can help to some extent by resolving spectra of individual light-harvesting complexes.[248,252] Figure 19a shows a plot of the fluorescence excitation spectra for the ensemble of LH2 complexes along with the spectra of five different individual LH2 complexes.[248] For the ensemble measurement, the figure shows structureless bands associated with the B800 and B850 rings. However, when considering the spectra of the individual complexes, the

DOI: 10.1021/acs.chemrev.6b00002
Chem. Rev. XXXX, XXX, XXX−XXX

transitions associated with the B800 and B850 rings are quite different. The spectrally narrow transitions of the B800 band are consistent with the absorption of individual BChl molecules of the B800 ring, whereas the broader transitions in the B850 band are assigned to excitonic states.

In Figure 19, we see evidence of both intercomplex and intracomplex disorder. Comparing the spectra of the different LH2 complexes, it is evident that each LH2 ring has a unique spectrum and, further, that disorder in the electronic transition energies of BChl chromophores within any ring makes the fluorescence excitation spectrum complex—quite different from the ideal case. Models of disordered rings have allowed for quantitative interpretation of single-molecule spectroscopic data of LH2, indicating also the presence of many complexes with relatively low fluorescence yields, attributed to the presence of a single red-shifted BChl in that complex. That subpopulation emits with a much smaller dipole strength than the typical, while its emission is characterized by a red shift and broadening compared to the "average" complex.[253,254] However, the LH2 ensemble emission spectrum should not be regarded as static, as single-molecule experiments performed by Kunz et al. directly visualized fluctuations of the electron−phonon coupling strength within a single pigment−protein complex, leading to continuous movement of the spectral peak position and variation of the spectral profile for each individual complex.[255]

A different method of estimating disorder involves measuring the delocalization of the exciton. In the case when no disorder is present in the system, theory predicts delocalization of the exciton over the entire ring, whereas delocalization on only a few BChl molecules is expected when disorder is taken into account (for a review, see ref 256). A useful indicator of exciton delocalization is superradiance.[243] Superradiance is a phenomenon whereby the collective emission of fluorescence in a molecular aggregate exhibits a higher radiative rate than the chromophores in isolation. The larger the delocalization, the higher the radiative rate.[257,258] There is a linear relationship between the dipole strength and the radiative rate of the fluorescing state, where a strong increase in the rate provides evidence for delocalization. Experiments performed by Monshouwer and co-workers[243] suggested that LH1 and LH2 complexes have an emitting dipole strength that is 3.8 and 2.8 times that of monomeric BChl *a*, respectively. These measurements of the superradiance combined with modeling suggest that, for the average emitting state, the exciton delocalization length is about 3−4 BChl molecules in LH2 and LH1.[243]

Other time-resolved spectroscopic studies have provided experimental evidence of exciton localization in the B850 ring of LH2.[259,260] These measurements relied on polarization dependent studies to understand how excitation energy flows through the LH2 complex. Jimenez et al. (1996) used polarization-dependent fluorescence upconversion measurements to explore the intraband dynamics of B850;[260] through careful modeling of fluorescence depolarization data, they demonstrated that, by including diagonal disorder in the theoretical model, one could successfully reproduce the experimental results. Furthermore, Jimenez and co-workers were able to determine that the electronic excited states are not delocalized over the entire B850 ring, but localized on approximately five BChls of the B850 ring.[260] This is consistent with pump−probe spectra and anisotropy measurements that suggested that the low-energy excited states of the B850 ring are localized on ∼4 ± 2 BChl molecules.[259,261]

In summary, purple bacteria utilize light-harvesting complexes 1 and 2 (LH1 and LH2), which bind carotenoids and bacteriochlorophylls. Spectral shifts in vivo of constituent chromophores can be attributed to specific coordination of amino acids with functional groups on the BChl *a* ring, local polarization of the protein environment, and subtle distortion of the chromophore and its local protein environment. LH1 has 32 closely spaced BChl *a* pigments that surround the reaction-center complex; LH1 absorption is centered at about 875 nm. LH2 is a nonamer (or octamer) and absorbs at about 800 nm (B800 ring) and 850 nm (B850 ring). In the B800 ring, chromophores are separated by ∼21.1 Å and are weakly coupled, associated with localized excitations. In the B850 ring, chromophores are separated by ∼9 Å, resulting in strong electronic coupling and delocalization of the excitation over the ring. Disorder results from variation in the relative positions or orientations of chromophores, as well as changes in the immediate molecular environment of pigments; the presence of disorder also accounts for the partial exciton delocalization over the B850 ring, in agreement with experimental observations. Adaptation to low-light conditions includes an increase in the LH2/LH1-RC ratio; also, structural modifications to LH2 have been found to be controlled genetically for low-light adaptation. Observed energy-transfer time scales are as follows: LH2 → LH1, 2−5 ps; LH1 → RC, 20−50 ps.

12. ENERGY-TRANSFER TIME SCALES

As a summary of the discussion on energy transfer, several light-harvesting proteins are used here to illustrate various strategies employed by organisms for efficient light harvesting, thereby emphasizing the mechanisms utilized for energy transfer, adopted pathways, and corresponding rates.

12.1. LH2 of Purple Bacteria

Energy-transfer pathways in LH2 complexes and their corresponding rates have been discussed in detail in several reviews and are summarized in Figure 15.[88,184,262,263] The highest rates (<100 fs) are achieved for energy migration within the B850 ring (and B875 ring of LH1 complex) as a result of the strong coupling between bacteriochlorophylls of the ring. In this strong coupling regime, the dynamics of the excitation are described by theories that incorporate excitons, and delocalization of the exciton must be taken into account.[243,256] Experimentally, EET within the ring is typically measured by fluorescence anisotropy or polarization-dependent transient absorption signals.[264−266] The B800 ring exhibits lower coupling between its bacteriochlorophylls, and EET takes place on the 400-fs time scale. Transfer of excitation from B800 to B850 is achieved within 0.7−1 ps depending on the species, strain, and data analysis and is described quite well by generalized Förster theory, as discussed in section 9.

In the isolated LH2 complexes, the excitation is eventually trapped in the lowest exciton state of the B850 ring and relaxes to the ground state within 1 ns, whereas in vivo, the excitons are transferred to other LH2 complexes or the B875 ring of the LH1 complex. For a review, see ref 184. The energy-transfer step from the accessory antenna, LH2, to the core antenna, LH1, depends on the species of the photosynthetic organisms, as the distribution and mutual arrangement of these antennas within the membrane have been found to vary widely. Cleary et al. (2013) noted the importance of the symmetry properties

DOI: 10.1021/acs.chemrev.6b00002
Chem. Rev. XXXX, XXX, XXX−XXX

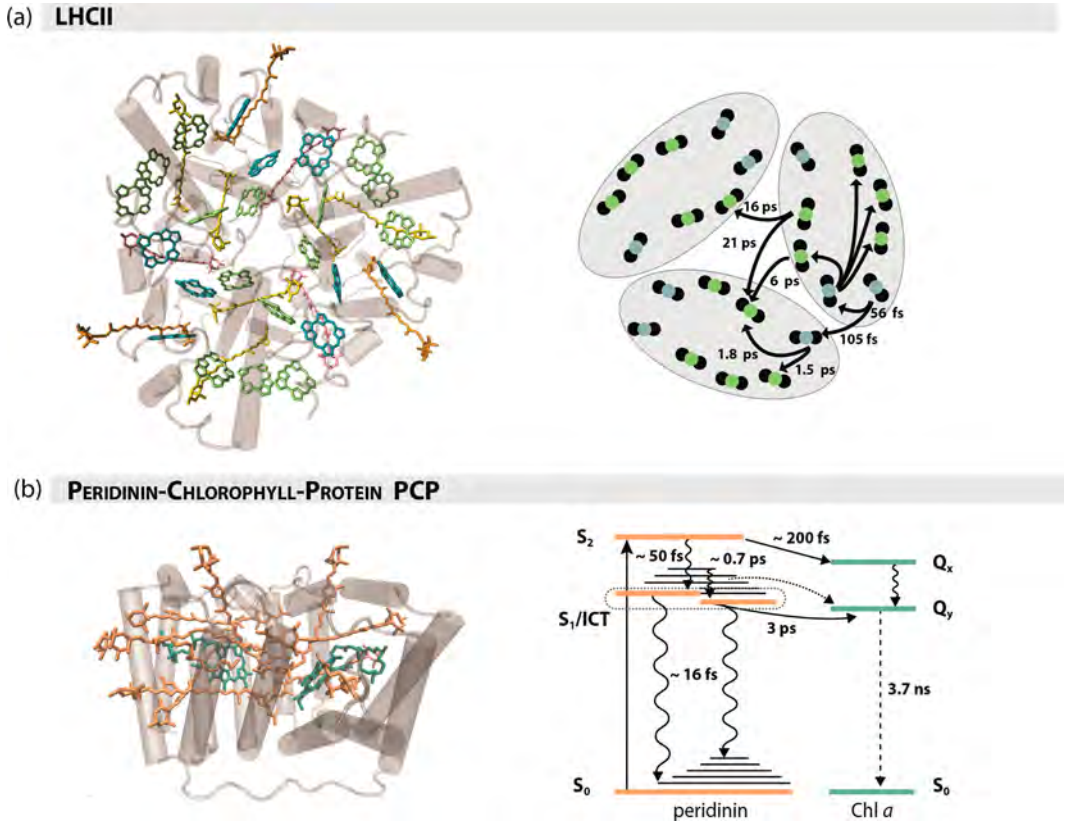

Figure 20. (a) Illustration of pigment arrangement in the LHCII trimer at the stromal side. Green, Chl *a*; blue, Chl *b*; yellow, lutein; orange, neoxanthin; pink, xanthophyll-cycle carotenoids (left). Schematic illustration of the energy-transfer pathways between Chl *a* (green) and Chl *b* (blue) molecules within the stromal-side layer of the LHCII trimer. Figure adapted from ref 277. (b) (Left) Structure of the peridinin-chlorophyll protein. (Right) Energy levels and energy-transfer pathways between peridinin and Chl *a*. For peridinin, the orange lines represent electronic levels, whereas the black lines denote vibrational levels. Figure adapted with permission from ref 297. Copyright 2002 National Academy of Sciences.

both of LH2 rings on the individual complex level, and of their organization on a supramolecular scale, as well as their impact on the efficiency of excitation energy transfer.[267]

An average time scale for energy transfer in LH2 is ∼2−5 ps (Figure 15).[221] A consequence of having circular light-harvesting complexes is that excitation energy migration for LH2 → LH2 or LH2 → LH1 is independent of the relative organization of the rings. In the LH1 complex, the final trapping of the harvested energy by the reaction-center special pair occurs as the energy is transferred from the B875 ring to the RC on a time scale of 20−50 ps.[268−270] This energy-migration step into the RC can be an uphill transfer, as the excited state of the LH1 antenna is lower in energy than the special BChl *a* pair in the reaction center. The slowest EET step occurs over a relatively larger distance because of the separation of B875 chromophores and the RC core (around 40 Å), but the efficiency of light harvesting is not diminished, as the singlet excited-state lifetime of LH1 is fairly long (1−2 ns) and provides more than enough time for efficient EET.

12.2. LHCII of Higher Plants

Higher plants and green algae contain a very heterogeneous light-harvesting apparatus comprising two RCs and numerous antenna proteins. Here, we have photosystem I, photosystem II, and several accessory antenna complexes. Each of the photosystems contains an RC and several inner antenna complexes bound to the RC. In addition, the apparatus contains an accessory antenna complex, LHCII, that can migrate within the membrane. Depending on physiological conditions LHCII associates with either of the photosystems to increase light-harvesting efficiency under low light conditions, or it is detached under excess light conditions. These are so-called "state transitions".[271−273] Excitation dynamics in LHCII attract significant attention because of its role in the nonphotochemical quenching of excited state of Chl *a*, which is discussed briefly below.[274]

In contrast to the LH2 complex of purple bacteria, the LHCII trimer does not have a highly symmetric structure, but rather consists of three monomer subunits, with each containing 13−15 chlorophylls *a* and *b* and 3−4 carotenoids, depending on the species.[275] Coupling between the chlorophylls varies, and thus, both Förster theory and Redfield theory have been used to model the excitation dynamics.[276−278] Carotenoids transfer their energy to chlorophylls on the time scale of <100 fs to the Q_x state and <1 ps to the Q_y state.[279,280] Chlorophyll *b* molecules typically serve as accessory pigments, but in the LHCII complex, some of them are strongly coupled to chlorophyll *a* molecules and, therefore, act as a single "exciton unit". The equilibration time scales between different chlorophyll exciton units vary significantly from <100 fs to >20 ps, as dictated by the coupling strength and the distance between the chlorophylls.[277,279−281]

As an example of possible EET pathways and rates, the results of the combined Förster−Redfield modeling of the LHCII are shown in Figure 20a. For details of the complete calculation based on a quantitative fit of the experimental linear spectra and transient absorption kinetics, see ref 277. It is worth

DOI: 10.1021/acs.chemrev.6b00002
Chem. Rev. XXXX, XXX, XXX−XXX

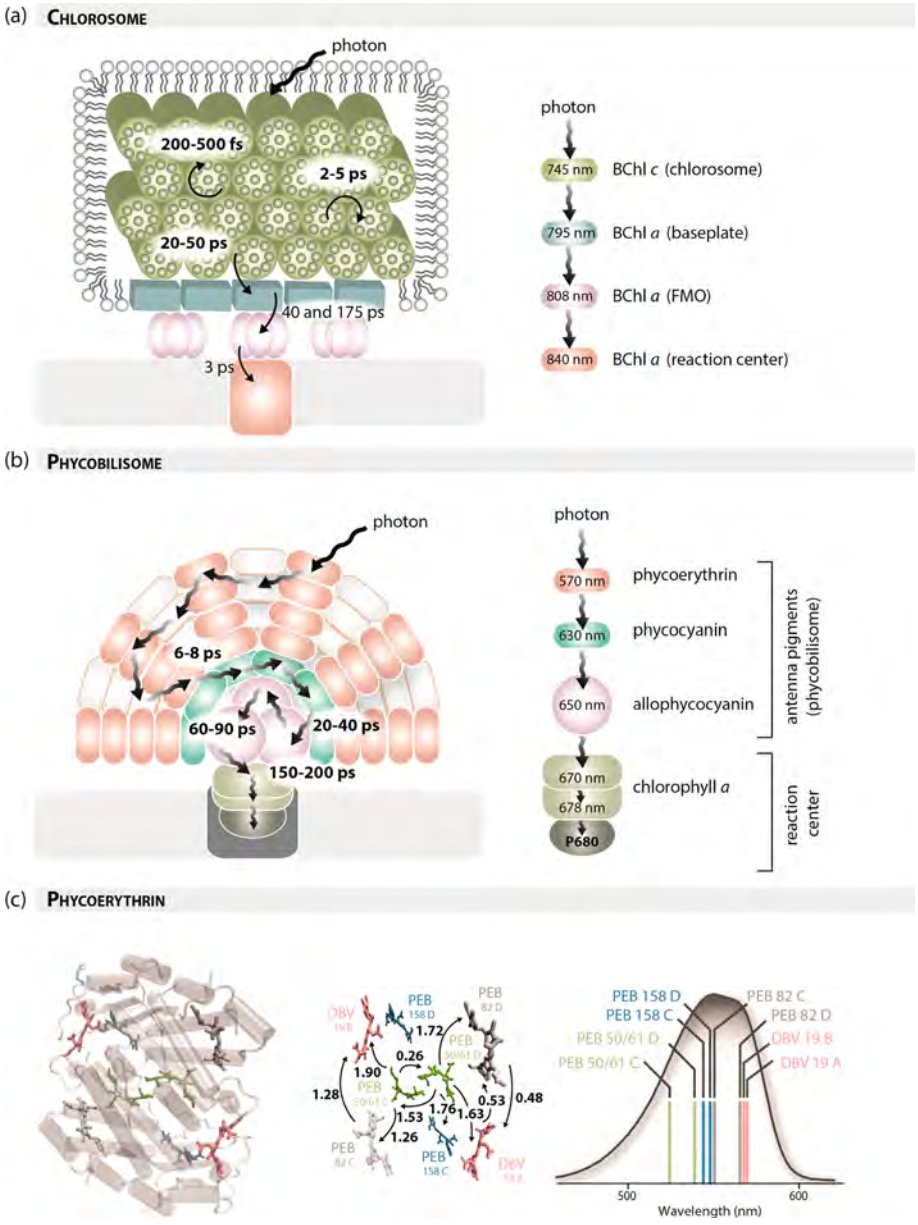

Figure 21. (a) Schematic representation of chlorosome from green bacteria, illustrating the energy-transfer pathway. (b) Architectural organization in a phycobilisome illustrating the energy-transfer steps as the excitation travels through a number of antenna molecules before it reaches the reaction-center chlorophyll (P680) in photosystem II. Figure adapted with permission from ref 300. Copyright 2011 Frontiers Media S.A. (c) Structure of the PE545 phycobiliprotein (left) detailing the time constants of energy transfer (picoseconds) among the eight light-absorbing bilin molecules (middle). Electronic absorption spectrum of the isolated PE545 protein with approximate absorption peaks corresponding to the bilin molecules. Figure adapted with permission from ref 327. Copyright 2013 American Chemical Society.

noting that, in a 2011 study,[282] the slow exciton transfer times were explained through the implicit treatment of the dynamic localization of the excitons in LHCII. The time scale of the transfer process became clear when the dynamical localization of the components was treated explicitly with a nonperturbative hierarchical equation of motion (HEOM) method, demonstrating that a Redfield treatment that neglects such localization effects can give transfer times that are an order of magnitude too fast.[283]

After equilibration in LHCII, the lifetime of the excitation depends significantly on the environment. In the case of isolated proteins (in a buffer solution), relaxation to the ground state takes place on a time scale of 4−5 ns; the LHCII embedded in the membrane has a shorter lifetime of ∼2 ns.[284] However, under high light conditions, additional excitation traps are created for fast quenching of the excess excitation in the antenna. The relaxation time to the ground state in that case can decrease to 200 ps.[285,286] The mechanisms of the nonphotochemical quenching of the excited state of Chl *a* are described in section 13.

12.3. FCP and PCP of Brown and Dinoflagellate Algae

A number of eukaryotic organisms, such as diatoms and dinoflagellates, contain antenna complexes with a high carotenoid-to-chlorophyll ratio (4:1). These carotenoids, fucoxanthin in fucoxanthin-chlorophyll complex (FCP) and peridinin in peridinin-chlorophyll protein (PCP), contain a carbonyl group that significantly alters the electronic properties of the molecule; that is, it results in a new intramolecular

DOI: 10.1021/acs.chemrev.6b00002
Chem. Rev. XXXX, XXX, XXX−XXX

charge-transfer (ICT) state and shifts the absorption spectrum of the carotenoid more to the visible range (500−600 nm).[287,288] Both FCP and PCP are the best examples of complexes where carotenoids make a significant contribution to light harvesting.[289]

Additionally, FCP utilizes chlorophyll *c* as an accessory pigment, which has a porphyrin structure in contrast to the chlorin-type chlorophyll *a*, and the diadinoxanthin carotenoid, which is involved in nonphotochemical quenching of excited-state Chl *a*.[290] The network of energy-transfer pathways has been studied by a number of investigators.[291−294] The fastest EET, ∼100 fs, occurs from the S_2 excited state of fucoxanthin to the Q_x state of chlorophyll *a*. Slower EET, 300−600 fs and 1−2 ps, was assigned to EET from the fucoxanthin S_1/ICT state to the Q_y state of chlorophyll *a*. Finally, the time constants of ∼5−10 ps and 1−3 ns are assigned to chlorophyll *a* Q_y-to-ground-state radiationless relaxation, and a ∼20-ps time constant is assigned to the S_1-to-ground-state radiationless relaxation of the carotenoid (diadinoxanthin and fucoxanthin). The EET from chlorophyll *c* to chlorophyll *a* was found to occur on a <100-fs time scale (below the temporal resolution of the experiment).[291,295] In contrast, Akimoto et al. (2014) assigned a slower EET of ∼600 fs to this pathway.[292]

The excitation dynamics in PCP is similar, but simpler, because of a more homogeneous pigment content (Figure 20b).[296] Again, EET from the peridinin S_2 state to the chlorophyll *a* Q_y state occurs on a <200-fs time scale, whereas 0.7- and 3-ps time constants were reported for peridinin S_1/ICT-to-chlorophyll Q_y energy transfer.[297−299] The radiationless relaxations to the ground states of peridinin and chlorophyll *a* were observed on a 16-ps time scale and a ∼1−3-ns time scale, respectively. It is important to note that the conventional dipole approximation often fails to describe the ultrafast energy transfer from carotenoid to neighboring chlorophyll because of the close proximity of these molecules and the long polyene backbone of the carotenoid. We suggest that the transition density cube (TDC) method, mentioned above, should be employed in this.[129]

12.4. Chlorosomes of Green Sulfur Bacteria

Another unique type of light-harvesting complex, the chlorosome, is present in green sulfur bacteria (Figure 21a). In contrast to most other light-harvesting complexes, chlorosomes do not contain a protein scaffold. Instead, an extremely large number of self-aggregated bacteriochlorophylls (∼200000) are organized in rods, packed in a lipid "sack". In addition to bacteriochlorophylls, chlorosomes contain small amounts of carotenoids, quinones, proteins, and lipids.[301] Detailed description of chlorosomes and bacteriochlorophyll arrangement within it can be found in papers by Ganapathy et al. (2009) and Oostergetel et al. (2010).[302,303] This organization of the pigments allows green sulfur bacteria to harvest light under extremely low-light conditions, possibly even including the tail of blackbody radiation from deep-sea hydrothermal vents.[304]

More typically, green sulfur bacteria are found in environments such as hot sulfur springs and aquatic microbial mats and communities. They photosynthesize only under very low light, at dawn and dusk. During the day, photosynthetic activity is likely suppressed by quenching excitations in the chlorosome. Chlorosomes from green sulfur bacteria are known to exhibit a redox-dependent quenching; this quenching appears to be activated under oxidizing conditions, suppressing energy transfer to the reaction centers.[305−310] We consider it likely that this unusual quenching might serve as a protection mechanism against the formation of toxic reactive oxygen species that might otherwise be a problem for the bacteria when they are exposed to oxygen. This quenching possibly involves the quinione chlorobiumquinone, found uniquely in green sulfur bacteria.

The light energy absorbed by chlorosomes (∼700−800-nm absorption band of bacteriochlorophyll *c*/*e*) is funnelled to the so-called "baseplate", a protein connecting the chlorosome to the membrane, and then, through the Fenna−Matthews−Olson (FMO) complex, to the reaction center. The excitation dynamics within the chlorosomes of various organisms has been a topic of numerous studies.[311−315] Typically, three lifetime components are resolved. The equilibration within a single bacteriochlorophyll rod occurs within 200−500 fs. Slower processes of 2−5 ps are assigned to inter-rod EET, and finally, the energy transfer from bacteriochlorophyll *c*/*e* of the chlorosome to bacteriochlorophyll *a* of the baseplate is known to occur within 20−50 ps. The chlorosomes have inspired research in the field of artificial photosynthesis, where the principles of self-organized chromophores are utilized for increasing the efficiency of solar devices.[316]

12.5. Phycobilisomes of Cyanobacteria

Phycobilisomes are peripheral membrane light-harvesting complexes in the thylakoid membrane (Figure 21b). This complex is a signature of cyanobacteria, the oldest photosynthetic organisms performing oxygenic photosynthesis, and incorporates several types of bilins, open-chain tetrapyrrole pigments. Structurally, phycobilisomes consist of protein rods attached radially to a core protein.[317,318] The elemental units of the phycobilisome are trimers, which are organized into disks. The rods are built of two types of disks, phycoerythrins (PEs) and phycocyanins (PCs). The trimers of the PCs and PEs contain three bilin pigments per trimer. The core, similarly, is built of allophycocyanin (APC) disks with six bilin pigments per monomer. All units (disks within a rod and rod to core) are connected by linker proteins.

The phycobilisome can migrate on the surface of the membrane and attach to either photosystem I or II. Excitation energy is funneled along the rods to the core and through the linker protein to the reaction center. The three types of the proteins, PE, PC and APC, absorb light in the spectral range between 550 and 650 nm, allowing cyanobacteria to increase the absorption cross section compared to those of the chlorophyll-containing antenna complexes of other organisms.

The excitation dynamics in phycobilisomes have been studied for more than 30 years.[319−323] A cascade of energy-transfer processes has typically been described by four components, with the fastest, describing equilibration in the PC complexes, being 6−8 ps, followed by EET from PC to APC on a ∼20−40-ps time scale. The last two steps describe dynamics within the core: EET from APC to the final emitter protein of the phycobilisome (∼60−90 ps) and energy transfer from the terminal emitter to the reaction center, which typically occurs on a 150−200-ps time scale. Over the past decade, the mechanism of photoprotection in cyanobacteria, which differs from nonphotochemical quenching in higher plants, has been of particular interest to many.[324]

12.6. Phycobiliproteins of Cryptophyte Algae

Cryptophytes emerged from cyanobacteria during evolution, which explains why phycobiliproteins are the main antenna

DOI: 10.1021/acs.chemrev.6b00002
Chem. Rev. XXXX, XXX, XXX−XXX

complexes of these algae (Figure 21c). However, in contrast to those of cyanobacteria, the antenna complexes of cryptophytes do not migrate over the membrane. Rather, they are found on the lumenal side of the thylakoid membrane and are arranged in a random matrix. Each cryptophyte species utilizes only one type of phycobiliprotein as its antenna, either a phycocyanin (PC) or a phycoerythrin (PE).[325] The variation in the absorption spectra of these phycobiliproteins stems from the remarkable range of constituent chromophores (bilins) found in the antenna complexes of cryptophytes (Figure 21c).[39] Bilins display a variation in the degree of conjugation, as well as in their oxidation states; they have evolved to absorb in the green, yellow, orange, or red part of the visible spectrum, coinciding with a spectral window that is complementary to chlorophyll *a* absorption.

The excitation dynamics in the antenna complexes of cryptophytes are dictated by the intraprotein coupling between different phycobilin molecules. The ~60-kDa antenna protein consists of four polypeptide chains, α_1, α_2 and two identical β subunits (labeled A, B, C, and D, respectively), which complex into an $\alpha_1\alpha_2\beta\beta$ dimeric structure ($\alpha_1\beta$ and $\alpha_2\beta$ monomers) with a boat-shaped geometry (approximately 75 Å × 60 Å × 40 Å).[326,327] Three time scales of energy migration within the PE and PC proteins can be distinguished: ultrafast equilibration/exciton relaxation within coupled phycobilins (<1 ps), intermediate step of EET between different neighboring phycobilins (1−8 ps), and energy transfer to the lowest-energy phycobilins (20−50 ps).[328,329] In the intact system, the energy-transfer pathways from phycobiliproteins to photosystems I and II exhibit similar time scales, and it becomes a challenging task to disentangle the excitation dynamics.[330]

Furthermore, particular interest in phycobiliproteins of cryptophyte algae has now arisen because two-dimensional electronic spectroscopy has revealed signatures of electronic coherence.[331−333] For reviews on coherence in photosynthetic antenna complexes, see refs 136, 334, and 335.

13. CAROTENOIDS AND PHOTOPROTECTION

Carotenoids are multifunctional chromophores and are vital components of biological tissues in both plants and animals. More than 600 varieties of carotenoids are found in different organisms.[336] Their roles vary greatly: For example, they act as building blocks by helping proteins to fold; they protect organisms against damaging oxygen species (antioxidant role) with potential anticancer function; they act as accessory pigments in plants, contributing to light-harvesting and energy-transfer processes; and they even participate in signaling in plants and animals, for instance, by changing the coloration of plumage and skin of birds.[337−340]

In photosynthetic organisms, carotenoids widen the absorption cross section and absorb light in the blue-green region of the solar spectrum and transfer excitation energy toward the red-shifted chlorophyll-type pigments, in the singlet−singlet EET step. The interpretation of the mechanisms of singlet−singlet EET from Cars to bacteriochlorophylls in LH complexes is complicated because of the proximity of the pigments, and it cannot be effectively described using Förster theory. Several researchers have attempted to calculate the EET rates in this system using different theoretical approaches.[129,236,341] The Car-to-BChl energy transfer can take place from the two lowest excited states of Cars, denoted S_2 and S_1 (Figure 22).

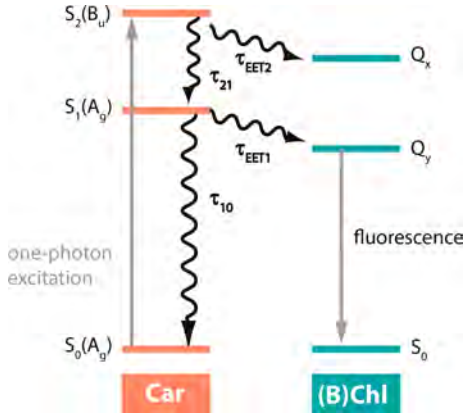

Figure 22. Energy level scheme for carotenoid−chlorophyll interactions. Figure adapted with permission from ref 116. Copyright 2006 Wiley.

There are cases in which Car-to-BChl energy transfer occurs only from the S_2 state of the carotenoids, which limits the overall efficiency of transfer to <60%, whereas in other systems, EET takes place with increased efficiency from both the S_2 and S_1 excited states.[88,342,343] Because of strong light absorption by the Car S_2 state, the efficiency of EET through S_2 can be determined in accordance with Förster theory. However, the full Coulombic interaction between Cars and BChls must be calculated, because the dipole−dipole approximation is invalidated by the close proximity of the interacting pigments.[129,344−346] In contrast, the Car S_1 state does not absorb light (it is called a "dark" state), and its participation in the energy transfer can be calculated only if the borrowing of intensity from the S_2 state is taken into account.[344−347] The presence of additional low-lying Car excited states between S_2 and S_1 has complicated the picture further.[348−350] Evidence for the participation of these additional excited singlet states has been experimentally demonstrated.[291,343,351−355]

Furthermore, carotenoids are well-known for their photoprotective role, particularly against singlet oxygen ($^1O_2$) and other reactive oxygen species (ROS). Singlet oxygen is formed from the ground triplet-state oxygen ($^3O_2$) with the help of the long-lived triplet state of sensitizer molecules, Chl in the case of oxygenic photosynthetic organisms. Carotenoids facilitate the deactivation of (B)Chl triplet excited states (^{3}Chl) through a triplet−triplet energy-transfer reaction.[337]

The ground state of oxygen is a triplet state ($^3O_2$); therefore, oxygen in its ground state can efficiently accept excitation energy from other molecules only if they are in the excited triplet state (e.g., eq 21a). $^1O_2$ is highly reactive and can oxidize pigments, proteins and lipids in the membrane, and therefore is lethal to living tissues.[337,356]

$$^3\text{BChl} + {}^3O_2 \rightarrow \text{BChl} + {}^1O_2 \quad (21a)$$

$$^3\text{BChl} + \text{Car} \rightarrow \text{BChl} + {}^3\text{Car} \quad (21b)$$

$$^1O_2 + \text{Car} \rightarrow {}^3O_2 + {}^3\text{Car} \quad (21c)$$

The mechanism of triplet−triplet energy transfer is different from Förster resonance energy transfer, because, as was mentioned above, de-excitation of any triplet state requires a change in the spin orientation and, therefore, is spin-forbidden (although the overall process of triplet−triplet EET is spin-allowed). Triplet−triplet EET rather proceeds through orbital-

DOI: 10.1021/acs.chemrev.6b00002
Chem. Rev. XXXX, XXX, XXX−XXX

overlap-dependent electronic coupling; see eq 8.[157,357−359] This mechanism is often referred to as Dexter EET, although, strictly, different kinds of interchromophore orbital overlap effects dominate compared to the exchanger interaction identified by Dexter.[157,358] The rate of the quenching of ^{3}BChl by carotenoids (eq 21b) is on the order of a few nanoseconds, 3 orders of magnitude larger than the rate of the bimolecular collision reaction with oxygen.[360,361]

Furthermore, carotenoids are also able to scavenge $^1O_2$ directly, if any is formed (eq 21c). The energy requirements for the role of carotenoids in photoprotection are illustrated in Figure 23. The energy level of the first triplet state of Car is

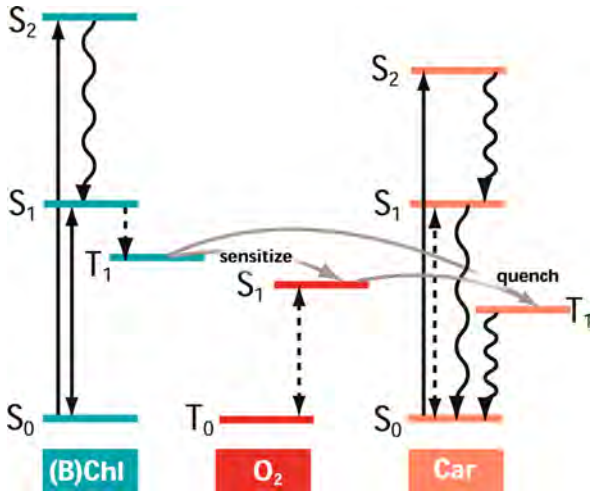

Figure 23. Schematic diagram illustrating the transitions in BChl, oxygen, and a carotenoid (with nine or more conjugated bonds). Solid arrows represent allowed transitions, and dotted arrows illustrate forbidden transitions, whereas wavy arrows show internal conversion. Figure adapted with permission from ref 366. Copyright 2005 Elsevier.

lower than that of BChl, to allow deactivation of that triplet state. Additionally, T_1(Car) must also be lower in energy than $S_1(O_2)$ so as to not act as a sensitizer in the production of singlet oxygen itself. These conditions are satisfied for carotenoids with nine or more conjugated bonds.[362,363] A number of reviews provide further information on these protective pathways.[363−365]

In addition to quenching already formed chlorophyll triplet states, carotenoids can also prevent their formation. Because the photochemical capacities of photosystems are limited under high-light conditions, the RC cannot utilize all of the excitation energy absorbed by antenna and chlorophyll excitation, which accumulates on photosynthetic complexes.[367] Utilizing sophisticated switch mechanisms, plants and algae transform their photosynthetic apparatus from an "efficient-light-harvesting" mode to an "excess-energy-dissipation" mode, where singlet excitation of chlorophylls is converted to heat, prior to the formation of chlorophyll triplet states.[128,368] The process of adaptive thermal dissipation of chlorophyll energy is known as nonphotochemical quenching (NPQ) of chlorophyll excited states and is shown in Figure 24. Carotenoids play a key role in the NPQ switch mechanisms by (i) changing the conformation of the LHCII protein into a quenched state, (ii) forming carotenoid−chlorophyll charge-transfer states, and (iii) opening up fast channels for the quenching of chlorophyll excited states through energy transfer to short-lived carotenoid excited states.[285,286,369−373] Of particular relevance are xanthophylls,

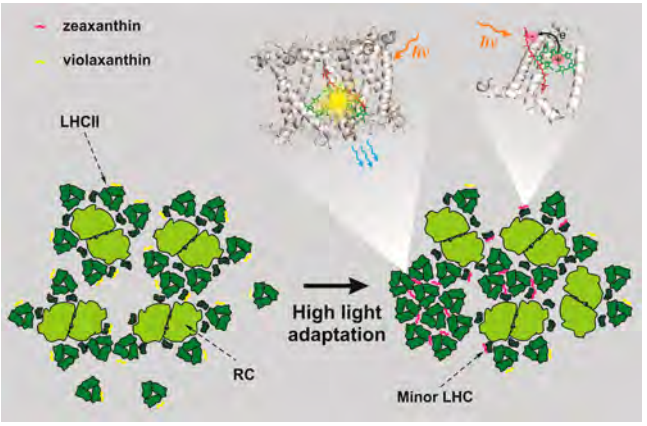

Figure 24. Schematic representation of nonphotochemical quenching of the excited state of chlorophyll in thylakoid membranes. (Left) Light-harvesting regime, (right) quenched regime, and (top) two NPQ mechanisms. Xanthophyll carotenoids in epoxidized (violaxanthin) and de-epoxidized (zeaxanthin) conformations are shown in yellow and red, respectively. Figure adapted with permission ref 284. Copyright 2012 Elsevier.

which experience conformational change in a cycle, triggered under excess light.[368,374] In a fully de-epoxidized conformation of a xanthophyll, zeaxanthin increases thermal dissipation of photosystem II, whereas in violaxanthin (in the epoxidized conformation of a xanthophyll), the light-harvesting function prevails. A detailed description of NPQ processes in photosynthetic organisms can be found in referenced articles and book chapters.[274,375−377]

In summary, carotenoids help proteins fold, protect organisms against damaging oxygen species, act as accessory pigments in plants, and participate in signaling. The Car-to-BChl energy transfer can occur from the Car S_1 or S_2 state. S_2 absorbs strongly and Förster theory with modifications (due to close proximity of chromophores) can be used to estimate rates of ensuing EET. S_1, however, is a dark state and energy transfer occurs by either a breakdown of the dipole approximation or by orbital overlap effects. Carotenoids play a photoprotective role by deactivating the BChl triplet excited states, which otherwise can transform ground triplet state of oxygen to a highly hazardous singlet form. Carotenoids also play a key role in nonphotochemical quenching, NPQ, allowing for thermal dissipation of excess chlorophyll energy by acting as a direct quencher, formating carotenoid-chlorophyll charge transfer states[284,372] and opening up fast channels for quenching of chlorophyll excited states via energy transfer to short lived carotenoid excited states.

14. TRAPPING OF ENERGY

An interesting activity would be to determine the rate-limiting step, or the position of the kinetic bottleneck, in the chain of events that follow absorption, energy migration (transfer), and final entry of excitation energy into the chain of electron-transfer processes at the reaction centers. The overall photochemical efficiency in a light-harvesting system will ultimately depend on the interconnected parameters describing the size of the antenna, the average transfer rates, and the competition between detrapping and photochemical processes that occur at the reaction centers. The dynamic aspects of exciton transport were also previously studied in molecular crystals, where the total rate of exciton trapping was attributed

DOI: 10.1021/acs.chemrev.6b00002
Chem. Rev. XXXX, XXX, XXX−XXX

to both the rate at which the excitons diffused into areas occupied by trap molecules and the rate of capture at which excitons decay to trap states once they enter the "sphere of influence" of the traps.[378,379] In analogy, in photosynthetic systems, following the original formation of an exciton, its lifetime can be subdivided into three stages: (a) exciton migration through transfer steps between constituent pigments of the light-harvesting assembly ($\langle\tau_{migr}\rangle$; i.e., the time required to reach the photoactive pigment of the reaction center for the first time after its generation), (b) delivery of the excitation energy to the reaction center ($\langle\tau_{del}\rangle$), and (c) trapping time in the reaction center ($\langle\tau_{trap}\rangle$)[380−382]

$$\langle\tau\rangle = \langle\tau_{migr}\rangle + \langle\tau_{del}\rangle + \langle\tau_{trap}\rangle \quad (22)$$

The value of the first passage time depends on the spatial and energetic landscapes of the integral antenna pigments, which dictate the number of transfer steps and their respective kinetics. Typical models describe the trapping time as dependent on the photochemical quenching parameter at the reaction centers, as well as the rate constants associated with the forward and backward transfer times of the exciton to the reaction-center chromophores, k_t and k_{-t}.[380] The relative values of the rate constants, k_t and k_{-t}, determine the classification of the trap. A deep trap is defined for $k_t/k_{-t} \gg 1$, where the migration of the excitation from the reaction center back to the antenna system is fairly low and the excitation is often irreversibly quenched as kinetics of photochemistry dominate over the time scale of detrapping. The irreversibility of the trapping essentially describes this model as "diffusion-limited", as the rate of trapping equals the rate of diffusion of the excitation energy to the trap, with $\langle\tau_{migr}\rangle$ as the dominating term in eq 22.

In the case of shallow traps, upon localization of the exciton at the reaction centers, the excitation is allowed to escape, so that excitons can visit a shallow trap a number of times before the excited state is photochemically quenched. This type of system is termed "trap-limited", as the excited-state lifetime is dominated by the term describing the ability of the reaction center to capture the excitation energy from the antenna pigments, $\langle\tau_{trap}\rangle$. The observed overall excited-state lifetime increases with the size of the antenna for both models. For the trap-limited model, the increase is linear and independent of the excitation wavelength. Physically, this implies that excitation of any pigment, independent of its energy and position, will result in energy-migration pathways that involve a number of detrapping steps and high probability of repopulation of the antenna system, so that location of the initial excitation is of no major importance.

Schatz and co-workers (1988) reported an increase in the overall lifetime for PSII complexes with different antenna sizes and suggested that PSII kinetics might follow a trap-limited model.[383] A special case involving a shallow trap was also described, where, even upon photochemical quenching, reverse electron transfer can lead to the re-creation of the excited state of the reaction-center chlorophyll, which can potentially diffuse back into the antenna system.[2] The simplicity of the original exciton-radical-pair-equilibrium (ERPE) model is attributed to the observed scaling law of the fluorescence decay time with N, but its main drawback is that it does not take into account crystal structural information.[87,383] The distances between the reaction center and the antenna pigments are relatively large, possibly necessary to prevent oxidation of antenna pigments, and these large distances were shown to create a bottleneck for the excitation energy transfer in structure-based calculations.[384] More recent studies consistent with structure-based calculations have revealed a more complex picture with slower fluorescence decay times than predicted by the original ERPE model.[385,386]

15. CONCLUDING REMARKS

Substantial advancements have been made toward elucidating the mechanistic details of excitation energy transfer in light-harvesting systems of photosynthetic organisms. Current research goes beyond the scope of deciphering the contributions of the photosynthetic organisms to optimizing this vital process, as the major goal is now to apply these fundamental concepts and employ mimicry for the realization of highly efficient artificial light harvestors. There are, however, some major concepts embedded in the blueprint of naturally occurring antenna complexes that have been revealed and from which researchers can learn to build efficient artificial systems. The total number, their mutual arrangement, their concentration, as well as the variety of pigments all provide vital information for the optimization of light-harvesting systems to be used in artificial systems. The architectural design of the energy landscape of the antenna depends both on the photophysics of the individual components and on the nature of their assembly, which, for example, leads to the variety of coupling regimes that were introduced in this review.

AUTHOR INFORMATION

Corresponding Author

*Tel.: +1 609-258-0729. E-mail: gscholes@princeton.edu.

Notes

The authors declare no competing financial interest.

Biographies

Tihana Mirkovic received her B.Sc. in Chemistry and Mathematics in 2003 from the University of Toronto. In 2009, she obtained her Ph.D. in Physical Chemistry, also from the University of Toronto, with Prof. G. D. Scholes and Prof G. A. Ozin, where her interdisciplinary research encompassed the development of nanomaterials and studies of the photophysical and dynamical aspects of nanoscale systems. As a Postdoctoral Fellow and Research Associate (2010−2014), she worked on elucidating the principles of light harvesting in cryptophyte algae. Currently, she is focusing on chemical education and works as a Sessional Lecturer at the University of Toronto in areas of materials and inorganic and physical chemistry.

Evgeny E. Ostroumov received his Ph.D. in Physics from University of Düsseldorf and Max-Planck-Institute for Bioinorganic Chemistry, where he worked with Prof. Alfred Holzwarth exploring the electronic properties of isolated chromophores and photoprotection mechanisms in high plants. He is currently an Associate Specialist at Princeton University, and his research interests include the development and application of nonlinear multidimensional ultrafast spectroscopy to study dynamics in natural and artificial photoactive systems with the aim of elucidating mechanisms of energy transfer and photoprotection and applications in diagnostics.

Jessica M. Anna is an Assistant Professor and Elliman Faculty Fellow in the Department of Chemistry at the University of Pennsylvania. Jessica joined the faculty at the University of Pennsylvania in July of 2014. Before this, she was a postdoctoral fellow in the Scholes group at the University of Toronto from 2011 to 2014. Before joining the Scholes group, Jessica received her Ph.D. in Physical Chemistry from the University of Michigan in 2011 under the guidance of Kevin

DOI: 10.1021/acs.chemrev.6b00002
Chem. Rev. XXXX, XXX, XXX−XXX

Kubarych and her B.S. from the University of Pittsburgh in 2006, where she worked with David Pratt. Her current research focuses on investigating electronic energy transfer and electron-transfer reactions in natural and artificial light-harvesting complexes and photocatalysts.

Rienk van Grondelle studied physics at VU University Amsterdam. He obtained his Ph.D. under the supervision of Prof. Dr. Lou Duysens. In 1982, he returned to VU University, and in 1987, he was appointed full professor. At VU University, he has built a large research group studying the early events in photosynthesis. R.v.G. has made major contributions to elucidating the fundamental physical mechanisms that underlie light harvesting and charge separation. He has developed theoretical tools for understanding complex spectroscopic data. Using multidimensional electronic spectroscopy, he recently showed that ultrafast charge separation is driven by specific molecular vibrations that allow electronic coherences to stay alive. He proposed a molecular model for photoprotection and demonstrated that the major plant light-harvesting complex operates as a nanoswitch, controlled by its biological environment. These results, of utmost importance for understanding photosynthesis, have inspired technological solutions for artificial and/or redesigned photosynthesis, as a route toward sustainable energy production.

Govindjee is Professor Emeritus of Biophysics, Biochemistry and Plant Biology at the University of Illinois at Urbana−Champaign (UIUC), Urbana, Illinois. He is a Series Editor of "Advances in Photosynthesis and Respiration" (Springer). He holds a B.Sc. (1952) and an M.Sc. (1954) from the University of Allahabad and a Ph.D. (1960; in Biophysics, under Eugene Rabinowitch) from UIUC. He is a fellow of the AAAS; recipient of a Lifetime Achievement Award from the Rebeiz Foundation for Basic Biology, a Liberal Arts and Sciences Alumni Achievement Award from UIUC, a Communication Award from the International Society of Photosynthesis Research, and a B. M. Johri Memorial Award (India) for Excellence in Plant Biology. Govindjee is an author of "Photosynthesis" (1969), has edited over 12 books, and has published over 400 research (and review) articles on photosynthesis. His research has focused on the primary photochemistry of oxygenic photosynthesis, excitation energy transfer in cyanobacteria and algae, and electron transfer from water to NADP. One of his major discoveries was on the unique role of bicarbonate in protonation of a reduced plastoquinone (Q_B^{2-}) on the electron-acceptor side of photosystem II of photosynthesis.

Greg Scholes is the William S. Tod Professor of Chemistry at Princeton University. Originally from Melbourne, Australia, he undertook postdoctoral training at Imperial College London and University of California, Berkeley. He started his independent career at the University of Toronto (2000−2014), where he was the D. J. LeRoy Distinguished Professor. Dr. Scholes is the Deputy Editor of the *Journal of Physical Chemistry Letters*; a Fellow of the Royal Society of Canada; a Senior Fellow in the Canadian Institute for Advanced Research program *Biology, Energy, Technology*; and a Professorial Fellow at the University of Melbourne. Dr. Scholes has had a long-standing interest in the mechanisms of electronic energy transfer and the photophysics of molecular excitons. Current research concerns working out the design principles for directing and regulating light-initiated energy flow in man-made and natural systems, such as proteins involved in photosynthesis.

ACKNOWLEDGMENTS

G.D.S. and R.v.G. acknowledge CIFAR, the Canadian Institute for Advanced Research, through its Bio-Inspired Solar Energy program. This work was supported partially as part of the Photosynthetic Antenna Research Center (PARC), an Energy Frontier Research Center funded by the U.S. Department of Energy, Office of Science, Basic Energy Sciences, under Award DE-SC0001035 and partially by the Natural Sciences and Engineering Research Council of Canada (G.D.S.). Govindjee thanks the Departments of Biochemistry and Plant Biology at the University of Illinois at Urbana−Champaign (UIUC) for supporting him during his retirement since 1999. R.v.G. was supported by VU University, by an Advanced Investigator grant from the European Research Council (No. 267333, PHOTPROT), and by EU FP7 project PAPETS (GA 323901). He gratefully acknowledges his Academy Professor grant from The Netherlands Royal Academy of Sciences (KNAW).

REFERENCES

(1) Rabinowitch, E.; Govindjee. *Photosynthesis*; Wiley: New York, 1969; available at http://www.life.illinois.edu/govindjee/g/Books.html (accessed July 1, 2016).
(2) Blankenship, R. E. *Molecular Mechanisms of Photosynthesis*; Wiley-Blackwell: Hoboken, NJ, 2014.
(3) Allen, J. F. Light, Time and Micro-Organisms. In *Microbial Responses to Light and Time*; Caddick, M. X., Baumberg, S., Hodgson, D. A., Phillips-Jones, M. K., Eds.; Cambridge University Press, 1998; pp 1−31. Available at http://www.jfallen.org/~john/webstar/ltm/ltm.pdf (accessed July 1, 2016).
(4) Abbott, D. Keeping the Energy Debate Clean: How Do We Supply the World's Energy Needs? *Proc. IEEE* **2010**, *98*, 42−66.
(5) Alstrum-Acevedo, J. H.; Brennaman, M. K.; Meyer, T. J. Chemical Approaches to Artificial Photosynthesis. 2. *Inorg. Chem.* **2005**, *44*, 6802−6827.
(6) Balzani, V.; Credi, A.; Venturi, M. Photochemical Conversion of Solar Energy. *ChemSusChem* **2008**, *1*, 26−58.
(7) Barber, J. Photosynthetic Energy Conversion: Natural and Artificial. *Chem. Soc. Rev.* **2009**, *38*, 185−196.
(8) Hambourger, M.; Moore, G. F.; Kramer, D. M.; Gust, D.; Moore, A. L.; Moore, T. A. Biology and Technology for Photochemical Fuel Production. *Chem. Soc. Rev.* **2009**, *38*, 25−35.
(9) Herrero, C.; Lassalle-Kaiser, B.; Leibl, W.; Rutherford, A. W.; Aukauloo, A. Artificial Systems Related to Light Driven Electron Transfer Processes in PSII. *Coord. Chem. Rev.* **2008**, *252*, 456−468.
(10) McConnell, I.; Li, G.; Brudvig, G. W. Energy Conversion in Natural and Artificial Photosynthesis. *Chem. Biol.* **2010**, *17*, 434−447.
(11) Ort, D. R.; Merchant, S. S.; Alric, J.; Barkan, A.; Blankenship, R. E.; Bock, R.; Croce, R.; Hanson, M. R.; Hibberd, J. M.; Long, S. P.; Moore, T. A.; et al. Redesigning Photosynthesis to Sustainably Meet Global Food and Bioenergy Demand. *Proc. Natl. Acad. Sci. U. S. A.* **2015**, *112*, 8529−8536.
(12) Eaton-Rye, J. J., Tripathy, B. C., Sharkey, T. D., Eds. *Photosynthesis: Plastid Biology, Energy Conversion and Carbon Assimilation*; Advances in Photosynthesis and Respiration; Springer: Dordrecht, The Netherlands, 2012; Vol. *34*.
(13) Hunter, C. N., Daldal, F., Thurnauer, M. C., Beatty, J. T., Eds. *The Purple Phototrophic Bacteria*; Advances in Photosynthesis and Respiration; Springer: Dordrecht, The Netherlands, 2009; Vol. *28*.
(14) Drews, G.; Golecki, J. R. Structure, Molecular Organization, and Biosynthesis of Membranes by Purple Bacteria. In *Anoxygenic Photosynthetic Bacteria*; Blankenship, R. E., Madigan, M. T., Bauer, C. E., Eds.; Advances in Photosynthesis and Respiration; Kluwer Academic Publishers: Dordrecht, The Netherlands, 1995; Vol. *2*, Chapter 12, pp 231−257.
(15) Overmann, J. Diversity and Ecology of Phototrophic Sulfur Bacteria. *Microbiol. Today* **2001**, *28*, 116−118.
(16) Nisbet, E. G.; Sleep, N. H. The Habitat and Nature of Early Life. *Nature* **2001**, *409*, 1083−1091.
(17) Govindjee; Govindjee, R. Primary Events in Photosynthesis. *Sci. Am.* **1974**, *231*, 68−82.
(18) Wolosiuk, R. A.; Buchanan, B. B. Photosynthesis: The Carbon Reactions. In *Plant Physiology and Development*, 6th ed.; Taiz, L.,

DOI: 10.1021/acs.chemrev.6b00002
Chem. Rev. XXXX, XXX, XXX−XXX

Zeiger, E., Møller, I. M., Murphy, A., Eds.; Sinauer Associates, Inc.: Sunderland, MA, 2015; Chapter 8.
(19) Emerson, R.; Arnold, W. The Photochemical Reaction in Photosynthesis. *J. Gen. Physiol.* **1932**, *16*, 191−205.
(20) Arnold, W.; Kohn, H. I. The Chlorophyll Unit in Photosynthesis. *J. Gen. Physiol.* **1934**, *18*, 109−112.
(21) Kohn, H. I. Number of Chlorophyll Molecules Acting as an Absorbing Unit in Photosynthesis. *Nature* **1936**, *137*, 706−706.
(22) Warburg, O.; Negelein, E. Über den Energieumsatz bei der Kohlensäureassimilation. *Z. Phys. Chem.* **1922**, *102*, 235−266.
(23) Nickelsen, K.; Govindjee. *The Maximum Quantum Yield Controversy: Otto Warburg and the "Midwest-Gang"*; Bern Studies in the History and Philosophy of Science; Institut für Philosophie, Universität Bern: Bern, Switzerland, 2011.
(24) Hill, J. F.; Govindjee. The Controversy over the Minimum Quantum Requirement for Oxygen Evolution. *Photosynth. Res.* **2014**, *122*, 97−112.
(25) Gaffron, H.; Wohl, K. Zur Theorie der Assimilation. *Naturwissenschaften* **1936**, *24*, 81−90.
(26) Wohl, K. The Mechanism of Photosynthesis in Green Plants. *New Phytol.* **1940**, *39*, 33−64.
(27) Clayton, R. K. The Biophysical Problems of Photosynthesis. *Science* **1965**, *149*, 1346−1354.
(28) Schmid, G. H.; Gaffron, H. Photosynthetic Units. *J. Gen. Physiol.* **1968**, *52*, 212−239.
(29) Mauzerall, D.; Greenbaum, N. L. The Absolute Size of a Photosynthetic Unit. *Biochim. Biophys. Acta, Bioenerg.* **1989**, *974*, 119−140.
(30) Hanzlik, C.; Hancock, L. E.; Knox, R. S.; Guard-Friar, D.; MacColl, R. Picosecond Fluorescence Spectroscopy of The Biliprotein Phycocyanin 612 − Direct Evidence for Fast Energy Transfer. *J. Lumin.* **1985**, *34*, 99−106.
(31) Ley, A. C.; Mauzerall, D. C. Absolute Absorption Cross-Sections for Photosystem II and the Minimum Quantum Requirement for Photosynthesis in *Chlorella Vulgaris*. *Biochim. Biophys. Acta, Bioenerg.* **1982**, *680*, 95−106.
(32) Green, R. B., Parson, W. W., Eds. *Light-Harvesting Antennas in Photosynthesis*; Advances in Photosynthesis and Respiration; Kluwer Academic Publishers: Dordrecht, The Netherlands, 2003; Vol. *13*.
(33) Clegg, R. M.; Sener, M.; Govindjee. From Förster Resonance Energy Transfer to Coherent Resonance Energy Transfer and Back (Invited Paper). In *Optical Biopsy VII: SPIE Proceedings*; Alfano, R. R., Ed.; SPIE: Bellingham, WA, 2010; Vol. *7561*, article 7561-12.
(34) van Grondelle, R. Excitation Energy Transfer, Trapping and Annihilation in Photosynthetic Systems. *Biochim. Biophys. Acta, Rev. Bioenerg.* **1985**, *811*, 147−195.
(35) Richardson, K.; Beardall, J.; Raven, J. A. Adaptation of Unicellular Algae to Irradiance − an Analysis of Strategies. *New Phytol.* **1983**, *93*, 157−191.
(36) Falkowski, P. G.; LaRoche, J. Acclimation to Spectral Irradiance in Algae. *J. Phycol.* **1991**, *27*, 8−14.
(37) Mirkovic, T.; Scholes, G. D. Photosynthetic Light Harvesting. In *Photobiology*; Björn, L. O., Ed.; Springer: New York, 2015; pp 231−241.
(38) Pierson, B. K.; Sands, V. M.; Frederick, J. L. Spectral Irradiance and Distribution of Pigments in a Highly Layered Marine Microbial Mat. *Appl. Environ. Microbiol.* **1990**, *56*, 2327−2340.
(39) Scholes, G. D.; Mirkovic, T.; Turner, D. B.; Fassioli, F.; Buchleitner, A. Solar Light Harvesting by Energy Transfer: From Ecology to Coherence. *Energy Environ. Sci.* **2012**, *5*, 9374−9393.
(40) Agrawal, S. C. Physical Factors Affecting the Flora. *Limnology*; APH Publishing Corporation: New Delhi, India, 1999; Chapter 5, pp 69−88.
(41) Rørslett, B.; Schwarz, A. M.; Hawes, I. Underwater Light Profiles in Some New Zealand Lakes: A Comparison of Log-Linear And Weibull Models. *N. Z. J. Mar. Freshwater Res.* **1996**, *30*, 477−484.
(42) Pierson, B.; Oesterle, A.; Murphy, G. L. Pigments, Light Penetration, and Photosynthetic Activity in the Multi-Layered Microbial Mats of Great Sippewissett Salt Marsh, Massachusetts. *FEMS Microbiol. Lett.* **1987**, *45*, 365−376.
(43) Perrine, Z.; Negi, S.; Sayre, R. Optimization of Photosynthetic Light Energy Utilization by Microalgae. *Algal Res.* **2012**, *1*, 134−142.
(44) Evans, J. R. The Dependence of Quantum Yield on Wavelength and Growth Irradiance. *Aust. J. Plant Physiol.* **1987**, *14*, 69−79.
(45) Terashima, I.; Fujita, T.; Inoue, T.; Chow, W. S.; Oguchi, R. Green Light Drives Leaf Photosynthesis More Efficiently than Red Light in Strong White Light: Revisiting the Enigmatic Question of Why Leaves are Green. *Plant Cell Physiol.* **2009**, *50*, 684−697.
(46) Emerson, R.; Lewis, C. M. The Dependence of the Quantum Yield of Chlorella Photosynthesis on Wave Length of Light. *Am. J. Bot.* **1943**, *30*, 165−178.
(47) Björn, L. O.; Govindjee. The Evolution of Photosynthesis and Its Environmental Impact. In *Photobiology: The Science of Light and Life*; Björn, L. O., Ed.; Springer Science+Business Media: New York, 2015; Chapter 12, pp 255−287.
(48) Kiang, N. Y.; Segura, A.; Tinetti, G.; Govindjee; Blankenship, R. E.; Cohen, M.; Siefert, J.; Crisp, D.; Meadows, V. S. Spectral Signatures of Photosynthesis. II. Coevolution with Other Stars and the Atmosphere on Extrasolar Worlds. *Astrobiology* **2007**, *7*, 252−274.
(49) Qin, L.; Kostić, N. M. Photoinduced Electron Transfer from the Triplet State of Zinc Cytochrome *c* to Ferricytochrome b_5 is Gated by Configurational Fluctuations of the Diprotein Complex. *Biochemistry* **1994**, *33*, 12592−12599.
(50) Mauzerall, D. Why Chlorophyll? *Ann. N. Y. Acad. Sci.* **1973**, *206*, 483−494.
(51) Björn, L. O.; Papageorgiou, G. C.; Blankenship, R. E.; Govindjee. A View Point: Why Chlorophyll a? *Photosynth. Res.* **2009**, *99*, 85−98.
(52) Björn, L. O. Why Are Plants Green? Relationships between Pigment Absorption and Photosynthetic Efficiency. *Photosynthetica* **1976**, *10*, 121−129.
(53) Granick, S. Evolution of Heme and Chlorophyll. In *Evolving Genes and Proteins*; Bryson, V., Vogel, H. J., Eds.; Academic Press: New York, 1965; pp 67−88.
(54) Emerson, R.; Lewis, C. M. The Photosynthetic Efficiency of Phycocyanin in Chroococcus and the Problem of Carotenoid Participation in Photosynthesis. *J. Gen. Physiol.* **1942**, *25*, 579−595.
(55) Haxo, F. T.; Blinks, L. R. Photosynthetic Action Spectra of Marine Algae. *J. Gen. Physiol.* **1950**, *33*, 389−422.
(56) Brody, M.; Emerson, R. The Quantum Yield of Photosynthesis in *Porphyridium cruentum*, and the Role of Chlorophyll *a* in the Photosynthesis of Red Algae. *J. Gen. Physiol.* **1959**, *43*, 251−264.
(57) Duysens, L. Transfer Of Light Energy Within the Pigment Systems Present in Photosynthesizing Cells. *Nature* **1951**, *168*, 548−550.
(58) Ghosh, A. K.; Govindjee. Transfer of the Excitation Energy in *Anacystis nidulans* Grown to Obtain Different Pigment Ratios. *Biophys. J.* **1966**, *6*, 611−619.
(59) Cho, F.; Govindjee. Low-Temperature (4−77 K) Spectroscopy of Chlorella; Temperature Dependence of Energy Transfer Efficiency. *Biochim. Biophys. Acta, Bioenerg.* **1970**, *216*, 139−150.
(60) Lichtlé, C. Effects of Nitrogen Deficiency and Light of High Intensity on *Cryptomonas rufescens* (*Cryptophyceae*): I. Cell and Photosynthetic Apparatus Transformations and Encystment. *Protoplasma* **1979**, *101*, 283−299.
(61) Rhiel, E.; Morschel, E.; Wehrmeyer, W. Correlation of Pigment Deprivation and Ultrastructural Organization of Thylakoid Membranes in *Cryptomonas Maculate* Following Nutrient Deficiency. *Protoplasma* **1985**, *129*, 62−73.
(62) Lewitus, A. J.; Caron, D. A. Relative Effects of Nitrogen or Phosphorus Depletion and Light Intensity on the Pigmentation, Chemical Composition, and Volume of *Pyrenomonas Salina* (Cryptophyceae). *Mar. Ecol.: Prog. Ser.* **1990**, *61*, 171−181.
(63) Arnon, D. I.; McSwain, B. D.; Tsujimoto, H. Y.; Wada, K. Photochemical Activity and Components of Membrane Preparations from Blue-Green Algae: I. Coexistence of Two Photosystems in

DOI: 10.1021/acs.chemrev.6b00002
Chem. Rev. XXXX, XXX, XXX−XXX

Relation to Chlorophyll *a* and Removal of Phycocyanin. *Biochim. Biophys. Acta, Bioenerg.* **1974**, *357*, 231−245.
(64) Campbell, N. A.; Reece, J. B. *Biology*, 7th ed.; Pearson Benjamin Cummings: San Francisco, 2005.
(65) Mader, S. *Biology*, 9th ed.; McGraw-Hill: New York, 2006.
(66) Govindjee; Govindjee, R. Primary Events in Photosynthesis. *Sci. Am.* **1974**, *231*, 68−82.
(67) Chen, M. Chlorophyll Modifications and Their Spectral Extension in Oxygenic Photosynthesis. *Annu. Rev. Biochem.* **2014**, *83*, 317−340.
(68) Tretiak, S.; Chernyak, V.; Mukamel, S. Chemical Bonding and Size Scaling of Nonlinear Polarizabilities of Conjugated Polymers. *Phys. Rev. Lett.* **1996**, *77*, 4656−4659.
(69) Scholes, G. D.; Fleming, G. R.; Olaya-Castro, A.; van Grondelle, R. Lessons From Nature About Solar Light Harvesting. *Nat. Chem.* **2011**, *3*, 763−774.
(70) Wientjes, E.; Roest, G.; Croce, R. From Red to Blue to Far-Red In Lhca4: How Does the Protein Modulate the Spectral Properties of the Pigments? *Biochim. Biophys. Acta, Bioenerg.* **2012**, *1817*, 711−717.
(71) Reddy, K. R.; Jiang, J.; Krayer, M.; Harris, M. A.; Springer, J. W.; Yang, E.; Jiao, J.; Niedzwiedzki, D. M.; Pandithavidana, D.; Parkes-Loach.; et al. Palette of Lipophilic Bioconjugatable Bacteriochlorins for Construction of Biohybrid Light-Harvesting Architectures. *Chem. Sci.* **2013**, *4*, 2036−2053.
(72) Yang, E.; Ruzie, C.; Krayer, M.; Diers, J. R.; Niedzwiedzki, D. M.; Kirmaier, C.; Lindsey, J. S.; Bocian, D. F.; Holten, D. Photophysical Properties and Electronic Structure of Bacteriochlorin−Chalcones with Extended Near-Infrared Absorption. *Photochem. Photobiol.* **2013**, *89*, 586−604.
(73) Wraight, C. A.; Clayton, R. K. The Absolute Quantum Efficiency of Bacteriochlorophyll Photooxidation in Reaction Centers of *Rhodopseudomonas Spheroides*. *Biochim. Biophys. Acta, Bioenerg.* **1974**, *333*, 246−60.
(74) Singsaas, E. L.; Ort, D. R.; DeLucia, E. H. Variation in Measured Values of Photosynthetic Quantum Yield in Ecophysiological Studies. *Oecologia* **2001**, *128*, 15−23.
(75) Rabinowitch, E. I. The Light Factor. I. Intensity. *Photosynthesis and Related Processes*; Interscience Publishers: New York, 1951; Vol. *II*, Part 1, Chapter 28, pp 964−1082.
(76) Moore, G. F.; Brudvig, G. W. Energy Conversion in Photosynthesis: A Paradigm for Solar Fuel Production. *Annu. Rev. Condens. Matter Phys.* **2011**, *2*, 303−27.
(77) Cho, H. M.; Mancino, L. J.; Blankenship, R. E. Light Saturation Curves and Quantum Yields in Reaction Centers from Photosynthetic Bacteria. *Biophys. J.* **1984**, *45*, 455−461.
(78) Loach, P. A.; Sekura, D. L. Primary Photochemistry and Electron Transport in *Rhodospirillum Rubrum*. *Biochemistry* **1968**, *7*, 2642−2649.
(79) Angerhöfer, A.; Cogdell, R. J.; Hipkins, M. F. A Spectral Characterization of the Light-Harvesting Pigment−Protein Complexes from *Rhodopseudomonas acidophila*. *Biochim. Biophys. Acta, Bioenerg.* **1986**, *848*, 333−341.
(80) Cogdell, R. J.; Hipkins, M. F.; MacDonald, W.; Truscott, T. G. Energy Transfer Between the Carotenoid and Bacteriochlorophyll Within the B800−850 Light-Harvesting Pigment−Protein Complex of *Rps. Sphaeroides*. *Biochim. Biophys. Acta, Bioenerg.* **1981**, *634*, 191−202.
(81) Wientjes, E.; van Amerongen, H.; Croce, R. Quantum Yield of Charge Separation in Photosystem II: Functional Effect of Changes in the Antenna Size upon Light Acclimation. *J. Phys. Chem. B* **2013**, *117*, 11200−11208.
(82) Betti, J. A.; Blankenship, R. E.; Natarajan, L. V.; Dickinson, L. C.; Fuller, R. C. Antenna Organization and Evidence for the Function of a New Antenna Pigment Species in the Green Photosynthetic Bacterium *Chloroflexus aurantiacus*. *Biochim. Biophys. Acta, Bioenerg.* **1982**, *680*, 194−201.
(83) van Dorssen, R. J.; Amesz, J. Pigment Organization and Energy Transfer in the Green Photosynthetic Bacterium Chloroflexus Aurantiacus. III. Energy Transfer in Whole Cells. *Photosynth. Res.* **1988**, *15*, 177−189.
(84) Vasmel, H.; VanDorssen, R. J.; DeVos, G. J.; Amesz, J. Pigment Organization and Energy Transfer in the Green Photosynthetic Bacterium *Chloroflexus aurantiacus* 1. The Cytoplasmic Membrane. *Photosynth. Res.* **1986**, *7*, 281−294.
(85) Schmidt am Busch, M.; Müh, F.; El-Amine Madjet, M.; Renger, T. The Eighth Bacteriochlorophyll Completes the Excitation Energy Funnel in the FMO Protein. *J. Phys. Chem. Lett.* **2011**, *2*, 93−98.
(86) Redlinger, T.; Gantt, E. A Mr 95,000 Polypeptide in *Porphyridium Cruentum* Phycobilisomes and Thylakoids: Possible Function in Linkage of Phycobilisomes to Thylakoids and in Energy Transfer. *Proc. Natl. Acad. Sci. U. S. A.* **1982**, *79*, 5542−5546.
(87) van Grondelle, R.; Dekker, J. P.; Gillbro, T.; Sundström, V. Energy Transfer and Trapping in Photosynthesis. *Biochim. Biophys. Acta, Bioenerg.* **1994**, *1187*, 1−65.
(88) Cogdell, R. J.; Gall, A.; Köhler, J. The Architecture and Function of the Light-Harvesting Apparatus of Purple Bacteria: From Single Molecules to in Vivo Membranes. *Q. Rev. Biophys.* **2006**, *39*, 227−324.
(89) Sprague, S. G.; Fuller, R. C. The Green Phototrophic Bacteria and Heliobacteria. In *Structure of Phototrophic Prokaryotes*; Stolz, J. F., Ed.; CRC Press: Boca Raton, FL, 1991; Chapter 4, pp 79−104.
(90) Bryant, D. A. *The Molecular Biology of Cyanobacteria*; Kluwer Academic Publishers: Dordrecht, The Netherlands, 1994.
(91) van de Meene, A. M.; Hohmann-Marriott, M. F.; Vermaas, W. F.; Roberson, R. W. The Three-Dimensional Structure of the Cyanobacterium *Synechocystis sp.* PCC 6803. *Arch. Microbiol.* **2006**, *184*, 259−270.
(92) Ruban, A. V.; Johnson, M. P. Visualizing the Dynamic Structure of the Plant Photosynthetic Membrane. *Nat. Plants* **2015**, *1*, 15161-1−15161-9.
(93) Kirchhoff, H. Architectural Switches in Plant Thylakoid Membranes. *Photosynth. Res.* **2013**, *116*, 481−487.
(94) Hohmann-Marriott, M. F.; Blankenship, R. E. Evolution of Photosynthesis. *Annu. Rev. Plant Biol.* **2011**, *62*, 515−548.
(95) Hohmann-Marriott, M. F., Ed. *The Structural Basis of Biological Energy Generation*; Advances in Photosynthesis and Respiration. Springer: Dordrecht, The Netherlands, 2014; Vol. *39*.
(96) Franck, J.; Teller, E. Migration and Photochemical Action of Excitation Energy in Crystals. *J. Chem. Phys.* **1938**, *6*, 861−872.
(97) Sauer, K.; Calvin, M. Molecular Orientation in Quantasomes. I. Electric Dichroism and Birefringence of Quantasomes from Spinach Chloroplasts. *J. Mol. Biol.* **1962**, *4*, 451−466.
(98) Park, R. B.; Pon, N. G. Chemical Composition and the Substructure of Lamellae Isolated from *Spineracea Oleracea* Chloroplasts. *J. Mol. Biol.* **1963**, *6*, 105−114.
(99) Pearlstein, R. M. Photosynthetic Exciton Theory in the 1960s. *Photosynth. Res.* **2002**, *73*, 119−126.
(100) Duysens, L. N. M. Transfer of Excitation Energy in Photosynthesis. Ph.D. Thesis, University of Utrecht, Utrecht, The Netherlands, 1952.
(101) Pearlstein, R. M. Migration and Trapping of Excitation Quanta in Photosynthetic Units. Ph.D. Thesis, University of Maryland, College Park, MD, 1966.
(102) Pearlstein, R. M. Migration and Trapping of Excitation Quanta in Photosynthetic Units. *Brookhaven Symp. Biol.* **1967**, *19*, 8−15.
(103) Robinson, G. W. Excitation Transfer and Trapping in Photosynthesis. *Brookhaven Symp. Biol.* **1967**, *19*, 16−48.
(104) Montroll, E. W. Random Walks on Lattices. III. Calculation of first-Passage Times with Application to Exciton Trapping on Photosynthetic Units. *J. Math. Phys.* **1969**, *10*, 753−765.
(105) Gulotty, R. J.; Mets, L.; Alberte, R. S.; Fleming, G. R. Picosecond Fluorescence Study of Photosynthetic Mutants of *Chlamydomonas Reinhardee*: Origin of the Fluorescence Decay Kinetics of Chloroplasts. *Photochem. Photobiol.* **1985**, *41*, 487−496.
(106) Lavorel, J.; Joliot, P. A Connected Model of the Photosynthetic Unit. *Biophys. J.* **1972**, *12*, 815−831.
(107) Paillotin, G. Motion of Excitons in Photosynthetic Units. In *Photosynthesis, Two Centuries After Its Discovery by Joseph Priestley: Proceedings of the IInd International Congress on Photosynthesis Research*;

DOI: 10.1021/acs.chemrev.6b00002
Chem. Rev. XXXX, XXX, XXX−XXX

Forti, G., Avron, M., Melandri, A., Eds.; N. V. Publishers: The Hague, The Netherlands, 1972; Vol. *1*, pp 331−336.
(108) Bernhardt, K.; Trissl, H. W. Theories for Kinetics and Yields of Fluorescence and Photochemistry: How, if at all, Can Different Models of Antenna Organization Be Distinguished Experimentally? *Biochim. Biophys. Acta, Bioenerg.* **1999**, *1409*, 125−142.
(109) Bakker, J. G. C.; van Grondelle, R.; den Hollander, W. T. F. Trapping, Loss and Annihilation of Excitations in a Photosynthetic System: II. Experiments with the Purple Bacteria *Rhodospirillum rubrum* and *Rhodopseudomonas capsulata*. *Biochim. Biophys. Acta, Bioenerg.* **1983**, *725*, 508−518.
(110) Vos, M.; van Grondelle, R.; van der Kooij, F. W.; van de Poll, D.; Amesz, J.; Duysens, L. N. M. Singlet-Singlet Annihilation at Low Temperatures in the Antenna of Purple Bacteria. *Biochim. Biophys. Acta, Bioenerg.* **1986**, *850*, 501−512.
(111) Sonneveld, A.; Rademaker, H.; Duysens, L. N. M. Chlorophyll a Fluorescence as a Monitor of Nanosecond Reduction of the Photooxidized Primary Donor P-680′ of Photosystem II. *Biochim. Biophys. Acta, Bioenerg.* **1979**, *548*, 536−551.
(112) Joliot, P.; Joliot, A. Étude cinétique de la réaction photochemique libérant l'oxygene au cours de la photosynthèse. *C. R. Acad. Sci., Paris* **1964**, *258*, 4622−4625.
(113) Paillotin, G.; Swenberg, C. E.; Breton, J.; Geacintov, N. E. Analysis of Picosecond Laser Induced Fluorescence Phenomena in Photosynthetic Membranes Utilizing a Master Equation Approach. *Biophys. J.* **1979**, *25*, 513−533.
(114) Den Hollander, W. T. F.; Bakker, J. G. C.; van Grondelle, R. Trapping, Loss and Annihilation of Excitations in a Photosynthetic System. I. Theoretical Aspects. *Biochim. Biophys. Acta, Bioenerg.* **1983**, *725*, 492−507.
(115) van Grondelle, R.; Novoderezhkin, V. I. Energy Transfer in Photosynthesis: Experimental Insights and Quantitative Models. *Phys. Chem. Chem. Phys.* **2006**, *8*, 793−807.
(116) Scholes, G. D.; Fleming, G. R. Energy Transfer and Photosynthetic Light Harvesting. *Adv. Chem. Phys.* **2005**, *13*, 57−129.
(117) Cheng, Y.-C.; Fleming, G. R. Dynamics of Light Harvesting in Photosynthesis. *Annu. Rev. Phys. Chem.* **2009**, *60*, 241−262.
(118) Renger, T.; Müh, F. Understanding Photosynthetic Light-Harvesting: A Bottom up Theoretical Approach. *Phys. Chem. Chem. Phys.* **2013**, *15*, 3348−3371.
(119) Olbrich, C.; Kleinekathöfer, C. Time-Dependent Atomistic View on the Electronic Relaxation in Light-Harvesting System II. *J. Phys. Chem. B* **2010**, *114*, 12427−12437.
(120) Olbrich, C.; Strümpfer, J.; Schulten, K.; Kleinekathöfer, U. Quest for Spatially Correlated Fluctuations in the FMO Light-Harvesting Complex. *J. Phys. Chem. B* **2011**, *115*, 758−764.
(121) Shim, S.; Rebentrost, P.; Valleau, S.; Aspuru-Guzik, A. Atomistic Study of the Long-Lived Quantum Coherences in the Fenna−Matthews−Olson Complex. *Biophys. J.* **2012**, *102*, 649−660.
(122) Curutchet, C.; Kongsted, J.; Munoz-Losa, A.; Hossein-Nejad, H.; Scholes, G. D.; Mennucci, B. Photosynthetic Light-Harvesting is Tuned by the Heterogeneous Polarizable Environment of the Protein. *J. Am. Chem. Soc.* **2011**, *133*, 3078−3084.
(123) Amarnath, K.; Bennett, D. I. G.; Schneider, A. R.; Fleming, G. R. Multiscale Model of Light Harvesting by Photosystem II in Plants. *Proc. Natl. Acad. Sci. U. S. A.* **2016**, *113*, 1156−1161.
(124) Stirbet, A. Excitonic Connectivity between Photosystem II Units: What Is It, and How to Measure It? *Photosynth. Res.* **2013**, *116*, 189−214.
(125) Perrin, J. Fluorescence et induction moléculaire par résonance. *C. R. Acad. Sci., Paris* **1927**, *184*, 1097−1100.
(126) Perrin, F.; Perrin, J. Activation et desactivation par induction moléculaire. In *Activation et Structure des Molécules*; Presses Universitaires de France (PUF): Paris, 1929; pp 354−382.
(127) Perrin, F. Théorie quantique des transferts d'activation entre molécules de même espèce. Cas des solutions fluorescentes. *Ann. Chim. Phys. (Paris, Fr.)* **1932**, *17*, 283−314.
(128) Scholes, G. D.; Ghiggino, K. P. Electronic Interactions and Interchromophore Exictation Transfer. *J. Phys. Chem.* **1994**, *98*, 4580−4590.
(129) Krueger, B. P.; Scholes, G. D.; Jimenez, R.; Fleming, G. R. Electronic Excitation Transfer from Carotenoid to Bacteriochlorophyll in the Purple Bacterium *Rhodopseudomonas Acidophila*. *J. Phys. Chem. B* **1998**, *102*, 2284−2292.
(130) Scholes, G. D.; Andrews, D. L. Damping and Higher Multipole Effects in the Quantum Electrodynamical Model for Electronic Energy Transfer in the Condensed Phase. *J. Chem. Phys.* **1997**, *107*, 5374−5384.
(131) van der Meer, B. W. Kappa-Squared: From Nuisance to New Sense. *Rev. Mol. Biotechnol.* **2002**, *82*, 181−196.
(132) Braslavsky, S. E.; Fron, E.; Rodriguez, H. B.; Roman, E. S.; Scholes, G. D.; Schweitzer, G.; Valeur, B.; Wirz, J. Pitfalls and Limitations in the Practical Use of Förster's Theory of Resonance Energy Transfer. *Photochem. Photobiol. Sci.* **2008**, *7*, 1444−1448.
(133) Knox, R. S.; van Amerongen, H. Refractive Index Dependence of the Förster Resonance Excitation Transfer Rate. *J. Phys. Chem. B* **2002**, *106*, 5289−5293.
(134) Förster, T. Energiewanderung und Fluoreszenz. *Naturwissenschaften* **1946**, *33*, 166−175.
(135) Olaya-Castro, A.; Scholes, G. D. Energy Transfer from Förster-Dexter Theory to Quantum Coherent Light-Harvesting. *Int. Rev. Phys. Chem.* **2011**, *30*, 49−77.
(136) Chenu, A.; Scholes, G. D. Coherence in Energy Transfer and Photosynthesis. *Annu. Rev. Phys. Chem.* **2015**, *66*, 69−96.
(137) Ishizaki, A.; Calhoun, T. R.; Schlau-Cohen, G. S.; Fleming, G. R. Quantum Coherence and Its Interplay with Protein Environments in Photosynthetic Energy Transfer. *Phys. Chem. Chem. Phys.* **2010**, *12*, 7319−7337.
(138) Fleming, G. R.; Cho, M. H. Chromophore-Solvent Dynamics. *Annu. Rev. Phys. Chem.* **1996**, *47*, 109−134.
(139) Oh, M. H. J.; Salvador, M. R.; Wong, C. Y.; Scholes, G. D. Three-Pulse Photon-Echo Peak Shift Spectroscopy and its Application for the Study of Solvation and Nanoscale Excitons. *ChemPhysChem* **2011**, *12*, 88−100.
(140) Stryer, L. Fluorescence Energy Transfer as a Spectroscopic Ruler. *Annu. Rev. Biochem.* **1978**, *47*, 819−846.
(141) Wallrabe, H.; Periasamy, A. Imaging Protein Molecules Using FRET and FLIM Microscopy. *Curr. Opin. Biotechnol.* **2005**, *16*, 19−27.
(142) Piston, D. W.; Kremers, G.-J. Fluorescent Protein FRET: the Good, the Bad and the Ugly. *Trends Biochem. Sci.* **2007**, *32*, 407−414.
(143) Beljonne, D.; Curutchet, C.; Scholes, G. D.; Silbey, R. J. Beyond Förster Resonance Energy Transfer in Biological Nanoscale Systems. *J. Phys. Chem. B* **2009**, *113*, 6583−6599.
(144) Ishizaki, A.; Fleming, G. R. Quantum Coherence in Photosynthetic Light Harvesting. *Annu. Rev. Condens. Matter Phys.* **2012**, *3*, 333−361.
(145) Scholes, G. D.; Curutchet, C.; Mennucci, B.; Cammi, R.; Tomasi, J. How Solvent Controls Electronic Energy Transfer and Light Harvesting. *J. Phys. Chem. B* **2007**, *111*, 6978−6982.
(146) Scholes, G. D.; Fleming, G. R. On the mechanism of light harvesting in Photosynthetic Purple Bacteria: B800 to B850 Energy Transfer. *J. Phys. Chem. B* **2000**, *104*, 1854−1868.
(147) Mukai, K.; Abe, S.; Sumi, H. Theory of Rapid Excitation-Energy Transfer from B800 to Optically-Forbidden Exciton States of B850 in the Antenna System LH2 of Photosynthetic Purple Bacteria. *J. Phys. Chem. B* **1999**, *103*, 6096−6102.
(148) Jang, S.; Newton, M. R.; Silbey, R. J. Multichromophoric Förster Resonance Energy Transfer. *Phys. Rev. Lett.* **2004**, *92*, 218301-1−218301-4.
(149) Yang, M.; Fleming, G. R. Influence of Phonons on Exciton Transfer Dynamics: Comparison of the Redfield, Förster, and Modified Redfield Equations. *Chem. Phys.* **2002**, *275*, 355−372.
(150) Scholes, G. D. Quantum-Coherent Electronic Energy Transfer: Did Nature Think of It First? *J. Phys. Chem. Lett.* **2010**, *1*, 2−8.
(151) Lambert, N.; Chen, Y.-N.; Cheng, Y.-C.; Li, C.-M.; Chen, G.-Y.; Nori, F. Quantum Biology. *Nat. Phys.* **2013**, *9*, 10−18.

DOI: 10.1021/acs.chemrev.6b00002
Chem. Rev. XXXX, XXX, XXX−XXX

(152) Levi, F.; Mostarda, S.; Rao, F.; Mintert, F. Quantum Mechanics of Excitation Transport in Photosynthetic Complexes: a Key Issues Review. *Rep. Prog. Phys.* **2015**, *78*, 082001.
(153) Ishizaki, A.; Fleming, G. R. Unified Treatment of Quantum Coherent and Incoherent Hopping Dynamics in Electronic Energy Transfer: Reduced Hierarchy Equation Approach. *J. Chem. Phys.* **2009**, *130*, 234111−10.
(154) Andrews, D. L. A Unified Theory of Radiative and Radiationless Molecular Energy Transfer. *Chem. Phys.* **1989**, *135*, 195−201.
(155) Scholes, G. D. Long-Range Resonance Energy Transfer in Molecular Systems. *Annu. Rev. Phys. Chem.* **2003**, *54*, 57−87.
(156) Andrews, D. L.; Curutchet, C.; Scholes, G. D. Resonance Energy Transfer: Beyond the Limits. *Laser Photon Rev.* **2011**, *5*, 114−123.
(157) Harcourt, R. D.; Scholes, G. D.; Ghiggino, K. P. Rate Expressions for Excitation Transfer. 2. Electronic Considerations of Direct and Through-Configuration Exciton Resonance Interactions. *J. Chem. Phys.* **1994**, *101*, 10521−10525.
(158) Scholes, G. D.; Ghiggino, K. P.; Oliver, A. M.; Paddon-Row, M. N. Through-Space and Through-Bond Effects on Exciton Interactions in Rigidly Linked Dinaphthyl Molecules. *J. Am. Chem. Soc.* **1993**, *115*, 4345−4349.
(159) Dow, J. D. Resonance Energy Transfer in Condensed Media from a Many-Particle Viewpoint. *Phys. Rev.* **1968**, *174*, 962.
(160) Iozzi, M. F.; Mennucci, B.; Tomasi, J.; Cammi, R. Excitation Energy Transfer (EET) Between Molecules in Condensed Matter: A Novel Application of the Polarizable Continuum Model (PCM). *J. Chem. Phys.* **2004**, *120*, 7029−7040.
(161) Jurinovich, S.; Viani, L.; Curutchet, C.; Mennucci, B. Limits and Potentials of Quantum Chemical Methods in Modelling Photosynthetic Antennae. *Phys. Chem. Chem. Phys.* **2015**, *17*, 30783−30792.
(162) Neugebauer, J. Photophysical Properties of Natural Light-Harvesting Complexes Studied by Subsystem Density Functional Theory. *J. Phys. Chem. B* **2008**, *112*, 2207−2217.
(163) Adolphs, J.; Renger, T. How Proteins Trigger Excitation Energy Transfer in the FMO Complex of Green Sulfur Bacteria. *Biophys. J.* **2006**, *91*, 2778−2797.
(164) Renger, T.; Müh, F. Theory of Excitonic Couplings in Dielectric Media: Foundation of Poisson-TrEsp Method and Application to Photosystem I Trimers. *Photosynth. Res.* **2012**, *111*, 47−52.
(165) Megow, J.; Renger, T.; May, V. Mixed Quantum-Classical Description of Excitation Energy Transfer in Supramolecular Complexes: Screening of the Excitonic Coupling. *ChemPhysChem* **2014**, *15*, 478−485.
(166) Louwe, R. J. W.; Vrieze, J.; Hoff, A. J.; Aartsma, T. J. Toward an Integral Interpretation of the Optical Steady-State Spectra of the FMO-Complex of *Prosthecochloris aestuarii*. 2. Exciton Simulations. *J. Phys. Chem. B* **1997**, *101*, 11280−11287.
(167) Adolphs, J.; Müh, F.; Madjet, M. E.; Schmidt am Busch, M.; Renger, T. Structure-Based Calculations of Optical Spectra of Photosystem I Suggest an Asymmetric Light-Harvesting Process. *J. Am. Chem. Soc.* **2010**, *132*, 3331−3343.
(168) Adolphs, J.; Müh, F.; El-Amine Madjet, M.; Renger, T. Calculation of pigment transition energies in the FMO protein: From simplicity to complexity and back. *Photosynth. Res.* **2008**, *95*, 197−209.
(169) Renger, T.; Madjet, M. E.; Schmidt am Busch, M.; Adolphs, J.; Müh, F. Structure-based modeling of energy transfer in photosynthesis. *Photosynth. Res.* **2013**, *116*, 367−88.
(170) Kasha, M. Energy Transfer Mechanisms and Molecular Exciton Model for Molecular Aggregates. *Radiat. Res.* **1963**, *20*, 55−70.
(171) Spano, F. C. Excitons in Conjugated Oligomer Aggregates, Films, and Crystals. *Annu. Rev. Phys. Chem.* **2006**, *57*, 217−243.
(172) Bardeen, C. J. The Structure and Dynamics of Molecular Excitons. *Annu. Rev. Phys. Chem.* **2014**, *65*, 127−148.
(173) Scholes, G. D.; Rumbles, G. Excitons in Nanoscale Systems. *Nat. Mater.* **2006**, *5*, 683−696.
(174) Spano, F. C. The Spectral Signatures of Frenkel Polarons in H- and J-Aggregates. *Acc. Chem. Res.* **2010**, *43*, 429−439.
(175) Murrell, J. N.; Tanaka, J. Theory of Electronic Spectra of Aromatic Hydrocarbon Dimers. *Mol. Phys.* **1964**, *7*, 363−380.
(176) Azumi, T.; McGlynn, S. P. Energy of Excimer Luminescence. III. Group Theoretical Considerations of Molecular Exciton and Charge Resonance States. *J. Chem. Phys.* **1965**, *42*, 1675−1680.
(177) Scholes, G. D.; Harcourt, R. D.; Fleming, G. R. Electronic Interactions in Photosynthetic Light-Harvesting Complexes: The Role of Carotenoids. *J. Phys. Chem. B* **1997**, *101*, 7302−7312.
(178) Beddard, G. S.; Porter, G. Concentration Quenching in Chlorophyll. *Nature* **1976**, *260*, 366−367.
(179) Watson, W. F.; Livingston, R. Self-Quenching and Sensitization of fluorescence of Chlorophyll Solutions. *J. Chem. Phys.* **1950**, *18*, 802−809.
(180) Kuhlbrandt, W.; Wang, D. N. Three-Dimensional Structure of Plant Light-Harvesting Complex Determined by Electron Crystallography. *Nature* **1991**, *350*, 130−134.
(181) Matthews, B. W.; Fenna, R. E.; Bolognesi, M. C.; Schmid, M. F.; Olson, J. M. Structure of a Bacteriochlorophyll *a*-Protein from the Green Photosynthetic Bacterium *Prosthecochloris Aestuarii*. *J. Mol. Biol.* **1979**, *131*, 259−285.
(182) Frigaard, N. U.; Takaichi, S.; Hirota, M.; Shimada, K.; Matsuura, K. Quinones in Chlorosomes of Green Sulfur Bacteria and Their Role in the Redox-Dependent Fluorescence Studied in Chlorosome-Like Bacteriochlorophyll *c* Aggregates. *Arch. Microbiol.* **1997**, *167*, 343−349.
(183) Ferretti, M.; Hendrikx, R.; Romero, E.; Southall, J.; Cogdell, R. J.; Novoderezhkin, V. I.; Scholes, G. D.; van Grondelle, R. Dark States in the Light-Harvesting Complex 2 Revealed by Two-Dimensional Electronic Spectroscopy. *Sci. Rep.* **2016**, *6*, 20834.
(184) Romero, E.; van Stokkum, I. H. M.; Novoderezhkin, V. I.; Dekker, J. P.; van Grondelle, R. Two Different Charge Separation Pathways in Photosystem II. *Biochemistry* **2010**, *49*, 4300−4307.
(185) Romero, E.; Augulis, R.; Novoderezhkin, V. I.; Ferretti, M.; Thieme, J.; Zigmantas, D.; van Grondelle, R. Quantum Coherence in Photosynthesis for Efficient Solar-Energy Conversion. *Nat. Phys.* **2014**, *10*, 676−682.
(186) Novoderezhkin, V. I.; Romero, E.; van Grondelle, R. How Exciton-Vibrational Coherences Control Charge Separation in the Photosystem II Reaction Center. *Phys. Chem. Chem. Phys.* **2015**, *17*, 30828−41.
(187) Novoderezhkin, V. I.; Romero, E.; Dekker, J. P.; van Grondelle, R. Multiple Charge-Separation Pathways in Photosystem II: Modeling of Transient Absorption Kinetics. *ChemPhysChem* **2011**, *12*, 681−688.
(188) Scholes, G. D.; Jordanides, X. J.; Fleming, G. R. Adapting the Förster Theory of Energy Transfer for Modeling Dynamics in Aggregated Molecular Assemblies. *J. Phys. Chem. B* **2001**, *105*, 1640−1651.
(189) Hu, X. C.; Ritz, T.; Damjanovic, A.; Schulten, K. Pigment Organization and Transfer of Electronic Excitation in the Photosynthetic Unit of Purple Bacteria. *J. Phys. Chem. B* **1997**, *101*, 3854−3871.
(190) Sumi, H. Theory on Rates of Excitation-Energy Transfer Between Molecular Aggregates Through Distributed Transition Dipoles with Application to the Antenna System in Bacterial Photosynthesis. *J. Phys. Chem. B* **1999**, *103*, 252−260.
(191) Scholes, G. D. Designing Light-Harvesting Antenna Systems Based on Superradiant Molecular Aggregates. *Chem. Phys.* **2002**, *275*, 373−386.
(192) Abasto, D. F.; Mohseni, M.; Lloyd, S.; Zanardi, P. Exciton Diffusion Length in Complex Quantum Systems: The Effects of Disorder and Environmental Fluctuations on Symmetry-Enhanced Supertransfer. *Philos. Trans. R. Soc., A* **2012**, *370*, 3750−3770.
(193) Krueger, B. P.; Scholes, G. D.; Fleming, G. R. Calculation of Couplings and Energy-Transfer Pathways Between the Pigments of LH2 by the ab Initio Transition Density Cube Method. *J. Phys. Chem. B* **1998**, *102*, 5378−5386.

DOI: 10.1021/acs.chemrev.6b00002
Chem. Rev. XXXX, XXX, XXX−XXX

(194) Valkūnas, L.; Kudžmauskas, Š.; Juzeliūnas, G. Excitation Transfer in Highly Concentrated Pseudoisocyanine Dye Solution. *Sov. Phys.-Coll.* **1985**, *25*, 41−47.
(195) Grover, M.; Silbey, R. Exciton Migration in Molecular Crystals. *J. Chem. Phys.* **1971**, *54*, 4843−4851.
(196) Jackson, B.; Silbey, R. On the Calculation of Transfer Rates Between Impurity States in Solids. *J. Chem. Phys.* **1983**, *78*, 4193−4196.
(197) Soules, T. F.; Duke, C. B. Resonant Energy Transfer between Localized Electronic States in a Crystal. *Phys. Rev. B* **1971**, *3*, 262−274.
(198) Kenkre, V. M. Relations Among Theories of Excitation Transfer II: Influence of Spectral Features on Exciton Motion. *Phys. Rev. B* **1975**, *12*, 2150−2160.
(199) Fleming, G. R.; van Grondelle, R. Femtosecond Spectroscopy of Photosynthetic Light-Harvesting Systems. *Curr. Opin. Struct. Biol.* **1997**, *7*, 738−748.
(200) Fotiadis, D.; Qian, P.; Philippsen, A.; Bullough, P. A.; Engel, A.; Hunter, C. N. Structural Analysis of the Reaction Center Light-Harvesting Complex I Photosynthetic Core Complex *Rhodospirillum Rubrum* Using Atomic Force Microscopy. *J. Biol. Chem.* **2004**, *279*, 2063−2068.
(201) Roszak, A. W.; Howard, T.; Southall, J.; Gardiner, A. T.; Law, C. J.; Isaacs, N. W.; Cogdell, R. J. Crystal Structure of the RC-LH1 Core Complex from *Rhodopseudomonas palustris*. *Science* **2003**, *302*, 1969−1972.
(202) Jungas, C.; Ranck, J.-L.; Rigaud, J.-L.; Joliot, P.; Vermeglio, A. Supramolecular Organization of the Photosynthetic Apparatus of *Rhodobacter sphaeroides*. *EMBO J.* **1999**, *18*, 534−542.
(203) Bahatyrova, S.; Frese, R. N.; Siebert, C. A.; Olsen, J. D.; van der Werf, K. O.; van Grondelle, R.; Niederman, R. A.; Bullough, P. A.; Otto, C.; Hunter, C. N. The Native Architecture of a Photosynthetic Membrane. *Nature* **2004**, *430*, 1058−1062.
(204) Scheuring, S.; Sturgis, J. N. Chromatic Adaptation of Photosynthetic Membranes. *Science* **2005**, *309*, 484−487.
(205) Hunter, C. N.; Tucker, J. D.; Niederman, R. A. The Assembly and Organisation of Photosynthetic Membranes in *Rhodobacter Sphaeroides*. *Photochem. Photobiol.* **2005**, *4*, 1023−1027.
(206) Allen, J. P.; Feher, G.; Yeates, T. O.; Rees, D. C.; Deisenhofer, J.; Michel, H.; Huber, R. Structural Homology of Reaction Centers from *Rhodopseudomonas Sphaeroides* and *Rhodopseudomonas Viridis* as Determined by X-Ray Diffraction. *Proc. Natl. Acad. Sci. U. S. A.* **1986**, *83*, 8589−8593.
(207) Scheuring, S.; Rigaud, J.-L.; Sturgis, J. N. Variable LH2 Stoichiometry and Core Clustering in Native Membranes of *Rhodospirillum Photometricum*. *EMBO J.* **2004**, *23*, 4127−4133.
(208) Jimenez, R.; van Mourik, F.; Yu, J. Y.; Fleming, G. R. Three-Pulse Photon Echo Measurements on LH1 and LH2 Complexes of *Rhodobacter sphaeroides*: A Nonlinear Spectroscopic Probe of Energy Transfer. *J. Phys. Chem. B* **1997**, *101*, 7350−7359.
(209) Chmeliov, J.; Songaila, E.; Rancova, O.; Gall, A.; Robert, B.; Abramavicius, D.; Valkūnas, L. Excitons in the LH3 Complexes from Purple Bacteria. *J. Phys. Chem. B* **2013**, *117*, 11058−11068.
(210) Ketelaars, M.; Segura, J. M.; Oellerich, S.; de Ruijter, W. P. F.; Magis, G.; Aartsma, T. J.; Matsushita, M.; Schmidt, J.; Cogdell, R. J.; Kohler, J. Probing the Electronic Structure and Conformational Flexibility of Individual Light-Harvesting 3 Complexes by Optical Single-Molecule Spectroscopy. *J. Phys. Chem. B* **2006**, *110*, 18710−18717.
(211) McLuskey, K.; Prince, S. M.; Cogdell, R. J.; Isaacs, N. W. The Crystallographic Structure of the B800−820 LH3 Light-Harvesting Complex from the Purple Bacteria Rhodopseudomonas Acidophila Strain 7050. *Biochemistry* **2001**, *40*, 8783−8783.
(212) McDermott, G.; Prince, S. M.; Freer, A. A.; Hawthornthwaite-Lawless, A. M.; Papiz, M. Z.; Cogdell, R. J.; Isaacs, N. W. Crystal Structure of an Integral Membrane Light-Harvesting Complex from Photosynthetic Bacteria. *Nature* **1995**, *374*, 517−521.
(213) Evans, K.; Fordham-Skelton, A. P.; Mistry, H.; Reynolds, C. D.; Lawless, A. M.; Papiz, M. Z. A Bacteriophytochrome Regulates the Synthesis of LH4 Complexes in *Rhodopseudomonas Palustris*. *Photosynth. Res.* **2005**, *85*, 169−180.
(214) Savage, H.; Cyrklaff, M.; Montoya, G.; Kühlbrandt, W.; Sinning, I. Two-Dimensional Structure of Light Harvesting Complex II (LHII) from the Purple Bacterium *Rhodovulum sulfidophilum* and Comparison with LHII from *Rhodopseudomonas acidophila*. *Structure* **1996**, *4*, 243−252.
(215) Permentier, H. P.; Neerken, S.; Overmann, J.; Amesz, J. A Bacteriochlorophyll *a* Antenna Complex from Purple Bacteria Absorbing at 963 nm. *Biochemistry* **2001**, *40*, 5573−5578.
(216) Hoogewerf, G. J.; Jung, D. O.; Madigan, T. Evidence for Limited Species Diversity of Bacteriochlorophyll *b*-Containing Purple Nonsulfur Anoxygenic Phototrophs in Freshwater Habitats. *FEMS Microbiol. Lett.* **2003**, *218*, 359−364.
(217) Beatty, T. J. *Genome Evolution of Photosynthetic Bacteria*, 1st ed.; Advances in Botanical Research; Elsevier Inc.: New York, 2013; Vol. *66*.
(218) Hirschler-Réa, A.; Matheron, R.; Riffaud, C.; Mouné, S.; Eatock, C.; Herbert, R. A.; Willison, J. C.; Caumette, P. Isolation and Characterization of Spirilloid Purple Phototrophic Bacteria Forming Red Layers in Microbial Mats of Mediterranean Salterns: Description of *Halorhodospira neutriphila* sp. nov. and Emendation of the Genus *Halorhodospira*. *Int. J. Syst. Evol. Microbiol.* **2003**, *53*, 153−163.
(219) Ma, F.; Kimura, Y.; Yu, L.-J.; Wang, P.; Ai, X.-C.; Wang, Z.-Y.; Zhang, J.-P. Specific Ca^{2+}-binding Motif in the LH1 Complex from Photosynthetic Bacterium *Thermochromatium tepidum* as Revealed by Optical Spectroscopy and Structural Modeling. *FEBS J.* **2009**, *276*, 1739−1749.
(220) Yang, F.; Yu, L.-J.; Wang, P.; Ai, X.-C.; Wang, Z.-Y.; Zhang, J.-P. Effects of Aggregation on the Excitation Dynamics of LH2 from *Thermochromatium tepidum* in Aqueous Phase and in Chromatophores. *J. Phys. Chem. B* **2011**, *115*, 7906−7913.
(221) (a) Hess, S.; Chachisvilis, M.; Timpmann, K.; Jones, M. R.; Fowler, G. J. S.; Hunter, C. N.; Sundström, V. Temporally and Spectrally Resolved Sub-Picosecond Energy Transfer within the Peripheral Antenna Complex (LH2) and from LH2 to the Core Antenna Complex in Photosynthetic Purple Bacteria. *Proc. Natl. Acad. Sci. U. S. A.* **1995**, *92*, 12333−12337. (b) Hess, S.; Åkesson, E.; Cogdell, R.; Pullerits, T.; Sundström, V. Energy Transfer in Spectrally Inhomogeneous Light-Harvesting Pigment−Protein Complexes of Purple Bacteria. *Biophys. J.* **1995**, *69*, 2211−2225.
(222) Pullerits, T.; Sundström, V. Photosynthetic Light-Harvesting Pigment−Protein Complexes: Toward Understanding How and Why. *Acc. Chem. Res.* **1996**, *29*, 381−389.
(223) Alia, A.; Matysik, J.; Soede-Huijbregts, C.; Baldus, M.; Raap, J.; Lugtenburg, J.; Gast, P.; van Gorkom, H. J.; Hoff, A. J.; de Groot, H. J. M. Ultrahigh Field MAS NMR Dipolar Correlation Spectroscopy of the Histidine Residues in Light-Harvesting Complex II from Photosynthetic Bacteria Reveals Partial Internal Charge Transfer in the B850/His Complex. *J. Am. Chem. Soc.* **2001**, *123*, 4803−4809.
(224) Alia, A.; Ganapathy, S.; de Groot, H. J. M. Magic Angle Spinning (MAS) NMR: A New Tool to Study the Spatial and Electronic Structure of Photosynthetic Complexes. *Photosynth. Res.* **2009**, *102*, 415−425.
(225) Papiz, M. Z.; Prince, S. M.; Howard, T.; Cogdell, R. J.; Isaacs, N. W. The Structural and Thermal Motion of the B800-B850 LH2 Complex from *Rps. Acidophila* at 2.0 Resolution and 100 K: New Structural Features and Functionally Relevant Motions. *J. Mol. Biol.* **2003**, *326*, 1523−1538.
(226) Fowler, G. J.; Visschers, R. W.; Grief, G. G.; van Grondelle, R.; Hunter, C. N. Genetically Modified Photosynthetic Antenna Complexes with Blueshifted Absorbance Bands. *Nature* **1992**, *355*, 848−850.
(227) Madjet, M. E.; Abdurahman, A.; Renger, T. Intermolecular Coulomb Couplings from Ab Initio Electrostatic Potentials: Application to Optical Transitions of Strongly Coupled Pigments in Photosynthetic Antennae and Reaction Centers. *J. Phys. Chem. B* **2006**, *110*, 17268−17281.

DOI: 10.1021/acs.chemrev.6b00002
Chem. Rev. XXXX, XXX, XXX−XXX

(228) Cogdell, R. J.; Howard, T. D.; Isaacs, N. W.; McLuskey, K.; Gardiner, A. T. Structural Factors Which Control the Position of the Q(Y) Absorption Band of Bacteriochlorophyll *a* in Purple Bacterial Antenna Complexes. *Photosynth. Res.* **2002**, *74*, 135−141.
(229) Mascle-Allemand, C.; Duquesne, K.; Lebrun, R.; Scheuring, S.; Sturgis, J. N. Antenna Mixing in Photosynthetic Membranes from *Phaeospirillum Molischianum*. *Proc. Natl. Acad. Sci. U. S. A.* **2010**, *107*, 5357−5362.
(230) Brotosudarmo, T. H. P.; Collins, A. M.; Gall, A.; Roszak, A. W.; Gardiner, A. T.; Blankenship, R. E.; Cogdell, R. J. The Light Intensity Under Which Cells Are Grown Controls the Type of Peripheral Light-Harvesting Complexes That are Assembled in a Purple Photosynthetic Bacterium. *Biochem. J.* **2011**, *440*, 51−61.
(231) Trissl, H.-W.; Law, C. J.; Cogdell, R. J. Uphill Energy Transfer in LH2-Containing Purple Bacteria at Room Temperature. *Biochim. Biophys. Acta, Bioenerg.* **1999**, *1412*, 149−172.
(232) Gall, A.; Robert, B. Characterization of the Different Peripheral Light-Harvesting Complexes from High- and Low-Light Grown Cells from *Rhodopseudomonas palustris*. *Biochemistry* **1999**, *38*, 5185−5190.
(233) Şener, M. K.; Strümpfer, J.; Timney, J. A.; Freiberg, A.; Hunter, C. N.; Schulten, K. Photosynthetic Vesicle Architecture and Constraints on Efficient Energy Harvesting. *Biophys. J.* **2010**, *99*, 67−75.
(234) Şener, M. K.; Olsen, J. D.; Hunter, C. N.; Schulten, K. Atomic-Level Structural and functional model of a Bacterial Photosynthetic Membrane Vesicle. *Proc. Natl. Acad. Sci. U. S. A.* **2007**, *104*, 15723−15728.
(235) Adams, P. G.; Hunter, C. N. Adaptation of Intracytoplasmic Membranes to Altered Light Intensity in *Rhodobacter Sphaeroides*. *Biochim. Biophys. Acta, Bioenerg.* **2012**, *1817*, 1616−1627.
(236) Hu, X.; Ritz, T.; Damjanovic, A.; Autenrieth, F.; Schulten, K. Photosynthetic Apparatus of Purple Bacteria. *Q. Rev. Biophys.* **2002**, *35*, 1−62.
(237) Sauer, K.; Cogdell, R. J.; Prince, S. M.; Freer, A.; Isaacs, N. W.; Scheer, H. Structure-Based Calculations of the Optical Spectra of the LH2 Bacterio-Chlorophyll-Protein Complex from *Rhodopseudomonas Acidophila*. *Photochem. Photobiol.* **1996**, *64*, 564−576.
(238) Kennis, J. T. M.; Streltsov, A. M.; Vulto, S. I. E.; Aartsma, T. J.; Nozawa, T.; Amesz, J. Femtosecond Dynamics in Isolated LH2 Complexes of Various Species of Purple Bacteria. *J. Phys. Chem. B* **1997**, *101*, 7827−7834.
(239) Scholes, G. D.; Gould, I. R.; Cogdell, R. J.; Fleming, G. R. Ab Initio Molecular Orbital Calculations of Electronic Couplings in the LH2 Bacterial Light-Harvesting Complex of *Rps. Acidophila*. *J. Phys. Chem. B* **1999**, *103*, 2543−2553.
(240) Visschers, R. W.; Chang, M. C.; van Mourik, F.; Parkesloach, P. S.; Heller, B. A.; Loach, P. A.; van Grondelle, R. Fluorescence Polarization and Low-Temperature Absorption Spectroscopy of a Subunit Form of Light-Harvesting Complex-I from Purple Photosynthetic Bacteria. *Biochemistry* **1991**, *30*, 5734−5742.
(241) van Mourik, F.; van der Oord, C. J. R.; Visscher, K. J.; Parkesloach, P. S.; Loach, P. A.; Visschers, R. W.; van Grondelle, R. Exciton Interactions in the Light-Harvesting Antenna of Photosynthetic Bacteria Studies with Triplet-Singlet Spectroscopy and Singlet-Triplet Annihilation on the B820 Subunit Form of *Rhodospirillum-Rubrum*. *Biochim. Biophys. Acta, Bioenerg.* **1991**, *1059*, 111−119.
(242) Koolhaas, M. H. C.; Frese, R. N.; Fowler, G. J. S.; Bibby, T. S.; Georgakopoulou, S.; van der Zwan, G.; Hunter, C. N.; van Grondelle, R. Identification of the Upper Exciton Component of the B850 Bacteriochlorophylls of the LH2 Antenna Complex, Using a B800-Free Mutant of *Rhodobacter Sphaeroides*. *Biochemistry* **1998**, *37*, 4693−4698.
(243) Monshouwer, R.; Abrahamsson, M.; van Mourik, F.; van Grondelle, R. Superradiance and Exciton Delocalization in Bacterial Photosynthetic Light-Harvesting Systems. *J. Phys. Chem. B* **1997**, *101*, 7241−7248.
(244) Novoderezhkin, V. I.; Razjivin, A. P. Exciton Dynamics in Circular Aggregates: Application to Antenna of Photosynthetic Purple Bacteria. *Biophys. J.* **1995**, *68*, 1089−1100.
(245) Fidder, H.; Knoester, J.; Wiersma, D. A. Optical Properties of Disordered Molecular Aggregates: A Numerical Study. *J. Chem. Phys.* **1991**, *95*, 7880−7890.
(246) Bakalis, L. D.; Coca, M.; Knoester, J. Optical Line Shapes of Dynamically Disordered Ring Aggregates. *J. Chem. Phys.* **1999**, *110*, 2208−2218.
(247) Mostovoy, M. V.; Knoester, J. Statistics of Optical Spectra from Single-Ring Aggregates and Its Application to LH2. *J. Phys. Chem. B* **2000**, *104*, 12355−12364.
(248) van Oijen, A. M.; Ketelaars, M.; Köhler, J.; Aartsma, T. J.; Schmidt, J. Unraveling the Electronic Structure of Individual Photosynthetic Pigment−Protein Complexes. *Science* **1999**, *285*, 400−402.
(249) Wu, H.-M.; Reddy, N. R. S.; Small, G. J. Direct Observation and Hole Burning of the Lowest Exciton Level (B870) of the LH2 Antenna Complex of *Rhodopseudomonas Acidophila* (Strain 10050). *J. Phys. Chem. B* **1997**, *101*, 651−656.
(250) Berlin, Y.; Burin, A.; Friedrich, J.; Köhler, J. Low Temperature Spectroscopy of Proteins. Part II: Experiments with Single Protein Complexes. *Phys. Life. Rev.* **2007**, *4*, 64−89.
(251) Krüger, T. P. J.; Wientjes, E.; Croce, R.; van Grondelle, R. Conformational Switching Explains the Intrinsic Multifunctionality of Plant Light-Harvesting Complexes. *Proc. Natl. Acad. Sci. U. S. A.* **2011**, *108*, 13516−13521.
(252) Oellerich, S.; Kohler, J. Low-Temperature Single-Molecule Spectroscopy on Photosynthetic Pigment−Protein Complexes from Purple Bacteria. *Photosynth. Res.* **2009**, *101*, 171−179.
(253) Novoderezhkin, V. I.; Rutkauskas, D.; van Grondelle, R. Dynamics of the Emission Spectrum of a Single LH2 Complex: Interplay of Slow and Fast Nuclear Motions. *Biophys. J.* **2006**, *90*, 2890−2902.
(254) Rutkauskas, D.; Novoderezkhin, V.; Cogdell, R. J.; van Grondelle, R. Fluorescence Spectral Fluctuations of Single LH2 Complexes from *Rhodopseudomonas acidophila* Strain 10050. *Biochemistry* **2004**, *43*, 4431−4438.
(255) Kunz, R.; Timpmann, K.; Southall, J.; Cogdell, R. J.; Freiberg, A.; Köhler, J. Fluctuations in the Electron−Phonon Coupling of a Single Chromoprotein. *Angew. Chem., Int. Ed.* **2013**, *52*, 8726−9730.
(256) Monshouwer, R.; van Grondelle, R. Excitations and Excitons in Bacterial Light-Harvesting Complexes. *Biochim. Biophys. Acta, Bioenerg.* **1996**, *1275*, 70−75.
(257) Meier, T.; Zhao, Y.; Chernyak, V.; Mukamel, S. Polarons, Localization and Excitonic Coherence in Superradiance of Biological Antenna Complexes. *J. Chem. Phys.* **1997**, *107*, 3876−3893.
(258) Palacios, M. A.; de Weerd, F. L.; Ihalainen, J. A.; van Grondelle, R.; van Amerongen, H. Superradiance and Exciton (De)localization in Light-Harvesting Complex II from Green Plants? *J. Phys. Chem. B* **2002**, *106*, 5782−5787.
(259) Pullerits, T.; Chachisvilis, M.; Sundström, V. Exciton Delocalization Length in the B850 Antenna of *Rhodobacter Sphaeroides*. *J. Phys. Chem.* **1996**, *100*, 10787−10792.
(260) Jimenez, R.; Dikshit, S. N.; Bradforth, S. E.; Fleming, G. R. Electronic Excitation Transfer in the LH2 Complex of *Rhodobacter Sphaeroides*. *J. Phys. Chem.* **1996**, *100*, 6825−6834.
(261) Novoderezhkin, V.; Monshouwer, R.; van Grondelle, R. Exciton (de)localization in the LH2 Antenna of *Rhodobacter Sphaeroides* as Revealed by Relative Difference Absorption Measurements of the LH2 Antenna and the B820 Subunit. *J. Phys. Chem. B* **1999**, *103*, 10540−10548.
(262) Sundström, V.; Pullerits, T.; van Grondelle, R. Photosynthetic Light-Harvesting: Reconciling Dynamics and Structure of Purple Bacterial LH2 Reveals Function of Photosynthetic Unit. *J. Phys. Chem. B* **1999**, *103*, 2327−2346.
(263) van Grondelle, R.; Novoderezhkin, V. I. Dynamics of Excitation Energy Transfer in the LH1 and LH2 Light-Harvesting

DOI: 10.1021/acs.chemrev.6b00002
Chem. Rev. XXXX, XXX, XXX−XXX

Complexes of Photosynthetic Bacteria. *Biochemistry* **2001**, *40*, 15057−15059.
(264) Ma, Y. Z.; Cogdell, R. J.; Gillbro, T. Energy Transfer and Exciton Annihilation in the B800−850 Antenna Complex of the Photosynthetic Purple Bacterium *Rhodopseudomonas Acidophila* (Strain 10050). A Femtosecond Transient Absorption Study. *J. Phys. Chem. B* **1997**, *101*, 1087−1095.
(265) Bergström, H.; Westerhuis, W. H. J.; Sundström, V.; van Grondelle, R.; Niederman, R. A.; Gillbro, T. Energy Transfer within the Isolated B875 Light-Harvesting Pigment−Protein Complex of *Rhodobacter sphaeroides* at 77 K Studied by Picosecond Absorption Spectroscopy. *FEBS Lett.* **1988**, *233*, 12−16.
(266) Hunter, C. N.; Bergström, H.; van Grondelle, R.; Sundström, V. Energy-Transfer Dynamics in Three Light-Harvesting Mutants of *Rhodobacter sphaeroides*: A Picosecond Spectroscopy Study. *Biochemistry* **1990**, *29*, 3203−3207.
(267) Cleary, L.; Chen, H.; Chuang, C.; Silbey, R. J.; Cao, J. Optimal Fold Symmetry of LH2 Rings on a Photosynthetic Membrane. *Proc. Natl. Acad. Sci. U. S. A.* **2013**, *110*, 8537−8542.
(268) Beekman, L. M. P.; van Mourik, F.; Jones, M. R.; Visser, H. M.; Hunter, C. N.; van Grondelle, R. Trapping Kinetics in Mutants of the Photosynthetic Purple Bacterium *Rhodobacter Sphaeroides*: Influence of the Charge Separation Rate and Consequences for the Rate-Limiting Step in the Light-Harvesting Process. *Biochemistry* **1994**, *33*, 3143−3147.
(269) Freiberg, A.; Allen, J. P.; Williams, J.; Woodbury, N. W. Energy Trapping and Detrapping by Wild Type and Mutant Reaction Centers of Purple Non-Sulfur Bacteria. *Photosynth. Res.* **1996**, *48*, 309−319.
(270) Visscher, K. J.; Bergström, H.; Sundström, V.; Hunter, C. N.; van Grondelle, R. Temperature Dependence of Energy Transfer from the Long Wavelength Antenna BChl-896 to the Reaction Center in Rhodospirillum Rubrum, Rhodobacter Sphaeroides (w.t. and M21 Mutant) from 77 to 177K, Studied by Picosecond Absorption Spectroscopy. *Photosynth. Res.* **1989**, *22*, 211−217.
(271) Allen, J. F.; Mullineaux, C. W. Probing the Mechanism of State Transitions in Oxygenic Photosynthesis by Chlorophyll Fluorescence Spectroscopy, Kinetics and Imaging. In *Chlorophyll a Fluorescence: A Signature of Photosynthesis*; Papageorgiou, G.C., Govindjee, Eds.; Advances in Photosynthesis and Respiration; Springer: Dordrecht, The Netherlands, 2004; Vol. *19*, pp 447−461.
(272) Papageorgiou, G. C.; Govindjee. Photosystem II Fluorescence: Slow Changes - Scaling from the Past. *J. Photochem. Photobiol., B* **2011**, *104*, 258−70.
(273) Wlodarczyk, L. M.; Snellenburg, J. J.; Ihalainen, J. A.; van Grondelle, R.; van Stokkum, I. H. M.; Dekker, J. P. Functional Rearrangement of the Light-Harvesting Antenna upon State Transitions in a Green Alga. *Biophys. J.* **2015**, *108*, 261−271.
(274) Demmig-Adams, B., Garab, G., Adams, W. W., III, Govindjee, Eds. *Non-Photochemical Quenching and Thermal Energy Dissipation in Plants, Algae and Cyanobacteria*; Springer: Dordrecht, The Netherlands, 2014; Vol. *40*.
(275) Liu, Z.; Yan, H.; Wang, K.; Kuang, T.; Zhang, J.; Gui, L.; An, X.; Chang, W. Crystal Structure of Spinach Major Light-Harvesting Complex at 2.72 Å Resolution. *Nature* **2004**, *428*, 287−292.
(276) Novoderezhkin, V. I.; Palacios, M. A.; van Amerongen, H.; van Grondelle, R. Excitation Dynamics in the LHCII Complex of Higher Plants: Modeling Based on the 2.72 Å Crystal Structure. *J. Phys. Chem. B* **2005**, *109*, 10493−10504.
(277) Novoderezhkin, V. I.; Marin, A.; van Grondelle, R. Intra- and Inter-Monomeric Transfers in the Light Harvesting LHCII Complex: the Redfield−Förster Picture. *Phys. Chem. Chem. Phys.* **2011**, *13*, 17093−17103.
(278) Novoderezhkin, V. I.; Palacios, M. A.; van Amerongen, H.; van Grondelle, R. Energy-Transfer Dynamics in the LHCII Complex of Higher Plants: Modified Redfield Approach. *J. Phys. Chem. B* **2004**, *108*, 10363−10375.
(279) Croce, R.; Müller, M. G.; Bassi, R.; Holzwarth, A. R. Carotenoid-to-Chlorophyll Energy Transfer in Recombinant Major Light-Harvesting Complex (LHCII) of Higher Plants. I. Femtosecond Transient Absorption Measurements. *Biophys. J.* **2001**, *80*, 901−915.
(280) Gradinaru, C. C.; van Stokkum, I. H. M.; Pascal, A. A.; van Grondelle, R.; van Amerongen, H. Identifying the Pathways of Energy Transfer between Carotenoids and Chlorophylls in LHCII and CP29. A Multicolor Pump-Probe Study. *J. Phys. Chem. B* **2000**, *104*, 9330−9342.
(281) Connelly, J. P.; Müller, M. G.; Hucke, M.; Gatzen, G.; Mullineaux, C. W.; Ruban, A. V.; Horton, P.; Holzwarth, A. R. Ultrafast Spectroscopy of Trimeric Light-Harvesting Complex II from Higher Plants. *J. Phys. Chem. B* **1997**, *101*, 1902−1909.
(282) Renger, T.; Madjet, M. E.; Knorr, A.; Müh, F. How the Molecular Structure Determines the Flow of Excitation Energy in Plant Light-Harvesting Complex II. *J. Plant Physiol.* **2011**, *168*, 1497−1509.
(283) Kreisbeck, C.; Kramer, T.; Aspuru-Guzik, A. Scalable High-Performance Algorithm for the Simulation of Exciton-Dynamics. Application to the Light Harvesting Complex II in the Presence of Resonant Vibrational Modes. *J. Chem. Theory Comput.* **2014**, *10*, 4045−4054.
(284) Ruban, A. V.; Johnson, M. P.; Duffy, C. D. P. The Photoprotective Molecular Switch in the Photosystem II Antenna. *Biochim. Biophys. Acta, Bioenerg.* **2012**, *1817*, 167−181.
(285) Ruban, A. V.; Berera, R.; Ilioaia, C.; van Stokkum, I. H. M.; Kennis, J. T. M.; Pascal, A.; van Amerongen, H.; Robert, B.; Horton, P.; van Grondelle, R. Identification of a Mechanism of Photoprotective Energy Dissipation in Higher Plants. *Nature* **2007**, *450*, 575−578.
(286) Miloslavina, Y.; Wehner, A.; Lambrev, P. H.; Wientjes, E.; Reus, M.; Garab, G.; Croce, R.; Holzwarth, A. R. Far-Red Fluorescence: a Direct Spectroscopic Marker for LHCII Oligomer Formation in Non-Photochemical Quenching. *FEBS Lett.* **2008**, *582*, 3625−3631.
(287) Büchel, C. Fucoxanthin-Chlorophyll Proteins in Diatoms: 18 and 19 kDa Subunits Assemble into Different Oligomeric States. *Biochemistry* **2003**, *42*, 13027−13034.
(288) Hofmann, E.; Wrench, P. M.; Sharples, F. P.; Hiller, R. G.; Welte, W.; Diederichs, K. Structural Basis of Light Harvesting by Carotenoids: Peridinin-Chlorophyll-Protein from *Amphidinium carterae*. *Science* **1996**, *272*, 1788−1791.
(289) Frank, H. A.; Cogdell, R. J. Carotenoids in Photosynthesis. *Photochem. Photobiol.* **1996**, *63*, 257−264.
(290) Büchel, C. Fucoxanthin-Chlorophyll-Proteins and Non-Photochemical Fluorescence Quenching of Diatoms. In *Non-Photochemical Quenching and Energy Dissipation in Plants, Algae and Cyanobacteria*; Demmig-Adams, B., Garab, G., Adams, W. W., III, Govindjee, Eds.; Advances in Photosynthesis and Respiration; Springer: Dordrecht, The Netherlands, 2014; Vol. *40*, Chapter 11, pp 259−275.
(291) Papagiannakis, E.; van Stokkum, I. H. M.; Fey, H.; Büchel, C.; van Grondelle, R. Spectroscopic Characterization of the Excitation Energy Transfer in the Fucoxanthin−Chlorophyll Protein of Diatoms. *Photosynth. Res.* **2005**, *86*, 241−250.
(292) Akimoto, S.; Teshigahara, A.; Yokono, M.; Mimuro, M.; Nagao, R.; Tomo, T. Excitation Relaxation Dynamics and Energy Transfer in Fucoxanthin−Chlorophyll a/c-Protein Complexes, Probed by Time-Resolved Fluorescence. *Biochim. Biophys. Acta, Bioenerg.* **2014**, *1837*, 1514−1521.
(293) Gildenhoff, N.; Amarie, S.; Gundermann, K.; Beer, A.; Büchel, C.; Wachtveitl, J. Oligomerization and Pigmentation Dependent Excitation Energy Transfer in Fucoxanthin-Chlorophyll Proteins. *Biochim. Biophys. Acta, Bioenerg.* **2010**, *1797*, 543−549.
(294) Gelzinis, A.; Butkus, V.; Songaila, E.; Augulis, R.; Gall, A.; Büchel, C.; Robert, B.; Abramavicius, D.; Zigmantas, D.; Valkūnas, L. Mapping Energy Transfer Channels in Fucoxanthin−Chlorophyll Protein Complex. *Biochim. Biophys. Acta, Bioenerg.* **2015**, *1847*, 241−247.
(295) Songaila, E.; Augulis, R.; Gelzinis, A.; Butkus, V.; Gall, A.; Büchel, C.; Robert, B.; Zigmantas, D.; Abramavicius, D.; Valkūnas, L. Ultrafast Energy Transfer from Chlorophyll c_2 to Chlorophyllin

DOI: 10.1021/acs.chemrev.6b00002
Chem. Rev. XXXX, XXX, XXX−XXX

Fucoxanthin−Chlorophyll Protein Complex. *J. Phys. Chem. Lett.* **2013**, *4*, 3590−3595.
(296) Polivka, T.; Frank, H. A. Molecular Factors Controlling Photosynthetic Light Harvesting by Carotenoids. *Acc. Chem. Res.* **2010**, *43*, 1125−1134.
(297) Zigmantas, D.; Hiller, R. G.; Sundstrom, V.; Polivka, T. Carotenoid to Chlorophyll Energy Transfer in the Peridinin−Chlorophyll-*a*−Protein Complex Involves an Intramolecular Charge Transfer State. *Proc. Natl. Acad. Sci. U. S. A.* **2002**, *99*, 16760−16765.
(298) van Stokkum, I. H. M.; Papagiannakis, E.; Vengris, M.; Salverda, J. M.; Polivka, T.; Zigmantas, D.; Larsen, D. S.; Lampoura, S. S.; Hiller, R. G.; van Grondelle, R. Inter-Pigment Interactions in the Peridinin Chlorophyll Protein Studied by Global and Target Analysis of Time Resolved Absorption Spectra. *Chem. Phys.* **2009**, *357*, 70−78.
(299) Bonetti, C.; Alexandre, M. T. A.; van Stokkum, I. H. M.; Hiller, R. G.; Groot, M. L.; van Grondelle, R.; Kennis, J. T. M. Identification of Excited-State Energy Transfer and Relaxation Pathways in the Peridinin−Chlorophyll Complex: An Ultrafast Mid-Infrared Study. *Phys. Chem. Chem. Phys.* **2010**, *12*, 9256−9266.
(300) Govindjee; Shevela, D. Adventures with Cyanobacteria: A Personal Perspective. *Front. Plant Sci.* **2011**, *2*, 1−17.
(301) Blankenship, R. E.; Matsuura, K. Antenna Complexes from Green Photosynthetic Bacteria. In *Light-Harvesting Antennas in Photosynthesis*; Green, B. R., Parson, W. W., Eds.; Advances in Photosynthesis and Respiration; Kluwer Academic Publishers: Dordrecht, The Netherlands, 2003; Vol. *13*, Chapter 6, pp 195−217.
(302) Ganapathy, S.; Oostergetel, G. T.; Wawrzyniak, P. K.; Reus, M.; Gomez Maqueo Chew, A.; Buda, F.; Boekema, E. J.; Bryant, D. A.; Holzwarth, A. R.; de Groot, H. J. M. Alternating Syn-Anti Bacteriochlorophylls form Concentric Helical Nanotubes in Chlorosomes. *Proc. Natl. Acad. Sci. U. S. A.* **2009**, *106*, 8525−8530.
(303) Oostergetel, G. T.; van Amerongen, H.; Boekema, E. J. The Chlorosome: A Prototype for Efficient Light Harvesting in Photosynthesis. *Photosynth. Res.* **2010**, *104*, 245−255.
(304) Beatty, J. T.; Overmann, J.; Lince, M. T.; Manske, A. K.; Lang, A. S.; Blankenship, R. E.; van Dover, C. L.; Martinson, T. A.; Plumley, F. G. An Obligately Photosynthetic Bacterial Anaerobe from a Deep-Sea Hydrothermal Vent. *Proc. Natl. Acad. Sci. U. S. A.* **2005**, *102*, 9306−9310.
(305) van Dorssen, R. J.; Gerola, P. D.; Olson, J. M.; Amesz, J. Optical and Structural Properties of Chlorosomes of the Photosynthetic Green Sulfur Bacterium *Chlorobium Limicola*. *Biochim. Biophys. Acta, Bioenerg.* **1986**, *848*, 77−82.
(306) Wang, J.; Brune, D. C.; Blankenship, R. E. Ejects of Oxidants and Reductants on the Effciency of Excitation Transfer in Green Photosynthetic Bacteria. *Biochim. Biophys. Acta, Bioenerg.* **1990**, *1015*, 457−463.
(307) Frigaard, N.-U.; Matsuura, K. Oxygen Uncouples Light Absorption by the Chlorosome Antenna and Photosynthetic Electron Transfer in the Green Sulfur Bacterium *Chlorobium Tepidum*. *Biochim. Biophys. Acta, Bioenerg.* **1999**, *1412*, 108−117.
(308) Alster, J.; Zupcanova, A.; Vacha, F.; Psencik, J. Effect of Quinones on Formation and Properties of Bacteriochlorophyll c Aggregates. *Photosynth. Res.* **2008**, *95*, 183−189.
(309) Frigaard, N. U.; Tokita, S.; Matsuura, K. Exogenous Quinones Inhibit Photosynthetic Electron Transfer in *Chloroflexus aurantiacus* by Specific Quenching of the Excited Bacteriochlorophyll *c* antenna. *Biochim. Biophys. Acta, Bioenerg.* **1999**, *1413*, 108−116.
(310) Tokita, S.; Frigaard, N.-U.; Hirota, M.; Shimada, K.; Matsuura, K. Quenching of Bacteriochlorophyll Fluorescence in Chlorosomes from Chloroflexus aurantiacus by Exogenous Quinones. *Photochem. Photobiol.* **2000**, *72*, 345−350.
(311) Pšenčík, J.; Polívka, T.; Němec, P.; Dian, J.; Kudrna, J.; Malý, P.; Hála, J. Fast Energy Transfer and Exciton Dynamics in Chlorosomes of the Green Sulfur Bacterium *Chlorobium tepidum*. *J. Phys. Chem. A* **1998**, *102*, 4392−4398.
(312) Prokhorenko, V. I.; Steensgaard, D. B.; Holzwarth, A. R. Exciton Dynamics in the Chlorosomal Antennae of the Green Bacteria *Chloroflexus aurantiacus* and *Chlorobium tepidum*. *Biophys. J.* **2000**, *79*, 2105−2120.
(313) Savikhin, S.; Zhu, Y.; Lin, S.; Blankenship, R. E.; Struve, W. S. Femtosecond Spectroscopy of Chlorosome Antennas from the Green Photosynthetic Bacterium. *J. Phys. Chem.* **1994**, *98*, 10322−10334.
(314) Savikhin, S.; Zhu, Y.; Blankenship, R. E.; Struve, W. S. Ultrafast Energy Transfer in Chlorosomes from the Green Photosynthetic Bacterium. *J. Phys. Chem.* **1996**, *100*, 3320−3322.
(315) Miller, M.; Cox, R. P.; Gillbro, T. Energy Transfer Kinetics in Chlorosomes from Chloroflexus Aurantiacus: Studies Using Picosecond Absorbance Spectroscopy. *Biochim. Biophys. Acta, Bioenerg.* **1991**, *1057*, 187−194.
(316) Huijser, A.; Marek, P.; Savenije, T.; Siebbeles, L. D. A.; Scherer, T.; Hauschild, R.; Szmytkowski, J.; Kalt, H.; Hahn, H.; Balaban, T. S. Photosensitization of TiO_2 and SnO_2 by Artificial Self-Assembling Mimics of the Natural Chlorosomal Bacteriochlorophylls. *J. Phys. Chem. C* **2007**, *111*, 11726−11733.
(317) Grossman, A. R.; Schaefer, M. R.; Chiang, G. G.; Collier, J. L. The Phycobilisome, a Light-Harvesting Complex Responsive to Environmental Conditions. *Microbiol. Rev.* **1993**, *57*, 725−749.
(318) MacColl, R. Cyanobacterial Phycobilisomes. *J. Struct. Biol.* **1998**, *124*, 311−334.
(319) Suter, G. W.; Holzwarth, A. R. A Kinetic Model for the Energy Transfer in Phycobilisomes. *Biophys. J.* **1987**, *52*, 673−683.
(320) Suter, G. W.; Mazzola, P.; Wendler, J.; Holzwarth, A. R. Fluorescence Decay Kinetics in Phycobilisomes Isolated from the Bluegreen Alga *Synechococcus* 6301. *Biochim. Biophys. Acta, Bioenerg.* **1984**, *766*, 269−276.
(321) Krumova, S. B.; Laptenok, S. P.; Borst, J. W.; Ughy, B.; Gombos, Z.; Ajlani, G.; van Amerongen, H. Monitoring Photosynthesis in Individual Cells of *Synechocystis sp.* PCC 6803 on a Picosecond Timescale. *Biophys. J.* **2010**, *99*, 2006−2015.
(322) Tian, L.; van Stokkum, I. H. M.; Koehorst, R. B. M.; Jongerius, A.; Kirilovsky, D.; van Amerongen, H. Site, Rate, and Mechanism of Photoprotective Quenching in Cyanobacteria. *J. Am. Chem. Soc.* **2011**, *133*, 18304−18311.
(323) Gillbro, T.; Sharkov, A. V.; Kryukov, I. V.; Khoroshilov, E. V.; Kryukov, P. G.; Fischer, R.; Scheer, H. Förster Energy Transfer Between Neighbouring Chromophoresin C-Phycocyanin Trimers. *Biochim. Biophys. Acta, Bioenerg.* **1993**, *1140*, 321−326.
(324) Kirilovsky, D.; Kaňa, R.; Prášil, O. Mechanisms Modulating Energy Arriving at Reaction Centers in Cyanobacteria. In *Non-Photochemical Quenching and Thermal Energy Dissipation in Plants, Algae and Cyanobacteria*; Demmig-Adams, B., Garab, G., Adams, W. W., III, Govindjee, Eds.; Advances in Photosynthesis and Respiration; Springer: Dordrecht, The Netherlands, 2014; Vol. *40*, Chapter 22, pp 471−501.
(325) Spear-Bernstein, L.; Miller, K. R. Unique Location of the Phycobiliprotein Light-Harvesting Pigment in the Cryptophyceae. *J. Phycol.* **1989**, *25*, 412−419.
(326) Novoderezhkin, V. I.; van Grondelle, R. Physical Origins and Models of Energy Transfer in Photosynthetic Light-Harvesting. *Phys. Chem. Chem. Phys.* **2010**, *12*, 7352−7365.
(327) Curutchet, C.; Novoderezhkin, V. I.; Kongsted, J.; Muñoz-Losa, A.; van Grondelle, R.; Scholes, G. D.; Mennucci, B. Energy Flow in the Cryptophyte PE545 Antenna Is Directed by Bilin Pigment Conformation. *J. Phys. Chem. B* **2013**, *117*, 4263−4273.
(328) Doust, A. B.; van Stokkum, I. H.; Larsen, D. S.; Wilk, K. E.; Curmi, P. M.; van Grondelle, R.; Scholes, G. D. Mediation of Ultrafast Light-Harvesting by a Central Dimer in Phycoerythrin 545 Studied by Transient Absorption and Global Analysis. *J. Phys. Chem. B* **2005**, *109*, 14219−14226.
(329) Marin, A.; Doust, A. B.; Scholes, G. D.; Wilk, K. E.; Curmi, P. M. G.; van Stokkum, I. H. M.; van Grondelle, R. Flow of Excitation Energy in the Cryptophyte Light-Harvesting Antenna Phycocyanin 645. *Biophys. J.* **2011**, *101*, 1004−1013.
(330) van der Weij-De Wit, C. D.; Doust, A. B.; van Stokkum, I. H. M.; Dekker, J. P.; Wilk, K. E.; Curmi, P. M. G.; Scholes, G. D.; van Grondelle, R. How Energy Funnels from the Phycoerythrin Antenna

DOI: 10.1021/acs.chemrev.6b00002
Chem. Rev. XXXX, XXX, XXX−XXX

Complex to Photosystem I and Photosystem II in Cryptophyte *Rhodomonas* CS24 Cells. *J. Phys. Chem. B* **2006**, *110*, 25066−25073.
(331) Collini, E.; Wong, C. Y.; Wilk, K. E.; Curmi, P. M. G.; Brumer, P.; Scholes, G. D. Coherently Wired Light-Harvesting in Photosynthetic Marine Algae at Ambient Temperature. *Nature* **2010**, *463*, 644−648.
(332) Wong, C. Y.; Alvey, R. M.; Turner, D. B.; Wilk, K. E.; Bryant, D. A.; Curmi, P. M. G.; Silbey, R. J.; Scholes, G. D. Electronic Coherence Lineshapes Reveal Hidden Excitonic Correlations in Photosynthetic Light Harvesting. *Nat. Chem.* **2012**, *4*, 396−404.
(333) Turner, D. B.; Dinshaw, R.; Lee, K.-K.; Belsley, M. S.; Wilk, K. E.; Curmi, P. M. G.; Scholes, G. D. Quantitative Investigations of Quantum Coherence for a Light-Harvesting Protein at Conditions Simulating Photosynthesis. *Phys. Chem. Chem. Phys.* **2012**, *14*, 4857−4874.
(334) Calhoun, T. R.; Fleming, G. R. Quantum Coherence in Photosynthetic Complexes. *Phys. Status Solidi B* **2011**, *248*, 833−838.
(335) Fassioli, G.; Dinshaw, R.; Arpin, P. C.; Scholes, G. D. Photosynthetic Light Harvesting: Excitons and Coherence. *J. R. Soc., Interface* **2014**, *11*, 20130901.
(336) Britton, G., Liaaen-Jensen, S., Pfander, H., Eds. *Carotenoids Handbook*; Birkhäuser Verlag AG: Basel, Switzerland, 2004.
(337) Britton, G.; Functions of Intact Carotenoids. In *Carotenoids, Vol. 4: Natural Functions*; Britton, G., Liaaen-Jensen, S., Pfander, H., Eds.; Birkhäuser Verlag AG: Basel, Switzerland, 2008; pp 189−212.
(338) Truscott, G. T.; Edge, R. Carotenoid radicals and the interaction of carotenoids with active oxygen species. In *The Photochemistry of Carotenoids*; Frank, H. A., Young, A., Britton, G., Cogdell, R. J., Eds.; Advances in Photosynthesis and Respiration; Springer: Dordrecht, The Netherlands, 2004; Vol. *8*, Chapter 12, pp 223−234.
(339) Telfer, A.; Pascal, A.; Gall, A. Carotenoids in Photosynthesis. In *Carotenoids, Vol. 4: Natural Functions*; Britton, G., Liaaen-Jensen, S., Pfander, H., Eds.; Birkhäuser Verlag AG: Basel, Switzerland, 2008; Chapter 14, pp 265−308.
(340) Blount, J. D.; McGraw, K. J. Signal Functions of Carotenoid Coloration. In *Carotenoids, Vol 4: Natural Functions*; Britton, G., Liaaen-Jensen, S., Pfander, H., Eds.; Birkhäuser Verlag AG: Basel, Switzerland, 2008; Chapter 11, pp 213−236.
(341) Nagae, H.; Kakitani, T.; Katoh, T.; Mimuro, M. Calculation of the Excitation Transfer-Matrix Elements Between the S2 or S1 State of Carotenoid and the S2 or S1 State of Bacteriochlorophyll. *J. Chem. Phys.* **1993**, *98*, 8012−8023.
(342) Maruta, S.; Kosumi, D.; Horibe, T.; Fujii, R.; Sugisaki, M.; Cogdell, R. J.; Hashimoto, H. The Dependence of Excitation Energy Transfer Pathways on Conjugation Length of Carotenoids in Purple Bacterial Photosynthetic Antennae. *Phys. Status Solidi B* **2011**, *248*, 403−407.
(343) Gradinaru, C. C.; Kennis, J. T. M.; Papagiannakis, E.; van Stokkum, I. H. M.; Cogdell, R. J.; Fleming, G. R.; Niederman, R. A.; van Grondelle, R. An Unusual Pathway of Excitation Energy Deactivation in Carotenoids: Singlet-to-Triplet Conversion on an Ultrafast Timescale in a Photosynthetic Antenna. *Proc. Natl. Acad. Sci. U. S. A.* **2001**, *98*, 2364−2369.
(344) Damjanovic, A.; Ritz, T.; Schulten, K. Energy Transfer Between Carotenoids and Bacteriochlorophylls in Light-Harvesting Complex II of Purple Bacteria. *Phys. Rev. E: Stat. Phys., Plasmas, Fluids, Relat. Interdiscip. Top.* **1999**, *59*, 3293−3311.
(345) Walla, P. J.; Linden, P. A.; Hsu, C.-P.; Scholes, G. D.; Fleming, G. R. Femtosecond Dynamics of the Forbidden Carotenoid S-1 State in Light-Harvesting Complexes of Purple Bacteria Observed After Two-Photon Excitation. *Proc. Natl. Acad. Sci. U. S. A.* **2000**, *97*, 10808−10813.
(346) Hsu, C.-P.; Walla, P. J.; Head-Gordon, M.; Fleming, G. R. The Role of the S_1 State of Carotenoids in Photosynthetic Energy Transfer: The Light-Harvesting Complex II of Purple Bacteria. *J. Phys. Chem. B* **2001**, *105*, 11016−11025.
(347) Zhang, J.-P.; Fujii, R.; Qian, P.; Inaba, T.; Mizoguchi, T.; Koyama, Y.; Onaka, K.; Watanabe, Y.; Nagae, H. Mechanism of the Carotenoid-to-Bacteriochlorophyll Energy Transfer via the S_1 State in the LH2 Complex from Purple Bacteria. *J. Phys. Chem. B* **2000**, *104*, 3683−3691.
(348) Tavan, P.; Schulten, K. The Low-Lying Electronic Excitations in Long Polyenes: A PPP-MRD-CI Study. *J. Chem. Phys.* **1986**, *85*, 6602−6609.
(349) Polívka, T.; Sundström, V. Dark Excited States of Carotenoids: Consensus and Controversy. *Chem. Phys. Lett.* **2009**, *477*, 1−11.
(350) Gradinaru, C. C.; Kennis, J. T. M.; Papagiannakis, E.; van Stokkum, I. H. M.; Cogdell, R. J.; Fleming, G. R.; Niederman, R. A.; van Grondelle, R. An Unusual Pathway of Excitation Energy Deactivation in Carotenoids: Singlet-to-Triplet Conversion on an Ultrafast Timescale in a Photosynthetic Antenna. *Proc. Natl. Acad. Sci. U. S. A.* **2001**, *98*, 2364−2369.
(351) Cerullo, G.; Polli, D.; Lanzani, G.; De Silvestri, S.; Hashimoto, H.; Cogdell, R. J. Photosynthetic Light Harvesting by Carotenoids: Detection of an Intermediate Excited State. *Science* **2002**, *298*, 2395−2398.
(352) Polli, D.; Cerullo, G.; Lanzani, G.; De Silvestri, S.; Yanagi, K.; Hashimoto, H.; Cogdell, R. J. Conjugation Length Dependence of Internal Conversion in Carotenoids: Role of the Intermediate State. *Phys. Rev. Lett.* **2004**, *93*, 163002-1−163002-4.
(353) Rondonuwu, F. S.; Yokoyama, K.; Fujii, R.; Koyama, Y.; Cogdell, R. J.; Watanabe, Y. The Role of the 11Bu− State in Carotenoid-To-Bacteriochlorophyll Singlet-Energy Transfer in the LH2 Antenna Complexes from *Rhodobacter Sphaeroides* G1C, *Rhodobacter Sphaeroides* 2.4.1, *Rhodospirillum Molischianum* and *Rhodopseudomonas Acidophila*. *Chem. Phys. Lett.* **2004**, *390*, 314−322.
(354) Ostroumov, E. E.; Mulvaney, R. M.; Cogdell, R. J.; Scholes, G. D. Broadband 2D Electronic Spectroscopy Reveals a Carotenoid Dark State in Purple Bacteria. *Science* **2013**, *340*, 52−56.
(355) Papagiannakis, E.; Kennis, J. T. M.; van Stokkum, I. H. M.; Cogdell, R. J.; van Grondelle, R. An Alternative Carotenoid-to-Bacteriochlorophyll Energy Transfer Pathway in Photosynthetic Light Harvesting. *Proc. Natl. Acad. Sci. U. S. A.* **2002**, *99*, 6017−6022.
(356) Foote, C. S.; Chang, Y. C.; Denny, R. W. Chemistry of singlet oxygen 10. Carotenoid Quenching Parallels Biological Protection. *J. Am. Chem. Soc.* **1970**, *92*, 5216−5218.
(357) de Winter, A.; Boxer, S. G. The Mechanism of Triplet Energy Transfer from the Special Pair to the Carotenoid in Bacterial Photosynthetic Reaction Centers. *J. Phys. Chem. B* **1999**, *103*, 8786−8789.
(358) Scholes, G. D.; Harcourt, R. D.; Ghiggino, K. P. Rate Expressions for Excitation Transfer. 3. An Ab-Initio Study of Electronic Factors in Excitation Transfer and Exciton Resonance Interactions. *J. Chem. Phys.* **1995**, *102*, 9574−9581.
(359) Closs, G. L.; Piotrowiak, P.; MacInnis, J. M.; Fleming, G. R. Determination of Long Distance Intramolecular Triplet Energy Transfer Rates. A Quantitative Comparison with Electron Transfer. *J. Am. Chem. Soc.* **1988**, *110*, 2652−2653.
(360) Bittl, R.; Schlodder, E.; Geisenheimer, I.; Lubitz, W.; Cogdell, R. J. Transient EPR and Absorption Studies of Carotenoid Triplet Formation in Purple Bacterial Antenna Complexes. *J. Phys. Chem. B* **2001**, *105*, 5525−5535.
(361) Ke, B. Role of Carotenoids in Photosynthesis. *Photosynthesis: Photobiochemistry and Photobiophysics*; Advances in Photosynthesis and Respiration; Kluwer Academic Publishers: Dordrecht, The Netherlands, 2001; Vol. *10*, Chapter 13, pp 229−250.
(362) Foote, C. S.; Denny, R. W. Chemistry of Singlet Oxygen 7. Quenching by Beta-Carotene. *J. Am. Chem. Soc.* **1968**, *90*, 6233−6235.
(363) Foote, C. S. Photosensitized Oxidation and Singlet Oxygen: Consequences in Biological Systems. In *Free Radicals in Biology*; Pryor, W. A., Ed.; Vol. *11*. Academic Press: New York, 1976; Vol. *II*, Chapter 3, pp 85−133.
(364) Krinsky, N. I. Carotenoid Protection Against Oxidation. *Pure Appl. Chem.* **1979**, *51*, 649−660.
(365) Siefermann-Harms, D. The Light-Harvesting and Protective Functions of Carotenoids in Photosynthetic Membranes. *Physiol. Plant.* **1987**, *69*, 561−568.

DOI: 10.1021/acs.chemrev.6b00002
Chem. Rev. XXXX, XXX, XXX−XXX

(366) Fiedor, J.; Fiedor, L.; Haessner, R.; Scheer, H. Cyclic Endoperoxides of β-Carotene, Potential Pro-Oxidants, as Products of Chemical Quenching of Single Oxygen. *Biochim. Biophys. Acta, Bioenerg.* **2005**, *1709*, 1−4.
(367) Demmig-Adams, B.; Adams, W. W. Photoprotection and Other Responses of Plants to High Light Stress. *Annu. Rev. Plant Physiol. Plant Mol. Biol.* **1992**, *43*, 599−626.
(368) Jahns, P.; Holzwarth, A. R. The Role of the Xanthophyll Cycle and of Lutein in Photoprotection of Photosystem II. *Biochim. Biophys. Acta, Bioenerg.* **2012**, *1817*, 182−193.
(369) Frank, H. A.; Cua, A.; Chynwat, V.; Young, A.; Gosztola, D.; Wasielewski, M. R. Photophysics of the Carotenoids Associated with the Xanthophyll Cycle in Photosynthesis. *Photosynth. Res.* **1994**, *41*, 389−395.
(370) Müller, M. G.; Lambrev, P.; Reus, M.; Wientjes, E.; Croce, R.; Holzwarth, A. R. Singlet Energy Dissipation in Photosystem II Light-Harvesting Complex Does Not Involve Energy Transfer to Carotenoids. *ChemPhysChem* **2010**, *11*, 1289−1296.
(371) Wahadoszamen, M.; Berera, R.; Ara, A. M.; Romero, E.; van Grondelle, R. Identification of Two Emitting Sites in the Dissipative State of the Major Light Harvesting Antenna. *Phys. Chem. Chem. Phys.* **2012**, *14*, 759−766.
(372) Avenson, T. J.; Ahn, T. K.; Zigmantas, D.; Niyogi, K. K.; Li, Z.; Ballottari, M.; Bassi, R.; Fleming, G. R. Zeaxanthin Radical Cation Formation in Minor Light-Harvesting Complexes of Higher Plant Antenna. *J. Biol. Chem.* **2008**, *283*, 3550−3558.
(373) Staleva, H.; Komenda, J.; Shukla, M. K.; Slouf, V.; Kana, R.; Polivka, T.; Sobotka, R. Mechanism of Photoprotection in the Cyanobacterial Ancestor of Plant Antenna Proteins. *Nat. Chem. Biol.* **2015**, *11*, 287−291.
(374) Gilmore, A. M. Mechanistic Aspects of Xanthophyll Cycle-Dependent Photoprotection in Higher Plant Chloroplasts and Leaves. *Physiol. Plant.* **1997**, *99*, 197−209.
(375) Ostroumov, E. E.; Khan, Y. R.; Scholes, G. D.; Govindjee. Photophysics of Photosynthetic Pigment−Protein Complexes. In *Non-Photochemical Quenching and Energy Dissipation in Plants, Algae and Cyanobacteria*; Demmig-Adams, B., Garab, G., Adams, W. W., III, Govindjee, Eds.; Advances in Photosynthesis and Respiration; Springer, 2014; Vol. *40*, Chapter 4, 97−128.
(376) Papageorgiou, G. C.; Govindjee. The Non-Photochemical Quenching of the Electronically Excited State of Chlorophyll a in Plants: Definitions, Timelines, Viewpoints, Open Questions. In *Non-Photochemical Quenching and Energy Dissipation in Plants, Algae and Cyanobacteria*; Demmig-Adams, B., Garab, G., Adams, W. W., III, Govindjee, Eds.; Advances in Photosynthesis and Respiration; Springer, 2014; Vol. *40*, Chapter 1, pp 1−44.
(377) Krüger, T. P. J.; Ilioaia, C.; Horton, P.; Alexandre, M. T. A.; van Grondelle, R. How Protein Disorder Controls Non-Photochemical Fluorescence Quenching. In *Non-Photochemical Quenching and Energy Dissipation in Plants, Algae and Cyanobacteria*; Demmig-Adams, B., Garab, G., Adams, W. W., III, Govindjee, Eds.; Advances in Photosynthesis and Respiration; Springer, 2014; Vol. *40*,Chapter 6, pp 157−185.
(378) Kenkre, V. M.; Parris, P. E.; Schmid, D. Investigation of the Appropriateness of Sensitized Luminescence to Determine Exciton Motion Parameters in Pure Molecular Crystals. *Phys. Rev. B: Condens. Matter Mater. Phys.* **1985**, *32*, 4946−4955.
(379) Silbey, R. Electronic Energy Transfer in Molecular Crystals. *Annu. Rev. Phys. Chem.* **1976**, *27*, 203−23.
(380) Pearlstein, R. M. Chlorophyll Singlet Excitons. In *Photosynthesis, Vol. 1: Energy Conversion by Plants and Bacteria*; Govindjee, Ed.; Academic Press: New York, 1982; Chapter 7, pp 293−330.
(381) Pearlstein, R. M. Coupling of Exciton Motion in the Core Antenna and Primary Charge Separation in the Reaction Center. *Photosynth. Res.* **1996**, *48*, 75−82.
(382) Kudžmauskas, Š.; Valkūnas, L.; Borisov, A. Y. A Theory of Excitation Transfer in Photosynthetic Units. *J. Theor. Biol.* **1983**, *105*, 13−23.
(383) Schatz, G. H.; Brock, H.; Holzwarth, A. R. Kinetic and Energetic Model for the Primary Processes in Photosystem II. *Biophys. J.* **1988**, *54*, 397−405.
(384) Raszewski, G.; Renger, T. Light Harvesting in Photosystem II Core Complexes Is Limited by the Transfer to the Trap: Can the Core Complex Turn into a Photoprotective Mode? *J. Am. Chem. Soc.* **2008**, *130*, 4431−4446.
(385) van der Weij-de Wit, C. D.; Dekker, J. P.; van Grondelle, R.; van Stokkum, I. H. M. Charge Separation Is Virtually Irreversible in Photosystem II Core Complexes with Oxidized Primary Quinone Acceptor. *J. Phys. Chem. A* **2011**, *115*, 3947−3956.
(386) Renger, T.; Schlodder, E. Optical Properties, Excitation Energy and Primary Charge Transfer in Photosystem II: Theory Meets Experiment. *J. Photochem. Photobiol., B* **2011**, *104*, 126−141.

DOI: 10.1021/acs.chemrev.6b00002
Chem. Rev. XXXX, XXX, XXX−XXX